

Distribution Agreement

In presenting this thesis or dissertation as a partial fulfillment of the requirements for an advanced degree from Emory University, I hereby grant to Emory University and its agents the non-exclusive license to archive, make accessible, and display my thesis or dissertation in whole or in part in all forms of media, now or hereafter known, including display on the world wide web. I understand that I may select some access restrictions as part of the online submission of this thesis or dissertation. I retain all ownership rights to the copyright of the thesis or dissertation. I also retain the right to use in future works (such as articles or books) all or part of this thesis or dissertation.

Signature:

Kathleen S. Gray

Date

THESIS APPROVAL FORM

A new gammaherpesvirus lytic gene promoter:
identification and epigenetic regulation

By
Kathleen S. Gray
Doctor of Philosophy

Graduate Division of Biological and Biomedical Science
Immunology and Molecular Pathogenesis

Samuel H. Speck
Advisor

Jeremy M. Boss
Committee Member

Joshy Jacob
Committee Member

Aron E. Lukacher
Committee Member

Paula M. Vertino
Committee Member

Accepted

Lisa A. Tedesco
Dean of the Graduate School

Date

A New Gammaherpesvirus Lytic Gene Promoter:
Identification and Epigenetic Regulation

By

Kathleen S. Gray
B.S., University of Michigan, 2002

Advisor: Samuel H. Speck, PhD

An abstract of a dissertation submitted to the Faculty of the Graduate School of Emory
University in partial fulfillment of the requirements for the degree of Doctor of Philosophy

Graduate Division of Biological and Biomedical Science
Immunology and Molecular Pathogenesis
2009

Abstract
A New Gammaherpesvirus Lytic Gene Promoter: Identification and Epigenetic Regulation
By Kathleen S. Gray

Gammaherpesviruses are characterized by their ability to establish a lifelong infection in cells of lymphoid origin. The human gammaherpesviruses Epstein-Barr (EBV or HHV-4), and to a lesser extent Kaposi's Sarcoma-Associated Herpesvirus (KSHV or HHV-8), are ubiquitous and associated with lymphomagenesis and lymphoproliferative disease in immunocompromised individuals. Although rare given the broad distribution of infection, gammaherpesvirus-associated pathologies have driven aggressive efforts to better understand gammaherpesvirus biology. Narrow host tropism human has necessitated animal models to study gammaherpesvirus infection and is exemplified by the Murine Herpesvirus-68 (MHV68) system.

One of the most conserved functional gammaherpesvirus proteins is that encoded by Orf50, termed Rta (for Replication and Transcriptional Activator), named for its key role in driving both initial lytic replication and reactivation from latent infection. For EBV and KSHV, Rta expression upon reactivation from latency has been well-studied using established latent cell lines, and therefore little is known about the mechanism to initially target Rta for repression in favor of latent infection.

In this study, we identify an additional Rta transcriptional unit conserved among EBV, KSHV, and MHV68 in the existence of a third Rta-coding exon and additional promoter. This promoter drives expression of Rta to sufficiently support lytic replication during both permissive infection and reactivation from latency in certain cell types. We demonstrate that DNA methylation and the de novo DNA methyltransferases (DNMTs) are

required to repress Rta transcription during early latency *in vivo*. Also, we provide evidence of strong selective pressure to methylate this new Rta promoter in infected B cells, even in the absence of DNMT3a and DNMT3b. In summary, we report the effect of de novo DNMT-mediated repression of Rta expression in B cells and demonstrate for the first time a direct requirement for de novo DNA methylation during the establishment of gammaherpesvirus latency.

A New Gammaherpesvirus Lytic Gene Promoter:
Identification and Epigenetic Regulation

By

Kathleen S. Gray
B.S., University of Michigan, 2002

Advisor: Samuel H. Speck, PhD

A dissertation submitted to the Faculty of the Graduate School of Emory University in partial fulfillment of the requirements for the degree of Doctor of Philosophy

Graduate Division of Biological and Biomedical Science
Immunology and Molecular Pathogenesis
2009

TABLE OF CONTENTS

Chapter 1: Introduction	1
1.I. Herpesviruses	
i. General background.....	1
ii. Gammaherpesvirus-associated pathologies: justification for study.....	3
iii. MHV68 as a model system.....	4
iv. MHV68 and human gammaherpesviruses: similarities and differences.....	6
1.II. The gammaherpesvirus Rta protein	
i. Gene structure and function in lytic replication.....	11
ii. Regulation of the Rta promoter.....	13
1.III. Epigenetic regulation via DNA methylation	
i. General background.....	15
ii. DNA methylation in health and disease.....	17
iii. Role of DNA methylation in lymphocytes.....	18
1.IV. Intersection of DNA methylation and gammaherpesviruses	
i. Role of DNA methylation in gammaherpesvirus pathogenesis.....	20
ii. Regulation of EBV latency programs.....	20
iii. Regulation of EBV latency programs by DNA methylation.....	23
iv. Regulation of gammaherpesvirus lytic replication by DNA methylation.....	24
v. The role of de novo DNA methylation in Rta promoter regulation.....	26
1.V. Figures and Tables	27
1.VI. Figure legends	35
Chapter 2: Alternatively initiated gene 50/RTA transcripts expressed during murine and human gammaherpesvirus reactivation from latency	37
2.I. Abstract	38
2.II. Introduction	40
2.III. Materials and Methods	43
2.IV. Results	53
2.V. Discussion	68
2.IV. Figure legends	77
2.VII. Figures	82

Chapter 3: Deregulated murine gammaherpesvirus gene 50/Rta transcription in vivo in the absence of the de novo methyltransferases DNMT3a and DNMT3b.....	89
3.I. Abstract.....	90
3.II. Introduction.....	92
3.III. Results.....	96
3.IV. Discussion.....	103
3.V. Materials and Methods.....	110
3.IV. Figures.....	117
3.VII. Figure legends.....	127
Chapter 4: Conclusions and Future Directions.....	130
4.I. Rta	
i. Rta transcription, splicing, and the function of Exon0.....	131
ii. Transcription factors regulating the Rta distal promoter.....	135
4.II. DNA methylation in MHV68 infection	
i. Role of de novo DNMTs in B cells.....	137
ii. De novo methyltransferases and human gammaherpesviruses.....	141
iii. Role of methylation in regulating gammaherpesvirus Rta: Relevance.....	144
4.III. Summary.....	145
4.IV. Figures.....	146
4.V. Figure legends.....	155
Literature Cited.....	158

LIST OF FIGURES and TABLES

Chapter 1:

Figures:

1. A. Kinetics of MHV68 lytic and latent infection
B. Model of MHV68 infection
2. A. Colinearity of gammaherpesvirus genomes
B. Annotation of transposon mutagenesis studies
3. Structure of gammaherpesvirus Rta-encoding transcripts
4. A. Model depicting DNA methylation in heterochromatin formation
B. Key domains of mammalian DNA methyltransferases
5. EBV latent gene transcription programs

Tables:

1. Frequency of MHV68 genome-positive cells
2. MHV68 genes and putative human gammaherpesvirus homologues

Chapter 2:

1. Conservation of G50/BRLF1/Rta coding region among gammaherpesviruses
2. Generation and confirmation of MHV68.G50pKO and MHV68.G50pKO-MR viruses
3. MHV68.G50pKO virus replicates *in vitro*
4. RACE and RT-PCR analyses identify an additional upstream G50 exon
5. Promoter activity in region immediately 5' to MHV68 E0
6. Quantitative RT-PCR analysis of distal versus proximal promoter-driven transcripts
7. Identification of upstream-initiated transcripts from treated EBV or KSHV latent cell lines
8. Exon 0 extends the EBV and KSHV G50 reading frames
9. G50pKO virus establishes latency *in vivo* but exhibits severe reactivation defect
10. Bisulfite PCR analysis of CpG methylation in regions containing the proximal and distal G50 promoters
11. G50pKO virus reactivates from peritoneal exudate cells following intraperitoneal infection

Chapter 3:

1. Methyltransferase inhibitor treatment induces MHV68 reactivation
2. In vitro methylation reduces distal Gene 50 promoter activity
3. Rearrangement of *Dnmt3a* and *Dnmt3b* alleles in *CD19^{+/Cre} Dnmt3a^{2loxP/2loxP} Dnmt3b^{2loxP/2loxP}* splenocytes
4. Evidence of ongoing lytic replication in CD19+/Cre mice during early latency
5. Gene 50 transcripts are elevated in CD19+/Cre mice at day 18
6. Bisulfite PCR analysis of the distal Gene 50 promoter region at day 18
7. Genome frequency at day 42 post-infection
8. Bisulfite PCR analysis of the distal Gene 50 promoter region at day 42 post-infection
9. Bisulfite PCR analysis of the v-cyclin and v-bcl2 promoter region at days 18 and 42 post-infection

Chapter 4:

1. A. Translation of N-terminus of hypothetical MHV68 E0-E2 protein
B. Summary of detected gammaherpesvirus Rta transcripts and translations
C. Results of structural prediction analysis of E0 vs E1-containing proteins
2. Rta can transactivate a methylated Orf57 promoter
3. A. Hypoxia-induced activation of the distal Rta promoter is dependent on a HIF binding site
B. HIF1 α activates the distal Rta promoter
C. HIF2 α activates the distal Rta promoter
4. Dnmt3a and Dnm3b transcripts are detectable in naïve B cells
5. Analysis of NP-specific antibody response in CD19+/Cre mice versus littermate controls:
A. ELISpot analysis of secondary antibody response following secondary immunization with NP-CGG
B. NP-specific antibody response following primary immunization
C. NP-specific antibody response following secondary immunization
6. Analysis of antibody response in MHV68-infected CD19+/Cre mice versus littermate controls:
A. MHV68-specific antibody response
B. ELISpot analysis of total IgM and IgG ASCs
7. A. Alternative splicing and promoter usage in transcription of MHV68-LANA
B. Bisulfite sequence analysis of LANA latent promoter region

Chapter 1: Introduction

1.I Herpesviruses

1.I.i. *General background*

Viruses are remarkable entities, with diverse morphology, host and cellular tropism, biological activity, and associated pathologies. Viral genomes are comprised of several nucleic acid forms, from single-stranded RNA to double-stranded DNA, and range in size from 3-4 kilobase hepadnaviruses to 250 kilobase poxviruses. Herpesviruses are a member of the double-stranded DNA virus family and have large, complex genomes around 100 to 200 Kb in size encoding 70+ genes. The genome is encapsidated and surrounded by a tegument layer consisting of various proteins of both known and unknown function, many of which aid in the efficient initiation of viral replication upon entry into the host cell. The outer layer of the virion is a lipid envelope containing various glycoproteins which mediate membrane fusion and viral entry.

The size and complexity of herpesvirus genomes is reflected in the sequential cascade of gene transcription during lytic replication. Upon delivery of the viral genome to the host nucleus (via the aid of both viral tegument and host cellular proteins), the first round of viral genes, known as immediate-early (IE) or α - genes, are transcribed. These genes are spliced and transported to the cytoplasm where they are translated; proteins are then transported back to the nucleus where they stimulate transcription of the next round of viral gene products, the early (E) or β - genes. These products of these genes primarily function in the control and shut-off of host cell processes and aid in viral DNA replication. DNA synthesis is initiated at

lytic origins of replication, and nascent viral genomes are transcribed as long concatamers via rolling-circle replication to provide templates to transcribe the final round of viral genes, the late (L) or γ - genes. Late proteins, such as surface glycoproteins (gPs) and various structural proteins, facilitate the packaging of viral genomes into viral particles and their subsequent export from the cell

All viruses usurp host cell machinery to replicate their genomes and produce infectious virions which are then released from the cell to go on and infect other healthy cells. Lytic infection is characterized by a high degree of viral gene transcription and the mass production of viral particles, such that the cell is filled with virions to the point of “lysis,” during which the host cell ruptures and infectious virus is released. Although the term “lytic replication” is often used to describe production viral infection, not all lytic replication results in the destruction of the host cell. Lytic or productive herpesvirus infection provides the basis for latent infection, a unique stage of the viral life cycle that defines the herpesvirus family. Latent infection is characterized as the presence of the viral genome in the cell with little or no virion production, as well as the ability of the virus to re-initiate productive lytic infection from this quiescent state, a process referred to as herpesvirus reactivation. Latent infection is distinct from persistent infection in that only a limited set of viral genes is being transcribed, and little or no infectious virus is produced.

Herpesviruses are categorized into three subfamilies: alpha, beta, and gamma. Members of all three families establish latent infection in host cells, but are sub-classified based on cellular tropism and other characteristics such as sequence homology. Alphaherpesviruses include Herpes Simplex Viruses-1 and 2 (HSV-1 and HSV-2), and Varicella-Zoster Virus (VZV), both of which infect and establish latent infection in neuronal

cells. Betaherpesviruses, such as murine and human cytomegalovirus (mCMV and hCMV), and human herpesviruses-6 and 7 (HHV6 and HHV7) exhibit broad cellular tropism for establishment of latency, while the third family, the gammaherpesviruses, establish latency primarily in cells of lymphoid origin. Gammaherpesviruses include the human pathogens Epstein-Barr Virus (EBV) and Kaposi's Sarcoma-associated Herpesvirus (KSHV), as well as the non-human primate herpesvirus saimiri (HVS), rhesus rhadinovirus (RRV), and several other non-primate pathogens. Based on DNA sequence homology, the gammaherpesvirus family is further divided into the γ -1 or lymphocryptovirus (EBV), and the γ -2 or rhadinovirus (KSHV, HVS, RRV) subfamilies. Murine herpesvirus-68 (MHV68) is a naturally-occurring pathogen of mice, voles, and other small rodents. MHV68 is a member of the γ -2 subfamily and the subject of the majority of this work and will be discussed in detail below.

1.I.ii *Gammaherpesvirus-associated pathologies: justification for study*

Viruses have proven to be invaluable tools in the study of normal cell biology; however, many viruses share the capacity to mediate cellular transformation and have been classified as DNA tumor viruses. Viruses in this family encode proteins capable of facilitating the transformation of host cells and initiating early events leading to tumorigenesis in infected individuals. Among the herpesviruses, EBV and KSHV have been associated with several malignancies in humans. EBV is implicated in the development of lymphomas (Hodgkin's (HL) and Burkitt's lymphoma (BL)), as well as gastric and nasopharyngeal carcinomas. KSHV is associated with the development of primary effusion lymphoma (PEL) and multicentric Castleman's disease (MCD), two tumors of lymphoid

origin. KSHV also induces Kaposi's sarcoma, a rare tumor of endothelium-associated lymphatic vessels from which the virus takes its name.

EBV is a ubiquitous pathogen—90% of the world population is estimated to be EBV positive. Despite the high incidence of seropositivity, EBV-related lymphomas are relatively rare, and often arise as a consequence of immunosuppression in post-transplant or AIDS patients. KSHV infection is less prevalent than EBV, but is highly concentrated in certain geographical areas, including regions in Africa and Asia. Although disease incidence is small compared to the frequency of infection, gammaherpesvirus-related pathologies are associated with high morbidity and mortality in susceptible individuals. For this reason, gammaherpesviruses have been a subject of intense study since the mid-20th century. Although tremendous progress has been made toward understanding these pathogens, research has been restricted by EBV and KSHV's strict human tropism. MHV68 infection of laboratory mice has gained acceptance as a model system to study gammaherpesvirus pathogenesis over the past fifteen years, and has proven to be a relevant and valuable tool in further understanding aspects of infection not readily studied in humans.

1.I.iii *MHV68 as a model system*

MHV68 is one of several strains of murine gammaherpesvirus isolated from wild murid rodents, along with MHV60, MHV72, MHV76, and MHV78 (11). Although originally identified in yellow-necked or wood mice and bank voles, murine gammaherpesviruses can infect a variety of species, including several strains of both inbred and outbred strains of mice. The natural route of MHV68 transmission is unknown. Although laboratory mouse strains support MHV68 infection, attempts at co-infection of naïve co-inhabiting mice have

been unsuccessful. Evidence suggests that natural transmission may be via low-dose intranasal infection (103). The course of infection in wild animals is also not fully deduced, but has been extensively studied in a laboratory setting. Intranasal infection of mice results in extensive lytic replication in the respiratory tract by day 4 in the nose and the lungs, the primary site of productive lytic infection. It is then hypothesized that B lymphocytes, either resident in lung tissue or recruited to the site of viral infection, are subsequently infected during this burst of virus replication. Infected B cells then migrate to the spleen where the initial stages of latent infection are thought to begin. Recent studies combining fluorescent recombinant virus and sophisticated imaging techniques have suggested that the path of MHV68 infection following intranasal infection also results in productive replication in the thymus and salivary glands (67, 103). Lytic virus can be detected by plaque or infectious center assay in the lung within four days of intranasal inoculation, with peak titers typically occurring around day 9 (83) (Fig.1A). Although viral genomes are present, lytic virus is typically not detected by plaque assay in the spleen or lungs beyond 12 days post-infection, although infection of certain transgenic mice or with recombinant virus can result in prolonged or persistent replication in the lung or spleen following intranasal infection (17, 83, 155, 183). Therefore, day 12 marks the beginning of MHV68 latency. Lytic virus is virtually absent in the spleen by day 18; however, approximately 1 in 500 splenocytes harbor MHV68 genomes, and approximately 1 in 5,000 splenocytes are capable of reactivation upon tissue culture explant (184). Based on the aforementioned definition of latency, day 18 is therefore often used to characterize aspects of what is considered “early” latent infection. By six weeks post-infection, genome-positive cells are still detected at an approximate frequency of 1 in 3,000-5,000 splenocytes, while *ex vivo* reactivation has dropped below the level of

detection in the standard tissue culture explant assay (184). However, it has been demonstrated that many of these cells are still capable of reactivation upon the administration of exogenous stimuli such as TLR ligation or B cell receptor and CD40 cross linking (48, 112). Lytic virus is rarely detected in normal BL/6 mice infected with wild-type MHV68 at day 42; however, similar to earlier time points, host failure to control viral latency in some transgenic mouse strains may result in virus recrudescence. In this case, infected cells traffic back to the initial site of infection and re-initiate lytic replication, enabling the detection of preformed lytic virus in the lung homogenates of infected mice (83, 98). Herpesviral infections typically persist for the lifetime of the host--the typical frequency of cells harboring viral genome is about 1 in 20,000 and 1 in 30,000 at three and six months post-infection, respectively (184). Although the frequency of genome-positivity decreases with time, MHV68 genome-positive cells are still detectable more than one year following initial infection and are thought to be maintained throughout the entire lifespan of the mouse (184). It is hypothesized that low-level reactivation in vivo produces infectious virus which infects new naïve B cells and effectively “re-seeds” the latency reservoir (Fig.1b). The mechanism of in vivo reactivation is not definitively known, but most likely requires a combination of extracellular signals and virus-mediated programming of latently infected cells, such that these cells are poised to reactivate in the optimal setting to faithfully maintain latent viral infection.

1.I.iv *MHV68 and human gammaherpesviruses: similarities and differences*

Epstein-Barr virus was identified and named by its discoverers in the 1960s, studies prompted by the physician Denis Burkitt who suggested that the unusual tumor endemic to

sub-Saharan African children (subsequently named Burkitt's lymphoma) may involve an infectious component. Since its initial characterization, EBV has been implicated in a wide variety of lymphomas, including Hodgkin's lymphoma, post-transplant lymphoproliferative disease (PTLD), and several AIDS-related malignancies. It has also been associated with non-lymphoid tumors, such as nasopharyngeal carcinoma and some gastric cancers. One of most striking aspects of EBV infection, however, is its prevalence—as many as 95% of Americans are thought to harbor latent EBV infection, with seropositivity at more than 80% worldwide. Perhaps surprisingly then, EBV-related pathology is relatively rare, especially given the ubiquity of EBV infection. The majority of primary EBV infection is thought to occur during early childhood and is not accompanied by noticeable symptoms. Following infection, the individual generates EBV-specific antibodies; EBV seropositivity endures for the lifetime of the infected person and is used as a clinical marker for exposure to and infection with EBV. If an individual is not infected during early childhood, they will most likely be exposed to the virus sometime during adolescence. The majority of people are EBV-positive by this stage of life, and studies have shown that healthy individuals actively shed virus from the oral epithelia (50, 68); EBV is therefore often referred to as the “kissing disease,” as oral transmission is thought to be the primary means of infection in young adults. Primary EBV infection at this age is not asymptomatic as in early childhood, but instead results in a condition known as infectious mononucleosis, named for the high viral loads and massive expansion of lymphocytes seen in the blood during this period (85). Symptoms are typically resolved within a few weeks of presentation, after which the individual, now seropositive, retains latently-infected EBV positive cells throughout the remainder of his or her life. Healthy individuals are able to control EBV infection without incidence of

pathology; however, immunocompromised individuals, such as post-transplant or AIDS-patients, are at risk of disease (16). This susceptibility to disease may arise from either a failure to control viral replication or dysfunctional tumor immunosurveillance, as well as other unknown factors.

Less is known about the etiology of latent Kaposi's sarcoma-associated herpesvirus (KSHV), which was first identified and isolated in the 1990s from biopsies of the rare, highly vascular tumor for which it is named (20). KSHV is like EBV in that it induces tumorigenesis in immunocompromised patients, such that Kaposi's sarcoma is sometimes referred to as the "AIDS rash (16)."

MHV68 shares several of these key pathogenic features with its human subfamily members. A hallmark of early latent MHV68 infection is marked splenomegaly, a presenting symptom in many infectious mononucleosis cases thought to be an inflammatory response to high levels of virus replication in the spleen. Like EBV, MHV68 induces a mononucleosis-like syndrome characterized by a massive expansion of lymphocytes cells during primary infection in laboratory mice (146). In addition, EBV infection has been shown to induce a dramatic expansion of activated monoclonal or oligoclonal cytotoxic CD8⁺ T cells with highly similar TCRs (15, 156). MHV68 also induces a clonal CD8⁺ T cell expansion, such that by four weeks post-infection, nearly half of all CD8⁺ T cells have TCRs of the V β 4 subtype, as opposed to only 4% in naïve mice (169). Like EBV and KSHV, MHV68 latent infection is primarily maintained in lymphocytes, while epithelial or endothelial cells support lytic replication and productive infection. Perhaps one of the most important similarities between EBV and MHV68 is the preferential maintenance of latent infection in the memory B cell population (180, 184). This is particularly significant to the duration of

gammaherpesvirus infection because memory B cells arise during the primary response to a pathogen and are maintained in the circulation indefinitely until subsequent exposure induces re-activation and effector function. In humans, resting, circulating, IgD-, CD27+ class-switched memory B cells are the primary reservoir for latent infection. Studies have confirmed that the majority of latent MHV68 is also maintained in the IgD- memory B cell population (184) at late times post-infection.

Regarding the role of MHV68 in tumorigenesis, the murine virus is similar to EBV and KSHV in that once lytic infection is controlled and latency is established in a wild-type mouse, the host is able to efficiently control viral replication and can live disease-free. However, as is the case in immunocompromised humans, transgenic mice with deletions in key immunoregulatory or tumor suppressor genes are more prone to MHV68-induced tumorigenesis. For example, BALB/c and BALB β 2-microglobulin-deficient mice are reported to develop lymphoproliferative disease and lymphomas as a result of MHV68 infection (160, 167).

The transforming potential of EBV has been well-documented and adapted as a powerful tool in generating lymphocyte cell lines, as infection with EBV results in the immortalization of human B cells. The genes conferring this ability have been extensively studied, and several functional homologues identified in KSHV. Although all direct homologues have not yet been identified in MHV68 (e.g. LMP1 or LMP2A), new evidence suggests that MHV68 may also possess lymphocyte transforming potential, and will perhaps provide insight into the initial events of gammaherpesvirus-induced tumorigenesis in vivo (X.Liang, personal communication).

Despite the lack of sequence homology for certain key EBV genes, considerable sequence and functional homology exists between members of the gammaherpesvirus family. The MHV68 genome was fully sequenced and analyzed in 1997, and revealed a high degree of sequence conservation between EBV, KSHV, HVS, and MHV68 (172). Many MHV68 structural proteins, such as glycoprotein B (gB) and the major capsid protein, share considerable homology with the primate viruses. Many genes encoding viral enzymes, such as the viral DNA polymerase, ribonucleotide reductase, and thymidine kinase, also share significant coding information. Although individual ORF sequence homology is variable, the overall organization of the gammaherpesvirus genomes is very highly conserved (Table 2 and Fig.2A). The EBV, KSHV, HVS, and MHV68 genomes are all between 150 and 180 Kb in size, and are compartmentalized into distinct regions containing lytic or latent genes. Each genome is flanked by highly repetitive, GC-rich sequence referred to as terminal repeats. Each virus also encodes several tRNAs of ambiguous function near the right end of the genome. The genes sharing little sequence homology with the other gammaherpesvirus family members are referred to as “unique” genes, and are clustered at either the far right or far left of the genome. Genes required for establishment or maintenance of viral latency are clustered into three distinct regions in the left, middle, and right portions of the genome. These latency-associated regions are separated by blocks containing key lytic genes, encoding structural, tegument, and envelope proteins, as well as vital processivity and transcription factors (173). Considerable effort has gone into determining the relative importance of the 60+ MHV68 predicted open reading frames; the combined analysis of transposon-insertion libraries and recombinant viral mutants has provided definitive information as to the role of several genes during viral latency or lytic replication (107, 148).

Deletion or disruption of many conserved genes results in varying degrees of compromised viral pathogenesis, either during the establishment or reactivation from latency, or during initial viral replication (Fig.2B).

2.II. The gammaherpesvirus Rta protein

2.II.i *Gene structure and function in lytic replication*

Perhaps one of the most deleterious mutations involves mutation or deletion of ORF50, encoding the KSHV/HVS (Rta) or EBV (BRLF1 or R protein) homologue. Rta, or Replication and Transcriptional Activator, is a protein of highly conserved function among all gammaherpesviruses and is critical for lytic replication during both primary infection and reactivation from latency. Rta is a potent activator of lytic viral gene transcription, such that ectopic expression of Rta in KSHV, MHV68, and some EBV latent cell lines is sufficient to induce lytic reactivation (5, 133, 137). Synthesis of MHV68 and KSHV Rta transcripts is insensitive to treatment with cyclohexamide, and Rta is therefore classified as an immediate-early gene (92, 159). In addition to Rta's sufficiency in inducing latent KSHV and MHV68 reactivation, it is also required for lytic replication, as Rta-null mutants fail to replicate both in vitro and in vivo (128, 188, 190). Therefore, transcription and translation of the Rta gene are key initial events following entry of viral DNA into the host cell during primary infection. In addition to autoactivation, Rta has been shown to potently upregulate transcription of other IE and E genes during lytic replication, including Orf57, which encodes a homologue of HSV ICP27 involved in mRNA nuclear export, and Orf59, a processivity factor involved in viral DNA replication (23, 80, 91, 94, 127, 177).

The organization of the Rta-coding region is extremely well-conserved among gammaherpesviruses. Previous studies have demonstrated that Rta is encoded by multiple exons; a short Exon1 (E1) splices to a long Exon2 (E2) to give rise to the full-length Rta transcript (Fig.3). In the case of the rhadinoviruses, the initiating ATG is actually located in Exon1, such that splicing of Exons 1 and 2 significantly extends the Rta open reading frame. Alternatively, the initiating ATG for EBV lies at the beginning of Exon2, and therefore Exon 2 encodes the entire full-length Rta protein. However, Exon1 is still retained and transcribed. A promoter upstream of Exon1 (Rp) drives transcription of the E1-E2 transcript, and has been considered the sole promoter driving Rta transcription. The spacing of Exons1 and 2 is similar among the four gammaherpesviruses, as is their placement relative to Orfs48 and 49, two genes encoded on the opposite strand in reverse orientation of Rta. Transcription in this area is highly compact, with a high degree of overlap between genes encoded on opposite strands. The role of transcriptional interference in control of EBV latent gene expression has been demonstrated, and it is likely that transcription in the direction opposite Rta also affects lytic gene transcription (131, 132, 187). The first half of this work addresses the identification of a third, conserved, upstream exon (termed E0) and an additional promoter driving expression of this multi-exon Rta transcript.

The Rta protein contains three functional domains: the N-terminus contains the DNA binding (encoded in part by Exon 1) and dimerization domain, the middle contains a proline-rich region, and the C-terminus contains an acidic activation domain which is essential for Rta-mediated transactivation. The protein also contains nuclear localization signals (NLS) that allow for its transport into the nucleus following cytoplasmic synthesis. The predicted size of MHV68 Rta is around 64 KDa, but runs at an apparent size of 90 KDa during SDS-

PAGE, a phenomenon also seen with KSHV and RRV Rta (96, 188). Analysis of the Rta amino acid sequence reveals many possible target residues for posttranslational modifications, and most likely explains this observation (96).

A key difference between EBV and rhadinovirus lytic replication is the EBV Z protein, or Zta, encoded by the BZLF1 gene. Although EBV also encodes an Rta homologue, Zta is the primary lytic switch protein, with the R protein playing a more secondary, yet still critically important role. In the case of EBV, Zta initiates the lytic cycle by binding to and activating the Rp promoter, which in turn leads to the activation of other lytic gene promoters. However, expression of EBV R protein is sufficient to induce reactivation and lytic replication in some EBV latent cell lines (54, 133, 197), and therefore still serves an important role in EBV lytic growth.

The cessation of lytic replication and establishment of latency defines a successful herpesvirus infection. Since Rta is sufficient to drive lytic replication, control of Rta expression is vital for true latency to be achieved. For this reason, the regulation of Rta expression has been studied in detail. Many factors contribute to the control of Rta transcription; epigenetic modifications, mRNA splicing, host transcription factors, and viral proteins, including Rta itself, have all been shown to regulate Rta expression, some of which will be discussed below.

2.II.ii Regulation of the Rta promoter

Given the high degree of organizational homology among the gammaherpesvirus Rta loci, as well as the overall similarities in viral pathogenesis described above, it is not surprising that these viruses also share in common many of the same mechanisms to regulate Rta transcription. For example, it has been demonstrated that KSHV and EBV Rta promoters are activated by AP-1, Sp1 and CBP/p300 binding (43, 55, 134, 162, 176, 193); although this interaction has not been directly shown for MHV68, there are AP-1, Sp1 and CBP/p300 consensus binding sites in the MHV68 Rta promoter (92). The plasma cell-specific transcription factor XBP-1 has also been shown to upregulate KSHV and EBV Rta expression (7, 30, 185, 195), and preliminary studies from our lab indicate that MHV68 lytic replication may also be upregulated by XBP-1 (X. Liang, unpublished). In addition, it has been demonstrated that cellular stressors can induce reactivation from latency. Conditions of low oxygen, for example, lead to the stabilization of hypoxia inducible factor α (HIF); studies have shown that both EBV and KSHV contain HIF-responsive elements in their lytic gene promoters, and this has recently been confirmed for MHV68 as well (13, 31, 58, 72, 129). The commonalities in lytic promoter regulation among the gammaherpesviruses is testament to the B cell-tropic physiological features shared by these viruses. Many of these transcription factors are effector molecules in pathways initiated by B-cell specific stimuli, such as B cell receptor cross-linking (Sp1), plasma cell differentiation (XBP-1), and inflammatory microenvironments (HIF). Pharmacological inducers of these stimuli, such as TPA treatment in the case of BCR cross-linking, induce reactivation of latent EBV, KSHV, and MHV68 latent cell lines (39, 44, 196, 200), and provide important clues as to the physiological cues leading to the induction of lytic replication *in vivo*.

Another key component in the control of gammaherpesvirus lytic transcription is epigenetic regulation. Both DNA methylation and histone modification play important regulatory roles in the establishment of and reactivation from latency, and will be discussed below. The observation that treatment with epigenetic modifying agents such as sodium butyrate (NaB), 5-azacytidine (AZA), and trichostatin A (TSA) induces lytic replication in EBV and KSHV latent cell lines prompted the investigation of DNA methylation status and chromatin accessibility of the Rta promoters (6, 22, 73, 95). These studies have delineated a clear role for DNA methylation in gammaherpesvirus pathogenesis, and provide the basis for the second half of this work.

1.III. Epigenetic regulation via DNA methylation

1.III.i *General background*

Epigenetics is primarily defined as heritable changes in gene expression that cannot be explained by alterations in genetic coding sequence. The last twenty years have seen an explosion of progress in the field studying how these changes lead to alterations in gene transcription, particularly in the context of embryonic development and tumorigenesis. Studies have expanded on the epigenetic premise that DNA architecture is a primary determinant of cell phenotype, demonstrating that nuclear organization of DNA on a genome-wide scale, as well as modifications at individual gene promoters, govern every aspect of cell fate and function. In terms of transcriptional regulation at the level of individual genes, the two primary epigenetic modifications are modification of histone tails, leading to changes in chromatin accessibility, and DNA methylation, which is primarily associated with transcriptional repression. Studies indicate that significant overlap exists

between these two branches of epigenetic regulation, such that DNA methylation facilitates the development of repressive heterochromatin, which in turn can promote further DNA methylation, allowing the cell to “re-emphasize” transcriptional silencing at a given locus (Fig.4a). A picture is emerging in which alterations in chromatin structure are the work of large, multi-subunit complexes with degrees of cell specificity, and much work is being done to characterize the interplay between these various epigenetic factors.

In mammalian cells, extensive lengths of DNA must be efficiently packaged to fit inside the cell. Each strand is organized into a nucleosome, a large multimeric subunit consisting of eight histone proteins comprising a histone octamer. Each histone octamer consists of two subunits each of four different histone proteins: H2A, H2B, H3 and H4. Other histone variants exist and are involved in the DNA damage response, inheritance, and DNA replication (61). The four primary histones, however, have been extensively studied for their role in shaping chromatin architecture. DNA double helices are wrapped around individual histones, which are part of the histone octamer, which comprise the nucleosome. DNA is wrapped around the histone octamer about 1.67 times, such that 146-147 bps of DNA is packaged into a nucleosome. Each nucleosome is then further packaged into strings of nucleosomes, connected by linker DNA, which are then supercoiled into compact chromatin fibers. These fibers are loaded onto scaffolding proteins and organized into the signature chromosome structure seen by standard karyotypic staining. Each histone has a long N-terminal tail extending out from the histone octamer. Modification of the protruding histone tails induces dramatic alterations in how DNA is looped and organized around each histone, and is a subject of intense study. Acetylation, methylation, sumoylation, phosphorylation, and ubiquitination are just some of the histone tail modifications that have been shown to

induce either the relaxing of chromatin structure to give rise to transcriptionally active euchromatin, or to lead to chromatin compaction and the formation of transcriptionally repressive heterochromatin. For example, methylation of H3 at a lysine residue at position 4 (H3K4) is associated with active transcription, while tri-methylation of a lysine at position 9 (H3K9) is associated with transcriptional repression.

Not only are the modifications and the target residues numerous, but now it is becoming clear that cross-talk exists between modifications on the same or even different histones, such that methylation of one residue is strongly correlated with phosphorylation of another residue (157). Histone modifications not only mark “on” and “off” genes, but also indicate recently transcribed regions, and are thought to serve as a code to be read and interpreted by transcriptional machinery (109). The “histone code” is complex and fascinating, and the subject of major investigation in the chromatin field.

The second major epigenetic modification is DNA methylation, which in mammals primarily involves the addition of methyl groups to the carbon in the 5th position of the nucleic acid base cytosine. Methylated cytosines are almost always immediately succeeded by a guanine base, and therefore mammalian DNA methylation is often referred to as “CpG” methylation (the “p” referring to the phosphate group linking the two bases). DNA methylation is most often studied in regions of high CpG density (called CpG islands (CGIs)), centromeric regions, and satellite repeats near chromosomal termini, but also has consequences in promoter regions, which do not necessarily contain CGIs or repeat regions. Methylation of promoters is most often associated with transcriptional silencing and reduced expression of the associated gene. The mechanism by which this repression occurs is not completely clear, but can involve 1) direct interference of transcription factor binding by

methylation of its cognate sequence, or 2) the recruitment of chromatin remodeling machinery to the methylated promoter via methyl binding domain-containing proteins (MBDs).

1.III.ii *DNA methylation in health and disease*

DNA methylation has been extensively studied in the context of disease; aberrant DNA methylation of tumor-suppressor genes and oncogenes has been demonstrated for nearly all tumor types, and has also been shown to play a role in certain neurological disorders, developmental disorders (Fragile X syndrome), and immunological disorders, such as systemic lupus erythematosus (SLE) and immunodeficiency, chromosomal instability, and facial anomalies (ICF) syndrome (3, 139). However, DNA methylation also plays a key role in many normal cellular processes. DNA methylation first becomes relevant during embryonic development-- when two germ cells fuse to generate an embryo, the cell from each parent carries alleles with a specific genetic “imprint” established by distinct DNA methylation patterns (136). For generation of normal, genetically diverse offspring, it is necessary to remove the parental methylation marks. This is accomplished through a wave of genome-wide demethylation, during which the methylation profile of the developing embryo is essentially “reset” or wiped clean.

In order for differentiation to proceed, a new pattern must be established (74, 106). This is accomplished through the action of DNA methyltransferases, or DNMTs (59, 75, 76). In mammals, there are five known DNMTs: DNMT1, DNMT2, DNMT3A, DNMT3B, and DNMT3L (24, 25, 51) (Fig.4b). To date, only DNMT1, DNMT3A, and DNMT3B have been shown to possess methyltransferase activity. The function of DNMT2 is involved in tRNA

methylation, while DNMT3L has been demonstrated to function as a chaperone protein involved in guiding catalytically active DNMTs to their target bases (21, 52, 71). The catalytically active DNMTs contain a domain that allows for the transfer of methyl groups from a donor molecule, S-adenosylmethionine (SAM), to the recipient cytosine. The action of these DNMTs is essential during development, as null mutations are either embryonic lethal (DNMT1, DNMT3B) or result in inviability past three weeks post-gestation (DNMT3A) (66, 122).

1.III.iii. Role of DNA methylation in lymphocytes

Another developmental pathway heavily regulated by DNA methylation is the generation of functional lymphocyte receptors during hematopoiesis. In order to achieve a wide breadth of immunological diversity, B cells and T cells must rearrange a specific set of genes encoding their BCRs and TCRs, respectively. This process involves the rearrangement and rejoining of multiple gene segments of V, D, or J type, referred to as V(D)J recombination, and gives rise to receptors of vast combinatorial diversity. In B cells, specific immunoglobulin generated in part by this process, are secreted to perform various effector functions upon activation of the B cell following recognition of its cognate antigen. Immunoglobulin receptors are comprised of a heavy chain and light chain, the latter of which can be generated from one of two loci, the lambda or kappa genes. Studies have demonstrated that in B cells, DNA methylation regulates not only V(D)J rearrangement, but also allelic exclusion and kappa-chain usage (65, 66, 114, 115). DNA methylation also plays another key role in lymphocytes in the regulation of several genes involved in various effector functions (113). It has also been shown that in T cells, methylation regulates the

expression of IFN-gamma in effector CD8⁺ T cells, as well as other cells of T-cell lineage (81, 102).

1.IV. Intersection of DNA methylation and gammaherpesviruses

1.IV.i *Role of DNA methylation in gammaherpesvirus pathogenesis*

The intimate relationship between gammaherpesviruses and B cells has long been recognized. Many key gammaherpesvirus genes are those which in effect mimic aspects of normal B cell physiology. EBV encodes LMP1 and LMP2A, proteins that mimic CD40 and BCR signaling, respectively. EBV, KSHV, and MHV68 encode genes that manipulate IL-6 and IL-10-responsive pathways, two cytokines with defined roles in B cell proliferation and survival. As previously mentioned, gammaherpesviruses reactivate in response to cues that induce specific B cell signaling pathways, demonstrating that gammaherpesvirus biology is inextricably linked to B cell-intrinsic mechanisms. It is therefore not surprising that gammaherpesviruses have evolved to also use many of the same transcriptional regulatory mechanisms well-established in B cells. Given the importance of DNA methylation in numerous normal lymphocyte functions, and that gammaherpesviruses contain dsDNA like their hosts, the discovery of DNA methylation as a mechanism orchestrating gammaherpesvirus gene transcription is not unexpected, yet is remarkable in design.

1.IV.ii *Regulation of EBV latency programs*

Until recently, the most well-known story for DNA methylation in gammaherpesviruses was that of the EBV latency programs. During EBV-mediated transformation of primary human B cells, the virus expresses a distinct set of genes required

for successful transformation, including LMP1, LMP2A, and LMP2B, as well as several EBNA genes (EBNAs 1,2,3a,3b,3c, and 4), EBERs, and BARTs. Seminal studies in the 1980s revealed that these genes are encoded by a single, highly-spliced transcript generated from one of two promoters located near the terminal repeats of the EBV genome (150). Analysis of transcription profiles in latent cell lines generated from BL, NPC, and other EBV tumor lines revealed that EBV latency is compartmentalized into distinct latency “programs,” characterized by the extent of latency gene transcription. A pattern emerged demonstrating that lymphoblastoid cell lines (LCLs), generated from infection of primary B cells, produced the long, highly-spliced transcript giving rise to the full profile of latency genes. Analysis of NPC cell lines (as well as some BL lines), revealed that these cells express a more restricted expression pattern, with the spliced transcript only containing exons encoding the LMP genes, EBNA1, and the EBERs. The most conservative transcription program was detected in BL lines, in which the transcript contained coding material only for EBNA1 and the EBERs. EBNA1 has been shown to be essential for maintaining the viral genome in latently infected cells, and homologues exist in both KSHV (kLANA, for Latency Associated Nuclear Antigen) and MHV68 (mLANA). The viral genome is maintained as a circular episome in latently infected cells, and EBNA1 is the protein that tethers the episome to host chromosomes to ensure its faithful replication within the host cell. The EBERs are small RNAs of ambiguous function, but are abundantly transcribed in latent cells and *in situ* hybridization used as a diagnostic tool for latent infection (27). This highly restricted expression profile has been termed Type I latency; the program in which EBNA1 and the LMPs are transcribed is known as Type II latency, and the most transcriptionally active form is known as Type III, or “growth-transforming” latency (Fig.5).

The extent of latent viral gene transcription is important during EBV infection because several latency genes contain epitopes recognizable by CD8⁺ cytotoxic T lymphocytes (CTLs) (14). It is thought that restricted gene expression minimizes the host immune response to EBV infection and favors the maintenance of viral latency. EBNA1, the only gene transcribed during restricted type 1 latency, contains several glycine-alanine repeats, which render it unable to be processed by the host proteasome (88, 89). EBNA1 thereby avoids antigen presentation, a strategy most likely acquired during EBV's co-evolution with the host immune system to allow sustained expression of the episomal tethering protein in latently infected cells. Following the identification of the highly spliced latency transcripts, it was soon discovered that their transcription was regulated by differential promoter usage (186). During type III latency, expression of the latency transcript is driven by a promoter termed W_p, immediately upstream of an internal repeat region encoding multiple W and Y exons. (Fig.5). Alternative splicing of these exons contributes to the generation of full-length latency transcripts (140). Later in infection, transcription is driven from an alternative, upstream promoter, termed C_p, and generates messages containing the W and Y exons as well as C exons. The promoter switch occurs via repression of W_p and activation of C_p by protein translated from the W_p-generated transcripts. Most transcripts in established LCL and NPC cell lines use C_p to drive expression of latency genes. Another promoter, termed Q_p, exists downstream of C_p and the W_p exons. This promoter is responsible for the generation of type I latency transcripts, and is the primary promoter active in BL cell lines (194).

1.IV.iii Regulation of EBV latency by DNA methylation

The generation of distinct latency transcripts by differential promoter usage is an exquisite example of complex gammaherpesvirus gene regulation. In addition to the numerous cis-elements involved in Wp/Cp/Qp transcription, subsequent analyses revealed that DNA methylation plays a key role in regulating promoter activity. Studies have demonstrated that in the peripheral blood of healthy, seropositive donors, latent EBV genomes contain high and intermediate levels of methylation at Wp and Cp, respectively, yet Qp is consistently hypomethylated (126). Transcriptional profiles from these cells reveal that the restricted type I latency program is operational. Therefore, it is hypothesized that DNA methylation of Wp and Cp is a mechanism to repress these promoters in normal cells, while Qp is protected from this repression and is the primary promoter driving latent gene expression. The kinetics with which this pattern is established was demonstrated by studies tracking DNA methylation at Wp, Cp, and Qp during the generation of LCLs (168). During the first few days following EBV infection, Wp is the primary promoter driving expression of latency transcripts and is devoid of methylation. By day 6 post-infection however, Wp-driven transcription begins to wane as Cp-driven transcription increases; this is accompanied by the accumulation of methylated CpGs within the Wp promoter region. By day 28 post-infection, transcription from Wp has largely ceased, and Cp is the functionally active promoter. At this point, Wp is hypermethylated, while Cp remains hypomethylated. These observations have been extended to latent EBV+ cell lines-- in LCL JYs, which express the broad repertoire of latency genes, Wp is hypomethylated and Cp remains hypomethylated (38) . In Raels however, a BL cell line with a restricted type I profile, both Wp and Cp are methylated, while Qp is hypomethylated (166). Therefore, the extent of DNA methylation

directly correlates with latent gene expression in latently-infected cells. Although higher order chromatin structure has been shown to also be involved in regulation of KSHV and EBV latency (41, 49, 77, 124, 152), these studies collectively demonstrate the integral role of de novo DNA methylation in the establishment of latent EBV infection and have made important contributions to the overall understanding of EBV gene transcription.

1.IV.iv *Regulation of gammaherpesvirus lytic replication by DNA methylation*

Although not as extensive as that for EBV latency programs, growing evidence exists to support a role for DNA methylation in regulating EBV lytic gene expression. As previously discussed, EBV encodes the Rta protein which facilitates the transcription of several other key lytic genes. But unlike KSHV and MHV68, in which Rta is considered the main lytic transactivator, the EBV gene BZLF1 encodes Zta, an additional transcription factor considered to be the primary lytic switch protein. As mentioned above, the EBV genome becomes extensively methylated during latent infection, yet retains the ability to reactivate from latency. Given that methylation has been shown to interfere with transcription factor binding, how EBV was able to extricate itself from a methylated state to initiated lytic replication was a mystery. Recent studies have provided a very plausible solution to this problem, demonstrating that Zta preferentially binds to methylated promoters over unmethylated promoters (8, 9, 34, 198). The Rp promoter, which drives Rta transcription, is methylated in latent cells and is a primary target of Zta transactivation (9, 134). It was shown that Zta binds to Rp more efficiently when Rp is methylated, a phenomenon not seen with any previously studied transcription factor, host or viral. These observations have been extended to show that Zta binds to other methylated viral promoters

as well (34), and it is therefore becoming evident that this unique capability is a remarkable evolutionary strategy by which EBV can exploit host-mediated DNA methylation to both establish and maintain lifelong latent infection.

That DNA methylation is involved in silencing lytic replication in latent cell lines has been demonstrated for both KSHV and EBV by treatment of latent cell lines with AZA (6, 22). In latent KSHV+ PEL cell lines, treatment with AZA induces the expression of KSHV lytic proteins (22). Bisulfite PCR analyses demonstrated that the Rta promoter is methylated in these cells and that AZA treatment results in demethylation of the promoter and re-expression of Rta. EBV+ cell lines respond with varying sensitivity to methyltransferase inhibitors; treatment of Akata and Rael BL cell lines, as well as EBV+ tumors, induces lytic replication and re-expression of lytic proteins, while other cells remain refractory to DNA demethylation alone (6, 18, 100). However, treatment with both histone deacetylase inhibitors (HDACs) and AZA provides a more potent chromatin-remodeling effect, and may induce lytic reactivation in AZA-refractory cell lines.

Studies such as those above provide strong evidence that human gammaherpesviruses are targeted for de novo DNA methylation during the establishment of latency in vivo. Reactivation from latency is associated with reduced methylation, which may occur through an active mechanism, such as enzymatic demethylation by an elusive host “demethylase”, or passively, by the replication of viral DNA at a rate beyond the capacity of Dnmt1 maintenance activity. However, because these pathogens are restricted to human infection, it has not been possible to study the dynamics of viral DNA methylation in vivo during the initial establishment of latency, nor has it been possible to study the specific role for various components of DNA methylation machinery in the context of infection. MVH68 provides a

model system by which to study early latency events, as well as to explore the consequences of deleting specific DNA methyltransferases at this critical junction in gammaherpesvirus infection.

1.IV.v *The role of de novo DNA methylation in Rta promoter regulation*

This work examines the role of de novo DNA methylation in the establishment of MHV68 latency, specifically focusing on its role in regulating MHV68 Rta transcription. In Chapter 2, we describe the identification of an additional layer of complexity in gammaherpesvirus G50 transcription, providing evidence for the existence of a third Rta coding exon conserved among the mouse and human gammaherpesviruses. A second Rta promoter lies upstream of this exon in MHV68, and appears to be differentially regulated in distinct latently infected cell populations. This promoter also becomes progressively methylated throughout MHV68 latency and is extensively methylated in latent cell lines. We then demonstrate that the de novo methyltransferases DNMT3A and DNMT3B play a role in methylating this alternative Rta promoter, and that this methylation is essential for repressing Rta transcription and lytic replication during early splenic latency. Finally, we provide evidence that DNA methylation is crucial for silencing Rta expression in particular, as even in the absence of DNMT3A and DNMT3B, an alternative mechanism exists to specifically methylate the Rta promoter while other viral promoters remain hypomethylated. Taken together, this work provides further insight into the complex regulation of a key gammaherpesvirus protein, and introduces a new set of questions to be answered regarding the function of this newly identified viral transcriptional element and its interface with host epigenetic machinery.

1.V. FIGURES AND TABLES

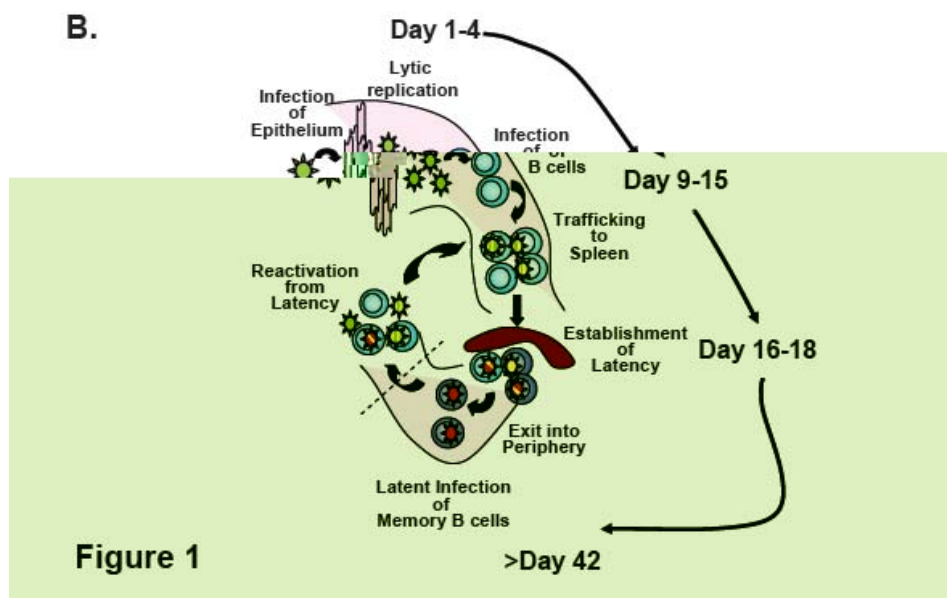
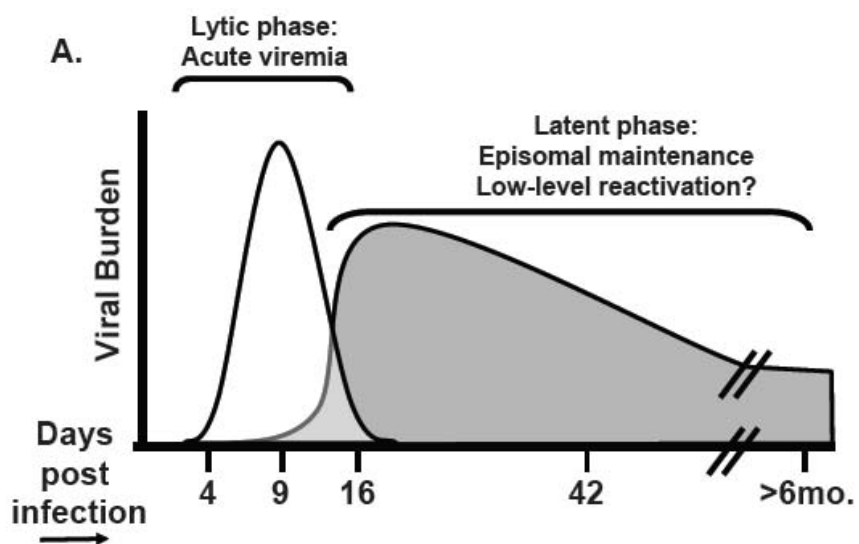
Chapter 1:

Figures:

1. A. Kinetics of MHV68 lytic and latent infection
B. Model of MHV68 infection
2. A. Colinearity of gammaherpesvirus genomes
B. Annotation of transposon mutagenesis studies
3. Structure of gammaherpesvirus Rta-encoding transcripts
4. A. Model depicting DNA methylation in heterochromatin formation
B. Key domains of mammalian DNA methyltransferases
5. EBV latent gene transcription programs

Tables:

1. Frequency of MHV68 genome-positive cells
2. MHV68 genes and putative human gammaherpesvirus homologues



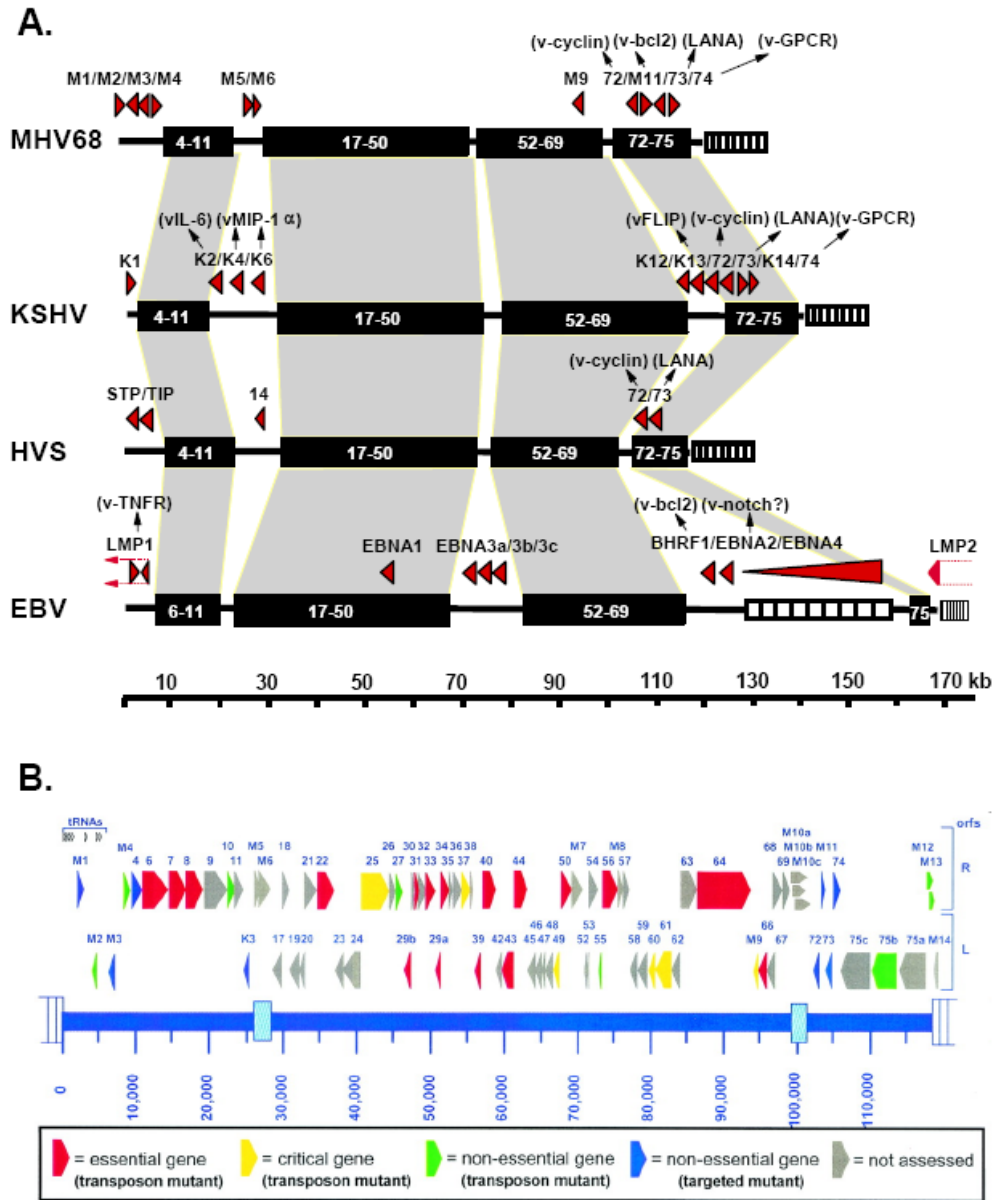


Figure 2

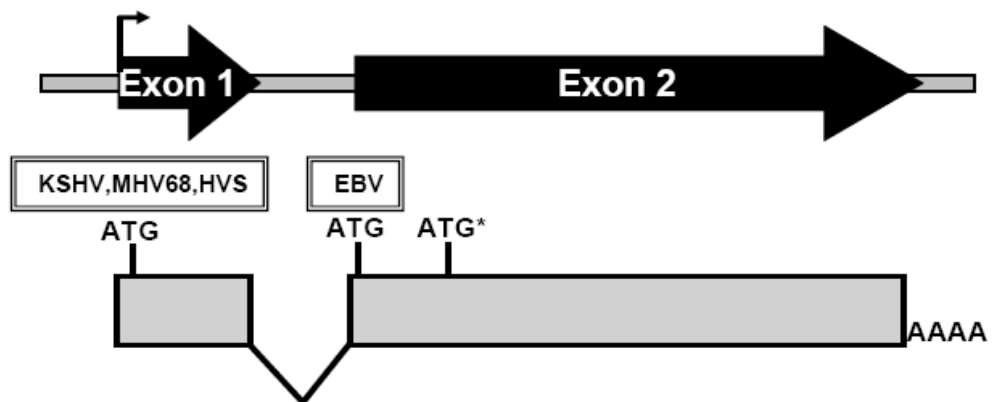


Figure 3

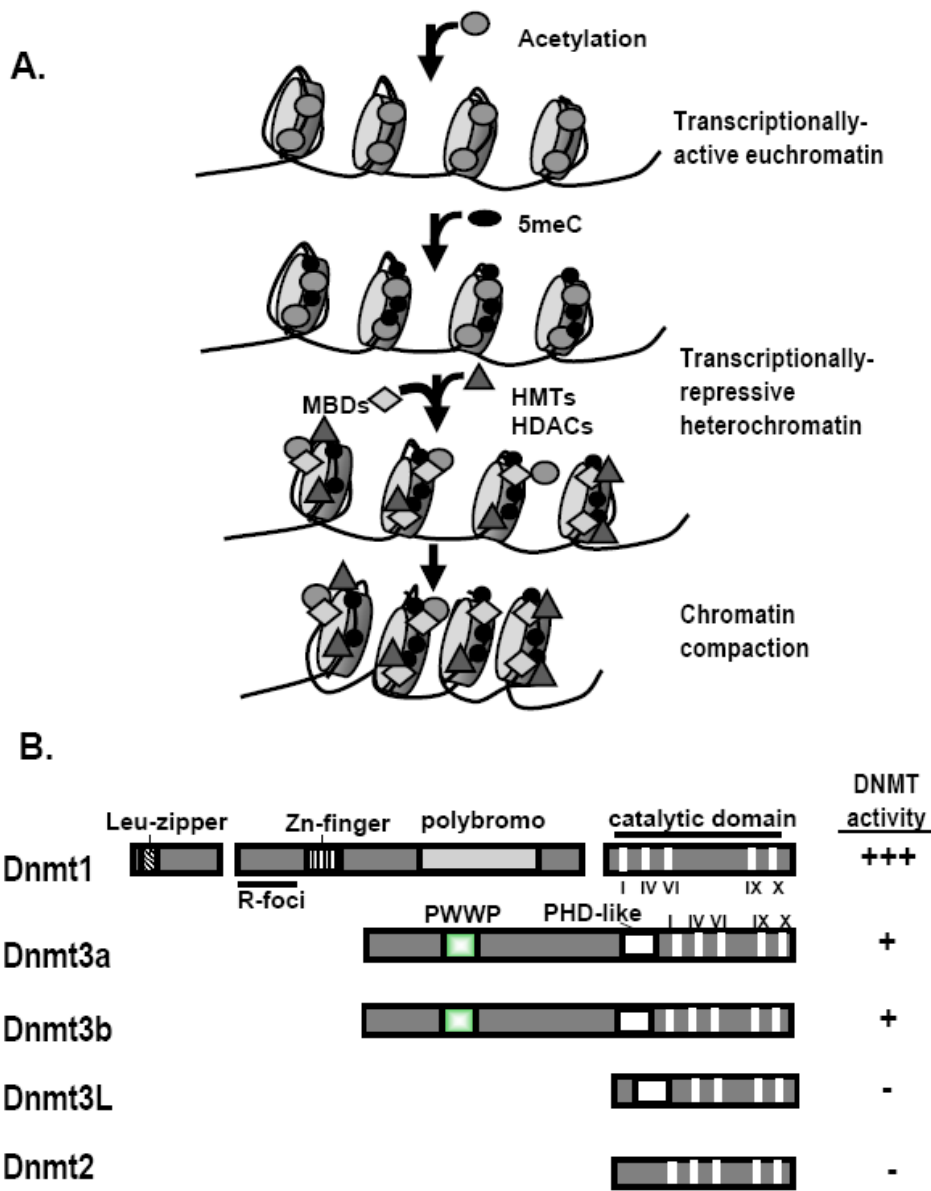


Figure 4

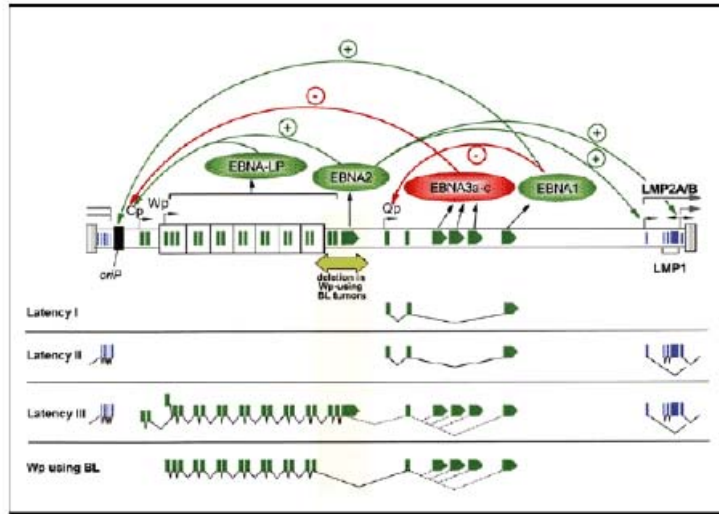


Figure 5

Cell fraction	Frequency of viral-genome-positive cells			
	dpi	Frequency ^a	Total no. of cells ^b	No. of latently infected cells ^c
Unsorted	16	1/200	8.1×10^7	405,000
	42	1/3,500	5.9×10^7	16,857
	182	1/18,500	3.8×10^7	2,054
CD19 ⁺	16	1/200	5.2×10^7	259,000
	42	1/4500	3.8×10^7	8,400
	182	1/28,000	2.4×10^7	868
CD19 ⁻	16	1/9000	2.9×10^7	3,244
	42	ND	2.1×10^7	NA
	182	ND	1.4×10^7	NA
CD19 ⁺ IgD ⁺	16	1/230	4.6×10^7	200,000
	42	1/12250	3.3×10^7	2,710
	182	ND	2.1×10^7	NA
CD19 ⁺ IgD ⁻	16	1/50	6.2×10^6	124,740
	42	1/700	4.5×10^6	6,586
	182	1/2000	2.9×10^6	1,465
Isotype-switched CD19 ⁺ IgD ^{-d}	84	1/1500	2.5×10^6	1692

^a Frequencies of viral-genome-positive cells represent the mean of at least three independent experiments with splenocytes pooled from 10 mice per experimental group. ND, not determined because values were below the limit of detection of the assay.

^b Cell numbers were derived from the calculated total number of spleen cells at days 16, 42, 84, and 182 postinfection (8.1×10^7 , 5.9×10^7 , 5.4×10^7 , and 3.8×10^7 , respectively) and from the percentage of total spleen cells that each subset represents, as calculated from FACS gating (CD19⁺, 64%; CD19⁻; 36%; CD19⁺ IgD⁺, 56.3%; CD19⁺ IgD⁻, 7.7%, isotype-switched IgD⁻ B cells, 4.7%).

^c The total number of latently infected cells was determined by using the experimental frequency data and the estimated total cell numbers per subset. NA, not applicable due to the inability to accurately estimate the frequency of cells harboring viral genome.

^d Isotype-switched memory B cells were stained and sorted by using a cocktail of antibodies directed against IgG1, IgG2a/b, IgG3, IgA, and IgE.

Table 1

Name	Genome location (bp)	Coding strand	Size (amino acids)				EBV name	% Identity to γ HV68			Possible function ^a
			γ HV68	KSHV	HVS	EBV		KSHV	HVS	EBV	
M1	2023-3282	R	420								Serpin
M2	4031-4627	L	199								
M3	6060-7277	L	406								
M4	8409-9785	R	459								
ORF 4	9873-11036	R	388	550	360			27.8	24.5		Complement regulatory protein
ORF 6	11215-14523	R	1,103	1,133	1,128	1,128	BALF2	40.3	42.2	39.6	Single-stranded DNA binding protein
ORF 7	14526-16481	R	652	695	679	685	BALF3	34.0	34.0	33.3	Transport protein
ORF 8	16505-19051	R	849	845	808	857	BALF4	51.1	45.6	38.2	Glycoprotein B
ORF 9	19217-22297	R	1,027	1,012	1,009	1,015	BALF5	55.8	55.1	49.2	DNA polymerase
ORF 10	22269-23522	R	418	418	407	422	RajILF1	19.9	18.2	12.4	
ORF 11	23488-24651	R	388	407	405	429	RajILF2	18.6	19.8	20.4	
K3	24733-25335	L	201	333				23.4			BHV4 IE1 homolog
M5	26178-26672	R	165								
M6	26554-28308	R	585								
ORF 17	28326-29957	L	544	553	475	605	BVRF3	32.7	28.3	28.3	Capsid protein
ORF 18 ^b	29917-30768	R	284	257	256	247	BVLF1.5	37.7	37.3	29.6	
ORF 19	30726-32273	L	516	549	543	570	BVRF1	36.2	38.8	34.5	Tegument protein
ORF 20	32119-32880	L	254	320	303	248	BXRF1	28.7	27.6	34.6	
ORF 21	32879-34810	R	644	580	527	607	BXLF1	19.6	19.9	20.8	Thymidine kinase
ORF 22	34833-37022	R	730	730	717	706	BXLF2	26.7	26.2	19.6	Glycoprotein H
ORF 23	37025-38167	L	381	404	253	425	BTRF1	25.2	13.6	21.5	
ORF 24	38103-40253	L	717	752	731	618	BcRF1	38.9	40.7	25.5	
ORF 25	40263-44381	R	1,373	1,376	1,371	1,381	BcLF1	56.8	57.2	52.4	Major capsid protein
ORF 26	44423-45319	R	299	305	304	301	BDLF1	42.1	38.8	33.8	Capsid protein
ORF 27	45329-46090	R	254	290	280	420	BDLF2	14.6	17.7	16.5	
ORF 29b	46395-47438	L	348	351	380	387	BDRF1	49.7	49.4	48.0	Packaging protein
ORF 30	47507-47746	R	80	77	75			27.5	32.5		
ORF 31	47710-48309	R	200	224	208	225	BDLF4	31.0	35.5	26.5	
ORF 32	48294-49625	R	444	454	441	507	BGLF1	20.7	23.0	20.5	
ORF 33	49588-50568	R	327	312	330	336	BGLF2	29.7	32.9	31.5	
ORF 29a	50540-51466	L	306	312	303	325	BGRF1	39.8	41.4	36.5	Packaging protein
ORF 34	51465-52460	R	332	327	316	332	BGLF3	28.0	31.6	27.7	
ORF 35	52423-52878	R	152	150	150	153	BGLF3.5	28.3	22.4	26.3	
ORF 36	52847-54157	R	437	444	431	455	BGLF4	23.8	18.8	24.3	Kinase
ORF 37	54129-55586	R	486	486	483	470	BGLF5	43.8	45.3	37.4	Alkaline exonuclease
ORF 38	55544-55768	R	75	61	66	75	BBLF1	20.0	20.0	24.0	Myristylated tegument protein
ORF 39	55802-56950	L	383	399	366	405	BBRF3	46.5	44.1	39.4	Glycoprotein M
ORF 40	57046-58875	R	610	457	450	541	BBLF2	18.4	20.5	13.1	Helicase-primase
ORF 42	58876-59634	L	253	278	265	278	BBRF2	33.6	35.6	28.9	
ORF 43	59634-61334	L	567	605	563	613	BBRF1	47.1	49.4	43.6	Capsid protein
ORF 44	61303-63630	R	776	788	781	809	BBLF4	54.8	53.1	47.0	Helicase-primase
ORF 45	63655-64272	L	206	407	257	214	BKRF4	33.0	13.1	13.6	
ORF 46	64275-65021	L	249	255	252	255	BKRF3	54.6	53.4	55.4	Uracil DNA glycosylase
ORF 47	65027-65545	L	173	167	141	137	BKRF2	20.2	15.6	13.9	Glycoprotein L
ORF 48	65584-66582	L	333	402	397	537	BKRF2	14.4	17.4	12.3	
ORF 49	66741-67643	L	301	302	303	310	BRRF1	14.6	16.0	12.6	
ORF 50	67907-69373	R	489	631	535	605	BRLF1	16.4	26.6	13.1	Transcriptional activator
M7	69466-70914	R	483								Glycoprotein 150
ORF 52	70960-71364	L	135	131	115	162	BLRF2	28.2	27.4	40.0	
ORF 53	71447-71701	L	85	110	90	102	BLRF1	30.6	30.6	27.1	
ORF 54	71806-72702	R	299	318	287	278	BLLF3	28.1	24.7	25.1	dUTPase
ORF 55	72744-73313	L	190	227	200	218	BSRF1	41.6	40.5	47.9	
ORF 56	73289-75793	R	835	843	835	874	BRLF1	35.3	35.7	30.5	DNA replication protein
M8	76015-76485	R	157								
ORF 57	76662-77159	R	166	275	416	438	BMLF1	21.7	25.3	22.3	Immediate-early protein
ORF 58	77214-78254	L	347	357	357	357	BMRF2	20.5	22.2	19.3	
ORF 59	78258-79439	L	394	396	368	404	BMRF1	32.7	26.1	24.4	DNA replication protein
ORF 60	79565-80479	L	305	305	305	302	BaRF1	61.3	62.3	56.1	Ribonucleotide reductase, small
ORF 61	80517-82865	L	783	792	767	826	BORF2	44.6	45.6	39.8	Ribonucleotide reductase, large
ORF 62	82871-84010	L	380	331	330	364	BORF1	25.0	20.2	22.1	Assembly/DNA maturation
ORF 63	83751-86564	R	938	928	899	1,239	BOLF1	21.6	21.0	17.3	Tegument protein
ORF 64	86567-93937	R	2,457	2,635	2,469	3,149	BPLF1	25.6	23.6	20.1	Tegument protein
M9	93962-94519	L	186								
ORF 66	94515-95741	L	409	429	435	591	BFRF2	31.1	29.6	23.0	
ORF 67	95738-96415	L	226	271	235	336	BFRF1	40.3	39.4	36.7	Tegument protein
ORF 68	96673-98052	R	460	545	436	525	BFLF1	31.7	29.1	29.3	Glycoprotein
ORF 69	98061-98936	R	292	225	261	318	BFLF2	33.9	35.6	32.9	
M10a	98903-101224	R	774								
M10b	99087-101204	R	706								
M10c	99187-101367	R	727								
ORF 72	102426-103181	L	252	257	254			25.0	21.0		Cyclin D homolog
M11	103418-103930	R	171	175	160	191	BHRF1	11.7	11.7	24.8	Bcl-2 homolog (gene 167)
ORF 73	103927-104868	L	314	1,162	407			24.2	7.3		Immediate-early protein
ORF 74	105057-106067	R	337	342	321			23.1	22.8		GCR (IL-8 receptor homolog?)
ORF 75c	106070-109999	L	1,310	1,296	1,299	1,318	BNRF1	24.7	23.4	22.4	Tegument protein/FGARAT ^c
ORF 75b	110077-113901	L	1,275	1,296	1,299	1,318	BNRF1	22.6	22.5	22.3	Tegument protein/FGARAT
ORF 75a	114032-117904	L	1,291	1,296	1,299	1,319	BNRF1	22.7	22.5	22.2	Tegument protein/FGARAT
M12	117992-118681	R	212								
M13	118149-118784	R	230								
M14	118808-119125	L	106								

Table 2

1.VI. FIGURE LEGENDS

Figure 1. A) Depiction of kinetics of MHV68 lytic and latent infection. Unshaded area represents lytic replication in the lung and spleen; lytic virus detectable by plaque assay in lung and spleen. Shaded area represents latent infection; viral genomes are present as determined by PCR analyses but lytic viral replication is limited or undetectable. (*Adapted from J.Upton*) B) Schematic illustrating progression of MHV68 infection following intranasal infection.

Figure 2. A) Gammaherpesvirus genomes contain blocks of conserved genes as well as unique genes. Conserved gene blocks are indicated by shaded areas; unique genes are depicted as arrowheads, the majority of which are clustered near the viral termini. B) Transposon mutagenesis identifies essential, critical, and non-essential genes for lytic replication. (**Moorman et al**, 2004. *J Virol* **78**:10282-90. (107))

Figure 3. Schematic illustrating basic Rta splicing. A promoter upstream of Exon1 (indicated by the small arrow) drives expression of a transcript containing Exon1 spliced to Exon2. For the gamma-2 herpesviruses (MHV68, KSHV, HVS), the first ATG start codon in Exon2 is located well within the exon (indicated by the asterisk); use of an ATG in Exon1 provides additional coding sequence for Rta. The gamma-1 herpesvirus EBV Exon2 ATG is located near the 5' end of Exon2 and is the translational start site for the full-length Rta protein, yet Exon1 is still retained in the genome.

Figure 4. A) Model depicting the role of DNA methylation in directing chromatin compaction and heterochromatin formation. Methyl-binding domain containing proteins (MBDs) bind to 5-methylcytosines (5meC) on DNA and recruit histone modifying proteins such as histone methyltransferases (HMTs) and histone deacetylases (HDACs). (*Adapted from K.Richardson* (<http://www.med.ufl.edu/biochem/keithr/>)) B) Functional domains of mammalian DNA methyltransferases. Dnmt1, Dnmt3a, and Dnmt3b contain catalytic domains conferring methyltransferase activity; Dnmt3L and Dnmt3L lack key catalytic domains and thus do not have methyltransferase activity. Leu-zipper, leucine-zipper; Zn-finger, zinc-finger motif; PHD-domain, cysteine-rich/ATRAX-homology region; R-foci, interacts with PCNA replication machinery; PWWP, PWWP motif. (*Adapted from Cheng, X., and R. M. Blumenthal.* 2008. *Structure* **16**:341-50. (25))

Figure 5. Alternative splicing and autoregulation in the EBV latent gene transcription. (From **Speck, S. H.** 2002. *Nat Med* **8**:1086-7. (149))

Table 1. Frequency of MHV68 genome-positive cells in various cell populations.
(From **Willer, D. O., and S. H. Speck.** 2003. *J Virol* **77**:8310-21. (184))

Table 2. List of MHV68 genes and homologues in KSHV, HVS, and EBV. (From **Virgin, H. W. t., P. Latreille, P. Wamsley, K. Hallsworth, K. E. Weck, A. J. Dal Canto, and S.H.Speck.** 1997. *J Virol* **71**:5894-904. (172))

Chapter 2: Alternatively initiated gene 50/RTA transcripts expressed during murine and human gammaherpesvirus reactivation from latency

2.I. Abstract

2.II. Introduction

2.III. Materials and Methods

2.IV. Results

2.V. Discussion

2.IV. Figure legends

2.VII. Figures

1. Conservation of G50/BRLF1/Rta coding region among gammaherpesviruses
2. Generation and confirmation of MHV68.G50pKO and MHV68.G50pKO-MR viruses
3. MHV68.G50pKO virus replicates *in vitro*
4. RACE and RT-PCR analyses identify an additional upstream G50 exon
5. Promoter activity in region immediately 5' to MHV68 E0
6. Quantitative RT-PCR analysis of distal versus proximal promoter-driven transcripts
7. Identification of upstream-initiated transcripts from treated EBV or KSHV latent cell lines
8. Exon 0 extends the EBV and KSHV G50 reading frames
9. G50pKO virus establishes latency *in vivo* but exhibits severe reactivation defect
10. Bisulfite PCR analysis of CpG methylation in regions containing the proximal and distal G50 promoters
11. G50pKO virus reactivates from peritoneal exudate cells following intraperitoneal infection

This work has been published in *Journal of Virology* (J Virol. 2009 Jan;83(1):314-28.) and has been reproduced here with permission (License number 2311950193431).

2.I. ABSTRACT

In the process of characterizing the requirements for expression of the essential immediate-early transcriptional activator (RTA) encoded by gene 50 of murine gammaherpesvirus 68 (MHV68), a recombinant virus was generated in which the known gene 50 promoter was deleted (G50pKO). Surprisingly, the G50pKO mutant retained the ability to replicate in permissive murine fibroblasts – albeit with slower kinetics than wild type MHV68. 5' RACE analyses of RNA prepared from G50pKO infected fibroblasts revealed a novel upstream transcription initiation site, which was also utilized during wild type MHV68 infection of permissive cells. Furthermore, the region upstream of the distal gene 50/RTA transcription initiation site exhibited promoter activity in both permissive NIH 3T12 fibroblasts, as well as in the murine macrophage cell line RAW 264.7. In addition, in RAW 264.7 cells the activity of the distal gene 50/RTA promoter was strongly upregulated (>20-fold) by treatment of the cells with LPS. Reverse transcriptase-PCR analyses of RNA prepared from KSHV and EBV infected B cell lines, following induction of virus reactivation, also revealed the presence of gene 50/RTA transcripts initiating upstream of the known transcription initiation site. The latter argues that alternative initiation of gene 50/RTA transcription is a strategy conserved among murine and human gammaherpesviruses. Infection of mice with the MHV68 G50pKO demonstrated the ability of this mutant virus to establish latency in the spleen and PECs. However, the G50pKO mutant unable to reactivate from latently infected splenocytes and also exhibited a significant reactivation defect from latently infected PECs - arguing in favor of a model where the proximal gene 50/RTA promoter plays a critical role in virus reactivation from latency, particularly from B cells. Finally, analyses of viral genome methylation in the regions

upstream of the proximal and distal gene 50/RTA transcription initiation sites revealed that the distal promoter is partially methylated in vivo, and heavily methylated in MHV68 latently infected B cell lines, suggesting that DNA methylation may serve to silence the activity of this promoter during virus latency.

2.II. INTRODUCTION

Herpesviruses contain large, double-stranded DNA genomes that encode an extensive array of viral proteins required for efficient infection and persistence in host organisms. These viruses establish life-long latent infection in a variety of cell types, a characteristic that is often accompanied by periodic virus reactivation and resumption of lytic replication and egress. Unlike the alpha and beta herpesviruses which exhibit neuronal or broad cellular tropism, the gammaherpesviruses are mainly lymphotropic, infecting and establishing latency in B or T lymphocytes. Gammaherpesviruses are associated with the development of lymphomas in both their natural host and in animal models, and have therefore been subject to intensive study in an effort to understand, treat, and prevent disease.

The γ 1-herpesvirus Epstein-Barr virus (EBV) is implicated in the development of several human malignancies, including Burkitt's lymphoma, Hodgkin's lymphoma, and nasopharyngeal carcinoma. Kaposi's sarcoma-associated herpesvirus (KSHV), a γ 2-herpesvirus, is likewise associated with tumor development in Kaposi's sarcoma, primary effusion lymphoma, and multicentric Castleman's disease. Although cell culture systems exist to study cells latently infected with these viruses, the narrow tropism of both EBV and KSHV has necessitated the use of animal models to intimately study the process of primary virus infection, and events that contribute to the perpetuation of viral latency in vivo. Murine gammaherpesvirus 68 (MHV68) is a naturally-occurring rodent pathogen that mimics several key aspects of both EBV and KSHV infection following experimental infections of inbred mice (11, 135, 161).

Substantial sequence homology is shared among the murine and primate gammaherpesviruses in the region of ORF50, which encodes the key lytic switch protein

RTA (172). Importantly, in all the characterized gammaherpesviruses the gene 50 transcript contains a short first exon that splices to a long coding exon (Fig. 1). For the γ 2-herpesviruses the ORF50/RTA reading frame is extended by the exon 1/exon 2 splice, with the translation initiation site located near the 3' end of exon 1. In the case of the γ 1-herpesvirus EBV, exon 1 does not contribute to the RTA coding sequence. Finally, the position of the short first exon is also well conserved among all the gammaherpesviruses, being located in the region between ORFs 48 and 49 (Fig. 1). RTA plays a pivotal role in lytic replication in both human and murine gammaherpesvirus infections, and ectopic expression of RTA is sufficient to trigger reactivation into the lytic cycle in latently-infected cell lines (133, 158, 197). Because gammaherpesviruses are thought to first infect permissive cells, followed by establishment of a latent infection within lymphocytes, potentially-antigenic lytic gene expression must be carefully controlled. This is important both during initial infection to allow for efficient establishment of latency, as well as during latency when the capability to reactivate remains. This level of regulation is accomplished for both latent and lytic genes by several mechanisms shared between EBV, KSHV, and MHV68, including multiple-promoter usage, extensive alternative splicing, and epigenetic modifications (2, 33, 46, 140, 142, 143, 187). We demonstrate here that expression of the MHV68 RTA homolog can be driven from a newly-defined promoter upstream of the promoter previously identified, and that this expression is sufficient to allow for lytic replication and establishment of latency. We also identified an additional exon included in the RTA-encoding transcript generated from this promoter, and provide evidence that the existence and utility of both the distal promoter and additional exon are conserved among the murine and human gammaherpesviruses. We provide evidence that DNA methylation may serve as a regulatory

mechanism for silencing the distal gene 50 promoter during latent infection and may potentially account for the severe reactivation defect observed in mice infected with a gene 50 mutant MHV68 lacking the proximal promoter. Finally, we demonstrate that although the G50pKO virus is defective for reactivation from latently-infected splenocytes, this virus is capable of reactivation from peritoneal exudate cells (PECs), indicating that activity of the newly identified distal promoter is regulated in a cell-type specific manner during latent infection.

2.III. MATERIALS AND METHODS

Viruses and tissue culture. Both virus mutants were generated from the wild-type MHV68 bacterial artificial chromosome (BAC) provided by Ulrich Koszinowski. Virus was passaged and titered as previously described (108). Mouse embryonic fibroblasts (MEFs), Vero-Cre, and NIH-3T12 cells were maintained in Dulbecco's Modified Eagle's Medium (DMEM) supplemented with 10% fetal calf serum, 2mM L-glutamine, 100 U penicillin per mL, and 100 mg streptomycin per mL. Vero-Cre cells were cultured with the addition of hygromycin (300 ug/ml). S11E, A20-HE1, A20-HE2, Akata, Clone-13, and BCBL-1 cell lines were maintained in RPMI medium 1640 supplemented with 10% fetal calf serum, 2mM L-glutamine, 100 U penicillin per mL, and 100 mg streptomycin per mL. A20-HE1 and A20-HE2 cells were maintained under hygromycin selection as previously described (45). All tissue culture was performed in a 5% CO₂ tissue culture incubator at 37 degrees C.

Generation of G50pKO and G50pKO.MR viruses. The MHV68.G50pKO virus generated by first using wild-type BAC DNA as a template in two separate round 1 50ul reactions. PCR was performed with Vent polymerase (New England Biolabs) with 25 cycles under the following parameters: 94C for 30seconds, 57C for 30seconds, and 72C for 1 minute. The internal primers were designed to introduce *HindIII* sites which would later be used for southern blot confirmation of mutant and marker rescue viruses. Reaction 1 used forward primer (5'-GATCATGACTTCTAGTCATATCC-3') and reverse primer (5'-GCTAGCTAAGCTTCTAGCCAGGGAATTTTGTTATGTGC-3') corresponding to nt66402. Reaction 2 used forward primer corresponding to nt66548 (5'-GCTAGAAGCTTAGCTAGCCTTCACGGGTTTCAAGGTCC-3') and reverse primer (5'-

GTTTCCTGACCTCTGTAGACG-3'). One microliter from each reaction was then used as template for a round 2 reaction using the reaction 1 forward primer and the reaction 2 reverse primer. The resulting product was gel purified, cloned into pCRBlunt (Invitrogen) and sequenced to verify the deletion of the G50 promoter region. The fragment was then excised from pCRBlunt and cloned in the suicide vector pGS284 using *NsiI*. Positive clones were identified using *BglII* and *NotI* digestion. Allelic exchange using the MHV68-BAC was performed as previously described (108). The MHV68.G50pKO.MR virus was generated by using the round 2 primers to amplify wild-type BAC DNA. The product was cloned into pGS284 as above and used in the allelic exchange protocol with the MHV68.G50pKO.MR BAC. Mutant and marker rescue BACs were confirmed by southern blot analyses following *HindIII* digestion and probed with a PCR-generated fragment encompassing the original site of amplification. Mutant and marker rescue BAC DNA was then transfected into Vero-Cre cells and propagated to generate virus stocks.

Plaque assays, in vitro growth, and determination of viral titers. NIH 3T12 cells were plated in six-well plates at 2×10^5 cells per well the day prior to infection. Virus stocks were diluted to a 200ul volume in cMEM for the indicated MOIs, and added to 3T12 monolayers. Plates were rocked every 15 min for 1 h at 37°C. For single-step growth analysis, viral inoculum was removed. After infection, cMEM was added and plates incubated under normal cell culture conditions until the indicated time post-infection, whereupon plates were stored at -80C until titer determination. Intracellular virus was liberated by freeze/thaw lysis, cell lysates diluted, and viral titers determined by plaque assay as previously described (171).

RACE analysis. RNA was prepared from NIH-3T12 cells 16 hours following infection with MHV68 G50pKO or wild-type virus (MOI=1) by GITC-phenol extraction, or from untreated A20-HE1 cells or A20-HE1 cells 24 hours following treatment with TPA (20 ng/uL) using Trizol Reagent (Invitrogen) per the manufacturer's instructions. For 3T12 analysis, polyA RNA was purified using the Sigma Gel-Elute kit, and 300ng converted to cDNA using the BD Smart RACE cDNA Amplification Kit (Clontech). For A20-HE1 and A20-HE2 analysis, RACE was performed using the GeneRacer system (Invitrogen). **For 3T12 analysis:** Nested PCR was performed using Vent polymerase with the 5' universal forward primer (Round1) and 5'universal nested forward primer (Round2) and reverse primer (5'GGTTGAGGTAGCTGTACC-3') at an annealing temperature of 60C. One microliter of round 1 product was used as the template for the round 2 reaction. **For A20-HE1 analysis:** Nested PCR was performed using AmplitaqGold DNA polymerase (see PCR mix below in Bisulfite PCR methods) under the following cycling conditions: For Round 1 (using 1ul of modified cDNA per 50ul reaction) 94C for 8 minutes, 10 cycles with denaturation at 95C for 30 seconds, annealing starting at 68C and decreasing 0.4C every 2 cycles, and extension at 72C for 2 minutes, then 25 cycles with denaturation at 95C for 30 seconds, annealing at 65C for 30 seconds, and extension at 72C for 2 minutes, followed by a final extension at 72C for 7 minutes. For Round 2- (using 1ul of Round1 product per 50ul reaction) performed with the conditions above. Both reactions were performed with the reverse gene-specific primer 5'-CCTTCTCATGGTCACATCTGTGTCTCACTGAAAAC-3'. PCR products were visualized by ethidium gel electrophoresis and excised bands purified using a Qiagen Gel Extraction Kit (Qiagen, Valencia,CA). Purified PCR products were ligated into pGEMT-Easy Vector (Promega) and analyzed by DNA sequencing.

Reporter plasmids. DNA fragments upstream of E0 were amplified from wild-type MHV68 BAC using AccuPrime Pfx Supermix (Invitrogen) at 64C with the same reverse primer in E0 (5-GATCGTCTAGAGTGCTGGGTTGTGAAG-3') and the following forward primers: - 100bp: (5' GATCGGCTAGCACTCGAAGTGTCCAGC-3'), 250bp: (5'-TGGCGGCTAGCTTAATCCTATATGGAGAT-3'), 500bp (5'-GATCGCTAGCGAAAACGCGGAGAG-3'), and -1000bp: (5'-GATCGCTAGCGAAAAGCGGGAGAG-3'). Products were gel purified and cloned into pCR-Blunt (Invitrogen) for sequence verification. Reporter fragments in pCR-Blunt were digested with *NheI* and *XbaI*, and the luciferase vector pGL4.10[luc2] (Invitrogen) digested with *NheI* and treated with calf intestinal phosphatase (CIP) prior to ligation. Digested products were gel purified and extracted using the Qiagen Gel Extraction Kit (Qiagen, Valencia, CA), resuspended in water, and ligated overnight at 16C. Ligations were transformed and screened for the presence and orientation of inserts by digestion with either *NheI* and *EcoRV* or *PvuII*. Positive clones were cultured and plasmid DNA isolated using the QiagenEndoFreeMaxi Kit (Qiagen, Valencia, CA).

Transfections and luciferase assays. One day prior to transfection, 2×10^5 NIH 3T12 fibroblasts or RAW 264.7 macrophages were plated in 6-well plates in cMEM. Immediately prior to transfection, cells were washed 2x in PBS and covered with serum-free media. NIH 3T12 transfections were performed with Lipofectamine and LipofectaminePlus reagent (Invitrogen) according to the manufacturer's instructions. RAW 264.7 transfections were performed with TransIT transfection reagent (Mirus) according to the manufacturer's

instructions. All transfections were performed with the recommended quantity of reporter plasmid DNA (2-2.5ug) as well as 5ng of pHR-Luc renilla luciferase vector as a transfection control. Empty pGL4.10[luc] and pGL4.13[luc] were used as negative and positive controls respectively. The GFP plasmid pMaxGFP (Amara) was used to monitor transfection efficiency. After 24 hours, macrophage cultures were stimulated with 5ug LPS (Sigma-Aldrich). After 48 hours, cell lysates were harvested and luminometric assays performed using the Dual Luciferase Assay System (Promega) according to manufacturer's instructions. Each transfection was performed in triplicate and data presented as Firefly:Renilla luciferase ratio over empty vector.

Cell lines and treatments. Induction of A20-HE1 cells at 1×10^6 cells/mL was performed by treatment with TPA (20 ng/uL). Akata cells at 1×10^6 cells/mL were induced by treatment with goat-anti-human-IgG (Jackson ImmunoResearch Laboratories, Inc) at 100ug/mL as previously described (ref Flemington). Clone-13 cells were treated at 1×10^6 cells/mL with TPA (20ng/mL) for 24 hours. BCBL-1 cells at 2×10^5 cells/mL were treated with TPA (20ng/mL) for 48 hours.

Quantitative RT-PCR. RNA from A20-HE2s or NIH-3T12s infected with MHV68 (MOI=10) was isolated using either Trizol reagent (Invitrogen) or the Qiagen RNeasy Maxi Kit (Qiagen). Three or five micrograms of RNA was treated with DnaseI (Invitrogen) according to manufacturer's instructions in a total volume of 50uL. Twenty microliters of Dnase-treated RNA was subsequently used in first-strand cDNA synthesis using SuperScriptII Reverse Transcriptase (Invitrogen). Five microliters of the cDNA reaction was

used in each quantitative amplification reaction. Quantitative PCR was performed using iQ Supermix (BioRad) with the following primers (at 900nM): **E1-E2:** Forward (5'-GGAATTTCTGCAGCGATGGCCTCT-3') Reverse (5'-CCTCTTTTGTTCAGCAGAGACTCCA-3') **E0-E1-E2:** Forward (5'-GCAGTCCGTAGCCGCTGGAGTGT-3') Reverse (5'-GCAGAGACTCCAATCAACTGGCTCAA-3') and **Taqman probe** (at 250nM): (5'-FAM-CTGGCACGGATCGAAGCAGGTCTACTAMRA-3') PCR was performed with the following cycle parameters: 95C for 3minutes, 40 cycles at 95C for 30seconds, 58C for 30seconds, 72C for 30seconds, 95C for 1minute. A standard curve was generated using a spliced E0-E1-E2 PCR product amplified from TPA-treated A20-HE2 cDNA using the conditions described below for MHV68 E0-E2 RT-PCR cloned into the pGEMT-Easy vector (Promega). qRT-PCR reactions were performed in a Becton-Dickinson iCycler and analyzed using BioRad iCycler software.

MHV68, EBV, and KSHV G50/RTA transcript analysis. EBV and KSHV genomic sequence (GenBank Accession Nos. NC007605 and U75698) were examined for the presence of putative splice donor sites. RNA was prepared from treated or untreated cells using Trizol Reagent as above. cDNA synthesis was performed with random hexamers using SuperScriptII reverse transcriptase (Invitrogen). All reactions were performed using GoTaqFlexi DNA polymerase (Promega) in a PCR mix of 1X GoFlexi Buffer, 1.5mM MgCl₂, dNTPs (0.2mM each), forward and reverse primers (0.2uM each) with the cycling parameters 94C for 5minutes, 30 cycles at 95C for 30seconds, annealing at indicated temperature for 30seconds, and extension at 72C for 1min30seconds, followed by a final

extension at 72C for 7minutes: **MHV68**. E0-E1 reaction: Forward primer (5'-CCAGGTCATCAAGGGTCCAAATACTC-3') Reverse primer (5'-GGAATCCGAGTCAGAGGCCAT-3'); annealing at 59C. E0-E2 reaction: Forward primer (same as E0-E1 reaction) Reverse primer (5'-GTCTGGTGGGATGTTGATGGCGT-3'); annealing at 58C. E1-E2 reaction: Forward primer (5'-CTGCTGGCAACCACCACCTTCA-3') Reverse primer (same as E0-E2 reaction); annealing at 58C. **EBV**: Forward primer (5'-CCATGGGTGATAACGTCCTGAACG -3') Reverse primer (5'-GCCCGTCTTCTTACCCTGTTGTTTCG-3'); annealing at 54C. **KSHV**: Forward primer (5'-GGCAAGCAAGCTGGTGTCTGGAT-3') Reverse primer (5'-CCTCCGATTGCAGACGAGTCG-3'); annealing at 56C. PCR products were visualized by ethidium-gel electrophoresis and cloned and sequenced as above.

Mice, organ harvests, and tissue preparation. Female C57BL/6 mice (The Jackson Laboratory) and Dnmt3b conditional knockout mice (170) were housed at the Yerkes or Whitehead vivarium in accordance with university and federal guidelines. C57BL/6 mice 8-12 weeks of age or Dnmt3b conditional knockout mice 3-4 months of age were inoculated intranasally with 1000pfu of either wild-type MHV68, MHV68.G50pKO, or MHV68.G50pKO.MR (C57BL/6 infections) or MHV68-Cre.MR (Dnmt3b conditional knockouts) (111) virus in 20uL cMEM following isofluorane anesthetization. Mice were sacrificed by asphyxiation or isofluorane inhalation and cervical dislocation. PECs were harvested by peritoneal lavage with 10mL cMEM, and spleens were harvested and splenocytes prepared by homogenization, and treated with Tris-ammonium chloride for red blood cell elimination as described previously (62). PECs or splenocytes were immediately

used for reactivation analyses, genomic DNA isolation, or stored in cMEM/10% DMSO at -80°C until prepared for quantitative or limiting-dilution PCR analyses.

Ex vivo limiting-dilution assays. To determine the frequency of genome positive cells in preparations of splenocytes or PECs, serially-diluted cells were subjected to nested PCR using primers to detect G50 as previously described (62). To determine the frequency of cells reactivating from latency, single-cell suspensions of splenocytes or peritoneal exudate cells (PECs) from mice at day 16-18 post-infection were plated in 2-fold serial dilutions onto mouse embryonic fibroblast monolayers (MEFs) in 96-well plates as previously described (62). At day 21 post-plating, each well was assessed for the presence of cytopathic effect (CPE). To determine the frequency of cells reactivating, the percentage of wells with CPE at each dilution was used in nonlinear regression analyses to calculate the frequency of reactivation per cell by Poisson distribution. Disrupted splenocytes and PECs were also plated in parallel as previously described to determine the contribution of preformed infectious virus to reactivation (62).

Quantitative PCR to determine frequency of viral genomes. Quantitative PCR was performed as described by Moorman et al (108). Briefly, DNA was extracted from splenocytes using the Qiagen DNeasy kit. DNA was quantitated in a fluorometer, and 0.5 µg of DNA was included in each PCR reaction. Glyceraldehyde-3-phosphate dehydrogenase (GAPDH)-specific PCR was also performed on each sample to control for variation in input DNA. A two-step PCR was used which consisted of the following steps: 2 min at 50°C, 10 min at 95°C, and 50 cycles of 95°C for 15 s, followed by 60°C for 30 s. The same PCR

conditions were used for both the ORF50 and GAPDH reactions. The number of copies of ORF50 and GAPDH in each sample was determined by comparison to a series of standard curve reactions using a plasmid control containing appropriate sequences. The standard curve dilutions used represented a range from 10^8 to 10^1 , in serial 10-fold dilutions, and were performed in a background of 0.5 μ g of splenic DNA from naive mice. All real-time PCRs were performed on a Becton Dickinson iCycler and analyzed in a minimum of two reactions. Data points represent the log square means of the replicate samples.

Genomic DNA isolation and bisulfite modification. Splenocytes were incubated for 12-18 hours at 50C in 100mM NaCl, 10mM Tris-Cl, 25mM EDTA, 0.5% SDS, and 0.1mg/mL proteinase K, followed by phenol chloroform extraction and ethanol precipitation. Genomic DNA (10-20ug) was digested 12-18 hours with HindIII and ethanol precipitated. Digested DNA (1-2ug) in a volume of 50uL was denatured at 37C for 10 minutes in 0.2M NaOH prior to bisulfite modification. Modification was performed by the addition of 30ul 10mM hydroquinone, 520ul 3M sodium bisulfite, and mineral oil overlay and 16-hour incubation at 50C. Modified DNA was purified using the GeneCleanII system (QBiogene), eluted in 50ul ddH₂O, and desulfonated by incubating in 0.3M NaOH for 5 minutes at 37C. DNA was ethanol precipitated and stored at -80C until use in PCR.

Bisulfite PCR analyses. Bisulfite-modified DNA was amplified using AmpliTaqGold DNA polymerase (AppliedBiosystems). Each nested and hemi-nested PCR reaction contained 1X Amplitaq Gold Buffer, 3mM MgCl₂, dNTPs (0.2mM each), and forward and reverse primers (0.2uM each). All reactions were performed in a BectonDickinson iCycler with the following

parameters: 95C for 10min (hot-start), 30 cycles of 95C for 30seconds, annealing at the indicated temperature for 30seconds, and 72C for 1 minute, followed by a final extension at 72C for 7minutes. For Round 1, 2ul of bisulfite-modified DNA was used in each 25ul reaction, and annealing was performed using a temperature gradient in 4 3.2-degree increments from 42-55C for 30 cycles. Round 1 products were combined, and 1ul used in 25ul Round 2 reactions. **Distal promoter region** Round 1: Forward primer (5'-ATGATGATTTATTAAAGAATTATGTTTT AGGT-3') Reverse primer (5'-CAACCTCACCAACTTTTACAATAAATA-3'). Round 2: Forward primer (same as Round 1) Reverse primer (5' CCCTTAATAACCTAATAAAAAACC CAATA-3'). Round 2 annealing was performed at 50C with 30 cycles.

Proximal promoter region Round 1: Forward primer (5'-GTTGGTGAGGTTGGGAAGTTAT-3') Reverse primer (5'-CTCTCTCCTCAACCTTTAAAAAACAT-3') with reaction conditions as above. Round 2: Forward primer (5'- GAATAGAAGGTAATTTTTTGAATAGAGT-3') Reverse primer (5'-CTACCAAATTTCCATAAAAATAAAAAACTA-3'). Round 2 annealing was performed at 53C with 30 cycles. PCR products were visualized by ethidium gel electrophoresis, purified using the GeneCleanII system as above, and ligated into pGEMT-Easy vector (Promega). Plasmid DNA was sequenced by Macrogen USA (Rockville, MD) and analyzed using VectorNTI AlignX software (Invitrogen).

2.IV. RESULTS

A recombinant MHV68 with a deletion spanning the known gene 50 promoter is replication competent in vitro

During the generation of a gene 50 null virus (G50.Stop), the ability to produce mutant virus stocks was confounded by the strict dependence of MHV68 on gene 50 expression for virus replication (188). To overcome this problem, the G50.Stop mutant was propagated on a stable cell line harboring a plasmid containing an intact copy of MHV68 gene 50 under the control of the human cytomegalovirus IE promoter (128). However, the presence of a wild type copy of gene 50 within the complementing cell line led to the generation of recombinant viruses harboring an intact gene 50 (revertants) – a problem that was exacerbated by the slow growth of the G50.Stop mutant on the complementing cell line. As such, any revertants that were generated had a significant growth advantage and quickly dominated the culture. In an attempt to circumvent this problem, we generated an MHV68 mutant that contained a 183-nt deletion (Δ 66401-66584), removing the entire core promoter sequence previously shown to drive G50 transcription (92) (Fig. 2). It was expected that this mutant virus, termed G50pKO, would be phenotypically identical to the G50.Stop virus (i.e., replication null) due to its inability to drive G50 expression. Furthermore, growth of this mutant on the gene 50 complementing cell line would not lead to the generation of wild type revertants since the RTA expression construct in this cell line lacked any gene 50 promoter sequences.

During the propagation of the G50pKO virus, we unexpectedly observed that not only was the mutant virus able to replicate in non-complementing NIH-3T12 fibroblasts, it was able to do so at appreciable levels compared to wild-type virus (Fig. 3). In single-step

growth analyses (MOI=10), the MHV68G50pKO virus exhibited a mild defect in both the initiation and magnitude of lytic replication compared to wild-type virus, which resulted in a nearly 2-log defect in viral replication at late times post-infection (Fig. 3A). Multistep viral growth curves (MOI= 0.1) revealed a similar defect, with delayed initiation of replication and an ca. 2-log deficit in viral titers at late times post-infection (Fig. 3B). These analyses revealed that, although the G50pKO virus is attenuated for lytic replication compared to wild-type virus at both high and low MOIs, deletion of the previously-defined core G50 promoter does not result in a replication null phenotype. This suggested the presence of a second promoter capable of driving gene 50 expression in the absence of the characterized promoter.

Identification of alternatively initiated gene 50 transcripts

Previous analyses demonstrated that MHV68 RTA, like RTA in other γ 2-herpesviruses, is encoded by a transcript generated from the splicing of a short exon, E1, to a long downstream exon, E2 (92, 96, 97, 99, 158, 182) (Fig. 1). The observation that the G50pKO mutant was capable of replicating in permissive fibroblasts argued for the presence of an alternatively initiated gene 50 transcript. 5' RACE analyses of RNA prepared from NIH 3T12 cells infected with the G50pKO virus, using a primer in exon 2, revealed a distinct transcription initiation site mapping upstream of the previously identified gene 50 transcription initiation site (Fig. 4A). The upstream initiated transcript gave rise to a spliced transcript containing an extended first exon (Fig. 4A). To assess whether this upstream initiation site was utilized by wild type MHV68, 5' RACE was performed with RNA prepared from NIH 3T12 fibroblasts infected with wild-type MHV68. These analyses

revealed that this transcription initiation site is utilized by wild type virus, and gives rise to a novel spliced gene 50 transcript containing 3 exons - a short exon, which we have termed E0, that splices to the previously identified exon 1, which in turn is spliced to exon 2 (Fig. 4A). Notably, the splice acceptor site for the E0/E1 splice is not present in the G50pKO virus due to the deletion introduced, and as such the E0/E1 splice was not observed in cells infected with this mutant virus.

We extended these analyses to assess whether the alternative gene 50 transcripts were present during MHV68 reactivation from latency. For these analyses we utilized a recently characterized MHV68 latently infected A20 B cell line (A20-A20-HE1) (45) treated with phorbol-12-myristate-13-acetate (TPA) to induce virus reactivation. 5' RACE analyses were conducted on cDNA from A20-A20-HE1 cells 24 hours after treatment with TPA; to eliminate contamination from unspliced message, amplification of A20-A20-HE1 cDNA was performed with a genome-specific primer encompassing the predicted E0-E1 splice junction (Fig. 4A). This analysis also identified a transcriptional start site at nt 65909, indicating that the E0-encoding transcript initiating upstream of E1 is produced both during infection of permissive fibroblasts, as well as during TPA-induced reactivation from latently-infected B cells. Importantly, the E0 containing spliced transcripts utilize a consensus splice donor site ($[(A/C)AGGT(A/G)AGT]$) at the 3' end of the E0 exon (nt 66088) and a consensus splice acceptor site ($[(Y)_n(C/T)AG/G]$) located just upstream of the previously identified proximal gene 50 transcription start site (E1 exon transcriptional start site at nt 66494). Notably, the E0/E1 splice product could readily be detected by RT-PCR with RNA prepared from A20-A20-HE1 cells treated with TPA, employing an upstream primer located in the E0 exon and downstream primers located in either the E1 or E2 exons (Fig. 4B). In addition to the

expected splice product (indicated with asterisks in Fig 4B), unspliced and partially spliced products were also detected (for details see legend to Fig. 4B). Taken together these data demonstrate that in addition to the E1/E2 spliced gene 50 transcript produced by a promoter proximal to the E1 exon, there is an additional gene 50 promoter upstream of the E1 exon which gives rise to a spliced transcript containing the E0, E1, and E2 exons. This promoter is utilized during virus replication in permissive fibroblasts and also during virus reactivation from B cells.

Identification of promoter activity mapping in the region immediately upstream of the E0 exon

To validate the existence of a bona fide promoter capable of producing E0-containing transcripts, we examined the region immediately upstream of the E0 transcriptional start site for promoter activity. Fragments containing the upstream region were cloned into the pGL4.10 luciferase reporter vector and the resulting reporter constructs transfected into either NIH 3T12 fibroblasts or the murine macrophage cell line RAW 264.7. While the -100bp fragment conferred little or no promoter activity, the -250bp fragment exhibited a 20-fold increase in activity over empty vector in NIH 3T12 fibroblasts, compared to a more modest 5-fold increase in unstimulated RAW 264.7 macrophages (Fig. 5). In both NIH 3T12s and RAW 264.7 cells, the inclusion of additional upstream sequences repressed the activity observed with the -250bp fragment alone. In 3T12s, the -1000bp fragment exhibited only ~3-fold higher activity than empty vector, and while this fragment still had some activity in stimulated macrophages (~18-fold), it was greatly reduced compared to the -250bp fragment. This suggests the existence of a repressive element(s) in the more distal

region of the E0-promoter that can attenuate activity of the distal promoter in these cell types. NIH 3T12 fibroblasts are a permissive cell line for MHV68 infection, while macrophages have been identified as a reservoir for latent MHV68 infection that are capable of reactivating virus in response to various stimuli. To determine if macrophage activation would increase promoter activity, we added LPS to the RAW 264.7 cultures for 24 hours prior to harvest. This stimulation led to a 30-fold increase in promoter activity with the -250bp reporter construct (ca. 150-fold over empty vector), -500bp construct (ca.30-fold over empty vector), and -1000bp constructs (ca. 15-fold over empty vector). These data demonstrate that the region upstream of the MHV68 gene 50 E0 exon displays significant promoter activity under conditions which are known to support lytic viral replication and gene 50 expression. In addition, since these transfections were performed in the absence of viral infection, the observed activity is independent of the expression of any viral proteins, and thus suggests a possible role for this promoter in MHV68 reactivation from latency in stimulated macrophages.

E0-containing transcripts are of low abundance relative to total gene 50 transcripts during permissive infection and reactivation from a latently infected B cell line

The identification of a second gene 50 promoter producing E1-E2 spliced transcripts raised questions regarding the relative abundance and kinetics of gene 50 transcripts arising from the distal versus the proximal gene 50 promoter. To address this issue, we used quantitative RT-PCR to determine the contribution of distal promoter-driven E0-E1-E2 transcripts to total E1-E2 transcripts in RNA from A20-HE2 cells at various times post-TPA treatment, as well as permissive NIH 3T12 fibroblasts 24 hours post-infection with wild-type

MHV68. To detect total E1-E2 transcripts, we used primers in E1 and E2 to amplify cDNA from TPA-treated A20-HE2s and infected NIH 3T12 cells and quantitated the amplification product using a Taqman probe specific for a region within the E2 exon. At 0 hours post-induction, very few copies of spliced E1-E2 transcripts were detected in the latently infected A20-HE2 cells, verifying the relatively low level of spontaneous reactivation previously seen in these cells (45) (Fig.6). TPA treatment resulted in a rapid accumulation of E1-E2 spliced transcripts by 4 hours post-induction, which peaked between 8 and 12 hours post-induction - kinetics in keeping with the rate viral replication seen previously upon TPA stimulation of this cell line and the classification of gene 50 as an immediate-early gene. E1-E2 spliced transcripts were also detected in NIH 3T12 fibroblasts 24 hours following MHV68 infection. This amplification reaction could also theoretically detect unspliced or anti-sense transcripts, an issue of concern given the high degree of complex, bi-directional transcription known to occur in the G50 region. These species could inflate the quantitation of E1-E2 spliced transcripts arising from the distal or proximal promoter. However, when visualized by gel electrophoresis, only a single 218-bp amplified product corresponding to the spliced E1-E2 transcript was observed, while distinct higher molecular weight species representing unspliced or antisense transcripts were not seen (data not shown). We therefore concluded that spliced E1-E2 transcripts comprise the majority of E2 exon containing transcripts detected in this assay, and any contribution by other transcript species was considered negligible for the purposes of this assay.

To detect E0-E1-E2 spliced transcript, generated from the distal gene 50 promoter, we used the same Taqman probe within the E2 exon, as described above, but with primers in E0 and E2. Unlike the readily quantifiable E1-E2 spliced transcripts, spliced E0-E1-E2

transcripts were not detected at early times following TPA induction of A20-HE2s, and only sporadically detected in 2 of 5 separate cDNA preparations from these cells at 24 hours. E0-containing transcripts were also undetectable at 48 hours, arguing against the possibility of the distal promoter exhibiting strong late promoter kinetics (data not shown). E0-E1-E2 spliced transcripts were detected at variable levels in NIH 3T12 cells 24 hours following infection, but at less than 1% of the level observed for E1-E2 spliced transcripts from the same cDNA preparation. The larger size of the E0-E1-E2 amplicon versus E1-E2 (218bp versus 377) was most likely not responsible for the discrepancy in copy number, as standard curve correlation coefficients and PCR efficiency were generated using the same plasmid containing E0-E1-E2 cDNA, and were very similar for both reactions (data not shown). Notably, previous attempts to detect E0-containing transcripts by northern blotting, using a splice junction-specific oligonucleotide probe complementary to the E0-E1 splice junction were unsuccessful - even when performed with significant quantities of purified mRNA. The scarcity of spliced E0-containing transcripts in both reactivating A20-HE2 and permissively infected NIH 3T12 cells, suggests that spliced G50 transcripts generated from the distal promoter are significantly less abundant than those generated from the proximal promoter during both reactivation from latency and permissive infection. It should be noted that, although in low abundance, transcripts originating from the distal promoter were detected in NIH 3T12 cells infected with wild-type MHV68. This corroborates the distal promoter activity seen in NIH 3T12 reporter.

Evidence for a conserved distal RTA promoter in human gammaherpesviruses

Although sequence variation exists among both γ 1- and γ 2- herpesviruses, the organization and function of lytic genes in the region encoding gene 50 is highly conserved (Fig. 1). The expression of E1/E2 spliced transcripts under the control of an E1 exon-proximal promoter is observed in both γ 1- (EBV) and γ 2 herpesviruses (MHV68, KSHV, HVS), and appears to represent a conserved strategy for expression of gene 50. In all four characterized gammaherpesviruses, open reading frames are arranged on opposite coding strands in a slightly overlapping orientation as illustrated in Fig. 1. The 5' end of ORF 48/BRRF2 is positioned adjacent to the 5' end of the E1 exon, and ORF 49/BRRF1 lies between the E1 and E2 exons in the opposite orientation. The high degree of organizational homology in this region led us to investigate whether the human gammaherpesviruses also express alternatively initiated gene 50 transcript(s). To do this, we adopted the strategy outlined in figure 7A – the region 1000bp upstream of the characterized transcriptional start site of both the KSHV and EBV E1 exon were examined for potential splice donor sites (using the consensus sequence [(A/C)AGGT(A/G)AGT]), which would represent the 3' terminus of an E0 exon, as well as for potential splice acceptor sites (using the consensus sequence [(Y)_n(C/T)AG/G] near the 5' end of the defined E1 exon. We then designed primers to flank these potential splice donor and acceptor sites and used them to perform RT-PCR on RNA from KSHV (BCBL-1) or EBV-infected B cell lines (Akata, Clone-13) treated with TPA or anti-IgG respectively to induce virus reactivation. RT-PCR products were gel purified, cloned, sequenced, and analyzed for the presence of spliced gene 50 transcripts.

Treatment of the latent EBV-positive Burkitt's lymphoma cell line Akata with anti-immunoglobulin led to the identification of two distinct transcript species (products A and B in Fig. 7B) utilizing the same splice acceptor site in the BRLF1 coding exon, but two distinct splice donor sites for splicing the E0 exon. Sequence analysis revealed that both products initiated at nt 94954 (F primer binding site), contained a portion of the putative E0 sequence, spliced to the E2 acceptor site at nt92897, and ending at nt92615 (R primer binding site). However, product B utilized a splice donor located at nt94862, while the product A splice utilized a splice donor located at nt94830. A third larger amplification product (product C) was identified that contained sequence from nt94954 to nt94693 and nt93371 to nt92615 (R primer binding site). Examination of the splice junction present in product C revealed that this corresponds to a spliced antisense transcript which that contains a portion of ORF49 (BRRF1) and ORF48 (BRRF2). Finally, a 1.4 Kb product (product D) was observed that corresponds to a partially spliced transcript (E0/E1-E2 product) in which the intron between exon 1 and exon 2 has not been removed (Note that this same partially-spliced product was detected following RT-PCR from TPA-treated A20-A20-HE2s, Fig.4B). As shown, the presence of the observed amplified products was dependent on both anti-immunoglobulin stimulation of virus reactivation and the inclusion of reverse transcriptase in the cDNA reaction (Fig. 7B). An analysis of potential translation products from the transcript corresponding to product B, an E0/E2 exon spliced transcript, reveals a possible extension of the BRLF1 open reading (Fig. 8A). This would be predicted to add a unique 31 a.a. extension at the N-terminus of RTA. Thus, one possible consequence of initiating from the distal promoter during EBV infection may be the generation of a functionally distinct form of

RTA. Future studies will be required to assess whether this predicted product is expressed and whether it has altered function(s).

To assess whether alternatively initiated gene 50 transcripts were also expressed during KSHV reactivation, RNA was prepared from the KSHV latently-infected BCBL-1 cell line 48 and 56 hours after treatment with TPA. As depicted in figure 7C, a forward primer positioned upstream of a putative splice donor site and a reverse primer in the gene 50 E2 exon identified a spliced transcript (product A) spanning nt 70436 (F primer binding site) to nt70728 and nt72572 to nt72722 (R primer binding site). The presence of consensus splice donor and acceptor sites at nt70728 and nt72572 respectively identifies this transcript as an authentic spliced transcript, rather than an artifact of the amplification reaction. The splice acceptor site at nt72572 is the same as that used to generate the E1/E2 spliced gene 50 transcript (96), confirming the validity of the junction produced between the putative E0 exon and the E2 exon. Another product (product B) was also detected that shared the same splice acceptor site as product A, but utilized a non-canonical splice donor at nt70823. The presence of both bands following RT-PCR was dependent on the inclusion of reverse transcriptase in the cDNA reaction (data not shown). The identification of upstream-initiated spliced transcripts containing the gene 50 E2 exon suggests that, like MHV68, the human rhadinovirus KSHV also encodes an additional distal gene 50 exon and promoter capable of generating a full-length gene 50 transcripts. Importantly, unlike MHV68, the identified transcripts lack the E1 exon raising the question of whether they give rise to a distinct RTA species. Translation of the lower molecular weight product A in figure 7C reveals the presence of a putative initiating methionine that would generate a product in frame with ORF50 and thus predicted to give rise to a functional RTA product (Fig. 8B). The E0 exon is

predicted to encode 10 a.a. at the N-terminus of RTA, while the E1 exon of E1/E2 spliced transcripts contributes 6 a.a. at the N-terminus of RTA (Fig. 8B). The inclusion of the additional sequence between nt70728 and nt70823 introduces stop codons, and thus translation of the longer Product B would not be predicted to encode an extended RTA product.

The proximal gene 50 promoter knockout mutant, G50pKO, establishes splenic latency in vivo, but is severely impaired for virus reactivation

Evidence of a distal gene 50 promoter capable of driving RTA expression prompted us to evaluate the relevance of the distal gene 50 promoter during virus infection in vivo. C57BL/6 mice were infected intranasally with 1000 PFU of either wild-type MHV68, the G50pKO virus, or a genetically repaired marker rescue virus G50pKO.MR. Levels of latent infection in splenocytes were determined by measuring the amount of viral genome present in the spleen at day 16 post-infection by quantitative PCR. The viral genome load was very similar between wild type, G50pKO and G50pKO.MR infected mice, with slightly lower levels observed in mice infected with the G50pKO (Fig. 9A). We have subsequently confirmed using a limiting dilution analyses that the G50pKO robustly establishes latency, but at a slightly lower level than wt or marker rescue virus (data not shown). Since we have previously shown that expression of RTA is required for establishment of latent infection in the spleen following intranasal infection (110), the presence of virus genome-positive splenocytes in G50pKO infected mice therefore corroborates the in vitro observations that, in the absence of the proximal gene 50 promoter, the distal gene 50 promoter is capable of driving sufficient levels of RTA expression to allow virus replication.

In addition to presence of genomes in latently infected cells, another parameter for assessing latent infection is determining the frequency of cells able to reactivate from latency and induce cytopathic effect (CPE) when plated in serial dilutions onto mouse embryonic fibroblast (MEF) monolayers. Remarkably, despite harboring nearly wild-type frequencies of viral genomes, splenocytes from G50pKO virus-infected animals displayed a complete inability to reactivate from latency (Fig. 9B). Splenocytes from both wild-type and G50pKO.MR infected mice reactivated at a frequency of approximately 1 in 6200 and 1 in 10300 respectively, while no detectable CPE was observed on MEFs cultured with splenocytes from G50pKO infected mice (Fig. 9B). Notably, no preformed infectious virus was detected in these splenocyte samples following mechanical disruption of the cells (data not shown). The G50pKO reactivation defect was not related to route of infection, as the same phenotype was observed upon intraperitoneal infection with an equivalent viral dose (data not shown). That the G50pKO mutant can establish latency at a relatively normal frequency, yet is completely unable to reactivate *ex vivo*, indicates that the distal G50 promoter can compensate for the proximal promoter during the establishment of latent infection *in vivo*, but not during reactivation from latently infected splenocytes, and corresponds to a defect in reactivation from B cells, the predominant latency reservoir in the spleen.

The distal gene 50 promoter is progressively methylated in splenocytes during in vivo infection and in latently-infected B cell lines

The reactivation defect exhibited by the G50pKO mutant suggests that distal gene 50 promoter activity may be differentially regulated during reactivation from latency and

primary lytic infection. This temporal discrepancy in promoter function suggested a possible role for epigenetic regulation of distal G50 promoter activity. A wealth of evidence exists supporting a role for DNA methylation in the regulation of both latent and lytic gene expression in KSHV and EBV (9, 22, 79, 87, 104, 126). To determine if DNA methylation regulates the MHV68 proximal and distal G50 promoters, we used bisulfite PCR analyses to examine the methylation status of CpG dinucleotides within the proximal and distal gene 50 promoters in viral genomes recovered from MHV68 latently infected B cell lines, as well as latently infected splenocytes recovered from mice at various times post-infection. Remarkably, the 110-nt gene 50 proximal promoter extending from nt 66442 to nt 66552 contains no CpGs, but is flanked by two CpGs located at nt 66430 and 66555. In contrast, the -250 region of the putative distal promoter and the 5' end of E0 contains five CpGs (Fig. 10). In splenocytes from wild-type MHV68 infected animals at day 16 post-infection, the two sites in the proximal promoter region were unmethylated in all clones examined, while significant methylation of the CpGs in the distal promoter were methylation. At day 42 post-infection, the percentage of methylated CpGs increased in both regions, but to a greater degree at the distal promoter sites (18% in proximal versus 42% in distal). At day 90 post-infection, the percentage of methylated CpGs had increased to 80% in the distal promoter region, but remained nearly equivalent to day 42 levels in the proximal promoter region (20%). This partitioning was also readily apparent in viral genomes present in MHV68 latently infected B cell lines. In the MHV68-positive lymphoma cell line S11E, hypermethylation of the CpGs in the distal gene 50 promoter was apparent, along with consistent methylation of the CpG upstream of the core proximal gene 50 promoter. This same pattern of methylation was also observed in the two independently generated A20 B

cell lines latently infected with an MHV68-hygromycin-EGFP virus (A20-HE1 and A20-HE2). These analyses demonstrate that not only does viral CpG methylation accumulate in the gene 50 region throughout the duration of latent viral infection, it is more concentrated in the distal than in the proximal gene promoter region. Methylation of CpGs in promoter regions is most often associated with silencing of the associated gene (105). Given that methylated CpGs accumulate in the distal promoter region during latent infection, we hypothesize that methylation-induced silencing of the distal gene 50 promoter reflects a general lack of distal promoter usage in latently-infected splenocytes and may contribute to the severe reactivation defect observed in latently infected splenocytes from G50pKO infected animals. The absence of significant methyl-CpG accumulation in the proximal promoter regions suggests that this promoter is refractory to DNA methylation and may therefore retain functional capacity in latently-infected splenocytes, even at late times post-infection.

G50pKO virus reactivates from peritoneal exudate cells

Given the pronounced reactivation defect of G50pKO virus-infected splenocytes, we questioned whether this mutant virus was capable of ex vivo reactivation from latently-infected cells. Peritoneal exudates are comprised mostly of macrophages and dendritic cells, both of which have been shown to harbor latent MHV68 (42). PECs from animals infected intraperitoneally typically exhibit a slightly enhanced frequency of reactivation during early latency compared to splenocytes. We therefore examined PECs from mice infected with G50pKO virus following intraperitoneal infection to determine if the distal promoter was sufficient to drive reactivation from this cell population. Frequencies of viral genome-

positive cells were reduced in splenocytes from G50pKO-infected animals relative to those infected with G50pKO.MR following intraperitoneal infection. This roughly 10-fold reduction in establishment is greater than would be expected given the slight reduction in viral genome copy number determined by qPCR following intranasal infection, and may reflect a differential requirement for the proximal G50 promoter during establishment of latent infection in splenocytes following intraperitoneal infection. (Fig.11A). Splenocytes from G50pKO.MR virus exhibited a similar frequency of reactivating cells as observed following intranasal infection, while PECs from G50pKO.MR-infected animals reactivated at a slightly higher frequency than splenocytes - as expected based on previous observations (69). The reactivation defect seen in splenocytes from G50pKO-infected animals following intranasal infection was also present following intraperitoneal infection (Fig.11B). Importantly, the establishment defect was not evident in PECs from G50pKO-infected animals, as the frequency of viral genome positive cells was equivalent to that in PECs from G50pKO.MR-infected animals (Fig.11A). Remarkably, PECs from animals infected with G50pKO virus were able to reactivate from latency at a frequency nearly identical to that of G50pKO.MR splenocytes (Fig.11B). This is in striking contrast to the complete absence of reactivation in G50pKO-infected splenocytes, and demonstrates that the distal promoter is sufficient to drive both establishment of latency and virus reactivation from PECs. These data suggest that the distal gene 50 promoter is regulated in a cell-type dependent manner, and may reveal a specific role for the distal promoter in driving the establishment and reactivation of latent infection in macrophages or dendritic cell populations.

2.V. DISCUSSION

Roles for alternatively initiated gene 50/BRLF1 transcription in gammaherpesvirus infection

In this paper we demonstrate that MHV68 gene 50 transcription is more complex than previously characterized, and involves transcription initiation from at least two independent promoters. This complexity appears to be shared among the murine and human gammaherpesviruses, and therefore most likely represents an evolutionarily conserved transcriptional strategy important to gene 50/BRLF1 transcription and successful gammaherpesvirus infection. However, pathogenesis experiments demonstrated that the distal gene 50 promoter was not sufficient to compensate for loss of the proximal gene 50 promoter during reactivation from latently infected splenocytes, but was able to drive an attenuated frequency of reactivation in PECs relative to G50pKO.MR virus. This suggests that the two promoters have evolved to have distinct regulatory functions, and that these functions are likely to be cell-type specific.

The identification of an E0 exon upstream of E1 and E2 exons elaborates the characterized G50 coding sequence. In MHV68, E1 contains an ATG initiation codon which, when spliced to E2, extends the G50 open reading frame by an additional 94 amino acids. This mechanism is shared among the other γ 2- herpesviruses KSHV and HVS, such that the utilization of the ATG in E1 as a translational start site produces an augmented RTA protein with a high level of sequence conservation at the amino terminus (158, 182). For EBV, a γ 1-herpesvirus, the E1/E2 spliced transcript contains the initiating ATG in the E2 exon, and as such the E1 exon is non-coding. However, the overall organization of gene

50/BRLF1 transcription still mirrors that of the γ 2-herpesviruses in that E1, although not providing any additional G50 coding sequence, is retained.

The splicing of KSHV RTA E1 and E2 provides an additional 6 amino acids at the N-terminus of RTA and was observed by several groups (97, 158). We were unable to detect a cDNA species containing the putative E0 exon spliced to the previously identified E1-E2 spliced transcript using this analysis. However, a transcript containing the putative E0 and E2 contains an ATG that, if used as the translational start site, encodes a protein with 10 unique N-terminal amino acids that splices in frame with the E2 reading frame previously characterized by the E1-E2 spliced product. We were also unable to detect a transcript containing the putative E0 exon spliced to the BRLF1 E1 exon in reactions from IgG-treated EBV-positive Akata cells. However, the EBV transcript using the upstream consensus splice donor site also contains an ATG within the putative E0 exon sequence presumably capable of translating an extended RTA protein that would extend the previously characterized BRLF1 reading frame. Analogous to the KSHV E0-E2 transcript, the addition of the EBV E0 exon sequence provides an additional 31 amino acids to the N-terminus of RTA. This configuration may be conserved in MHV68 as well, as translating a hypothetical E0-E1-E2 spliced product using an ATG in E0 cannot produce a full-length amino acid sequence in any frame, while translating an E0-E2 product provides 14 additional amino acids from E0 that would splice in-frame with the previously identified E2 reading frame used by the E1-E2 spliced product.

The observation of an anti-IgG, reverse transcriptase-dependent product (C in figure 7B) in the Akata RT-PCR corroborates the complex bi-directional gene transcription in this area of the genome observed for both KSHV and EBV (32, 130), and perhaps represents a

form of lytic gene self-regulation by the generation of anti-sense gene 50 transcripts during reactivation from latency. RT-PCR analysis was also performed in a second latent EBV-positive Burkitt's lymphoma cell line, clone-13, following treatment with TPA to induce reactivation. Only the longer E0-E2 species containing the splice site at nt94830 was detected in RT-PCR analysis of this cell line; neither the shorter splice variant nor the spliced anti-sense transcript were detected despite a lack of any sequence variation between the two cell lines. This suggests that regulation of G50 splicing in the context of reactivation from latent EBV infection may be strain or cell-type dependent.

The existence of multiple gene 50 promoters has been reported by Whitehouse et al. upon the observation that HVS uses two different promoters to drive transcription of two distinct RTA products (182). The promoter immediately upstream of E1 drives transcription of the spliced E1-E2 product which encodes the functional RTA protein, while a second promoter situated within E2 gives rise to an unspliced transcript encoding a truncated RTA product of unknown function. The activity of these promoters is temporally regulated, with the first having immediate-early kinetics while the unspliced transcript produced by the second promoter was sensitive to cyclohexamide treatment. These observations suggest the intriguing possibility that different RTA promoters have unique kinetic profiles and produce distinct gene 50 transcripts. Given the lytic growth defect and reactivation defect of the proximal promoter knockout virus, it was not surprising to find that the distal gene 50 promoter generates significantly fewer spliced gene 50 transcript than the proximal promoter. It may be that generation of spliced transcripts encoding functional gene 50 is only one of the roles for the distal gene 50 promoter. In addition to contributing to the pool of gene 50 protein-producing transcripts, it is possible that transcripts from the distal gene 50 promoter,

either spliced or unspliced, play a role in regulating transcription from the proximal promoter following initiation of the lytic replication program. This may occur either through competition for transcriptional machinery or direct interference with transcription from the proximal gene 50 promoter, a mechanism used to explain promoter switching and exclusion of the “proximal” Wp promoter in favor of the “distal” Cp promoter during the establishment of EBV latency (131). Although no detectable levels of E0-E1-E2 spliced transcripts were detected at 48 hours post induction of A20-HE2s, the presence of E0-E1-E2 transcripts in 3T12s 24 hours post-infection, along with low level detection of E0-initiated transcript in A20-HEs at 24 hours post-induction at a time when E1-E2 transcripts appear to be decreasing, could still support the hypothesis that distal promoter-generated transcripts arise with delayed kinetics relative to proximal promoter-generated transcripts. These transcripts may in fact serve to modulate gene 50 expression in favor of dampening the lytic cascade during establishment or reactivation from latency. In the context of the G50pKO virus, it may be that distal promoter activity is increased, or sustained at low levels for such time that sufficient G50 transcripts accumulate to allow for lytic growth both in vitro and in vivo. Another possibility is that gene 50 transcripts initiating from the distal promoter is to serve as an alternative mechanism for modifying gene 50 expression at a distinct stage of virus infection or in distinct cell populations (e.g., macrophages). The ability of the G50pKO virus to reactivate from latently-infected PECs but not splenocytes strongly supports this latter hypothesis. Finally, it is possible that altering the 5' UTR present in the gene 50 transcript impacts either transcript stability or efficiency of translation initiation. None of these possibilities are mutually exclusive, and further studies on these alternative gene 50 transcripts and distinct forms of RTA will be required to determine their importance during

gammaherpesvirus infection. The relationship between the previously characterized gene 50 promoter and the distal gene 50 promoter identified here may provide valuable insights into the regulation of gene 50 transcription in MHV68 as well as in the human gammaherpesviruses, and requires further characterization.

CpG suppression and DNA methylation in gammaherpesviruses

Gammaherpesviruses are unique among the herpesvirus family in that they exhibit overall CpG suppression, suggesting that their genomes have been subjected to extensive CpG methylation throughout their evolution within vertebrate hosts (63, 78). The MHV68 genome is particularly sparse in terms of CpG distribution, with only a 0.4 ratio of CpG:GpC dinucleotide frequency, compared to roughly 0.6 for EBV and 0.8 for KSHV. As was described for the region encompassing the KSHV lytic genes RTA and K8 (22), the locus containing MHV68 gene 50 is also CpG-suppressed to a greater degree than the overall genome, with an overall CpG:GpC ratio of only 0.26. Even more remarkably, while the 250nt region upstream of the MHV68 E0 exon (containing the core distal gene 50 promoter) exhibits a CpG:GpC ratio of 0.33, the ratio for the 250nt region upstream of the E1 exon (containing the core proximal gene 50 promoter) is only 0.09. The 110 bp within this region previously shown to be required for proximal gene 50 promoter activity by reporter assays, and for efficient reactivation from splenocytes in this study, are completely devoid of CpGs. This may represent a characteristic viral adaptation such that the proximal promoter is refractory to this form of host-directed epigenetic silencing and thus more readily responsive to reactivation stimuli. The distal promoter region, though still suppressed relative to the

entire MHV68 genome, has a higher frequency of CpGs than the ORF48/49/50 locus as a whole. This suggests that the few CpG dinucleotides that have been retained amidst a presumed sea of cytosine nucleotide substitutions may represent key elements of MHV68 gene regulation, and that their methylation status is likely of significant relevance to the control of MHV68 lytic gene expression.

During lytic replication in the early stages of G50pKO infection, when the majority of viral DNA is packaged in virions and therefore unmethylated, it appears that the distal gene 50 promoter drives RTA expression to sufficient levels to allow for the establishment of splenic latency at levels comparable to wild-type infection. However, as the viral genome is maintained in the relatively quiescent memory B cell latency reservoir, it accumulates higher proportions of methylated CpGs. This progressive methylation of the viral genome has been seen at the latency promoters Wp and Cp during the generation of lymphoblastoid cell lines following EBV-induced transformation of B lymphocytes (168) and in seropositive individuals (126). With respect to RTA expression, reactivation of latent gammaherpesvirus infection has been shown to be accompanied by a loss of CpG methylation in the KSHV RTA promoter upon treatment of latent BCBL-1 cells with TPA (22). Similarly, treatment with the demethylating agent 5-azadeoxycytidine induces reactivation in both KSHV and EBV latently infected cell lines, presumably due to demethylation of key lytic gene promoters (6, 22). Biopsies from KSHV-positive tumors demonstrated that the majority of viral genomes in these samples contain unmethylated gene 50 promoters, suggesting that reactivation of latent KSHV either requires or results in loss of CpG methylation at lytic gene promoters (22).

In the context of wild-type MHV68 lytic infection, the core proximal gene 50 promoter is not subjected to methylated-CpG-induced silencing, and therefore may be required to drive G50 expression from the methylated latent state to induce reactivation and subsequent lytic replication. A possible scenario is that in a wild-type infection, rapid viral DNA synthesis induced upon reactivation overwhelms the capabilities of host methyltransferases and as such results in a passive “demethylation” of the distal promoter, rendering it once again active during the later stages of virus reactivation. In a G50pKO infection, however, the proximal promoter is no longer present to initiate gene 50 transcription and subsequent reactivation from the methylated viral genome. The distal gene 50 promoter, which was unmethylated and therefore able to facilitate lytic replication in absence of the proximal promoter during establishment, is now repressed by CpG methylation and therefore no longer able to drive gene 50 expression and thus unable to promote virus reactivation from latency.

It is worth noting that the RTA promoters defined for EBV and KSHV contain a higher density of CpGs than either the proximal or distal promoter regions of MHV68, and that these CpG “islands” are heavily methylated in latent cell lines (8, 22). There does not appear to be a “methylation-free” region in these promoters analogous to that seen in the 110 bp region of the MHV68 proximal G50 promoter. However, EBV and KSHV differ from MHV68 in that they encode a bZIP protein (Zta and K8 respectively) immediately downstream of gene 50/BRLF1. Recent studies have demonstrated that the EBV Zta protein, unlike many mammalian transcription factors whose binding is inhibited by methylated cytosines within their recognition site, preferentially binds to and transactivates a methylated RTA promoter (8, 9, 79). Although Zta and K8 differ in both their ability to bind to DNA

and induce lytic replication, the two proteins share significant homology with respect to host-cell protein interactions (147). It is possible that cellular factors associated with these bZIP proteins may confer a unique resistance to promoter methylation, and thus may circumvent the need for a “methylation-free” EBV-BRLF1 or KSHV-RTA promoter in order to initiate virus reactivation and subsequent viral replication. It is hypothesized that the ability to reactivate from latency is an important aspect in the maintenance of long-term gammaherpesvirus infection. Therefore, MHV68, which does not encode a known bZIP protein, may have evolved a CpG-free gene 50 promoter to retain resistance to the host-mediated epigenetic silencing that occurs during latent infection.

Mutations in Orf48 do not recapitulate the G50pKO phenotype

The original intention in generating a gene 50 promoter knock-out virus was to obtain a mutant virus that was essentially G50-null and could be used in place of the G50.Stop virus to avoid recombination during propagation on RTA-expressing stable cell lines. For this reason, the G50pKO virus was engineered to completely ablate the region containing the core 110-nt proximal gene 50 promoter, and thus contains a large deletion of the first 820-nt of ORF48, a tegument-associated protein of unknown function encoded on the opposite strand (12) (see Fig. 1). However, it is unlikely that the splenic reactivation phenotype observed with the G50pKO virus is due to disruption of ORF48, since previous studies using an ORF48-deletion virus did not reveal a splenic latency defect (101). In contrast, a study examining MHV68 mutants generated from transposon insertions reported that ORF48 was essential for lytic growth in vitro, as an insertion at nt 66462 within the first 200nt of the gene resulted in a replication-incompetent phenotype (148). However, this likely represents

a complex phenotype since this transposon insertion disrupts the proximal gene 50 promoter, and the introduction of a large transposon between the distal gene 50 promoter and exon 1 undoubtedly interferes with RTA expression driven by the distal gene 50 promoter. Notably, the absence of CPE observed upon infection with the transposon mutant is a much more severe than the defect in virus replication observed with the G50pKO virus. With respect to the replication defect observed with the G50pKO mutant there are two likely explanations. First, the deletion introduced removed the E0/E1 splice acceptor site, leading to production of a transcript from the distal gene 50 promoter containing the E0-E1 intron in addition to E0 and E1 exon sequences. Retaining the E0-E1 intron introduces a number of short open reading frames that likely interfere with efficient translation of RTA from this transcript. Second, the kinetics of gene 50 expression from the proximal promoter may not be suited to efficiently express RTA in the absence of transcription initiation from the proximal gene 50 promoter. Thus, these seemingly incongruous results likely arise from the fact that, like many other gammaherpesvirus genes, transcription of MHV68 gene 50 and the surrounding genes is extremely complex and varies according to infected cell type. Much further investigation is required to fully understand the regulation and contribution of transcription in this critical region of the viral genome to virus replication and reactivation.

2.VI. FIGURE LEGENDS

Figure 1. Conservation of G50/BRLF1/Rta coding region among gammaherpesviruses.

Schematic representation of the G50/BRLF1/Rta coding regions of MHV68, EBV, KSHV, and HVS. The nucleotide positions for G50 exons 1 and 2 are provided. The box drawn around exon1 demonstrates the conserved juxtaposition of exon1 relative to open reading frames encoded on the opposite strand.

Figure 2. Generation and confirmation of MHV68.G50pKO and MHV68.G50pKO-MR viruses. (A) Schematic depicting the organization of open reading frames in G50 region. The upright arrow indicates the relative position of the characterized G50 promoter, and the hatched area indicates the region of the deletion in the MHV68.G50pKO virus. The indicated splicing of E1 to E2 gives rise to a full-length G50-encoding transcript. Wild-type sequence contains HindIII sites at bp64898 and bp57541; the MHV68.G50pKO BAC contains an additional HindIII site at 66549 (indicated by the asterisk). (B) Hind-III digest of MHV68-wildtype, G50pKO, and G50pKO-MR virus BACs. The arrows indicate the fragments produced by the introduction of the additional HindIII site in A. (C) Southern blot hybridization using the PCR-generated probe indicated in A.

Figure 3. MHV68.G50pKO virus replicates in vitro. (A) Single-step growth analysis. NIH 3T12 cells were infected with wild-type or MHV68.g50pKO virus. Cells were infected at MOI=10 and harvested at the indicated times post infection for determination of viral titers. (B) Multi-step growth analysis. Cells were infected at MOI= 0.1 and harvested at the indicated times post-infection.

Figure 4. RACE and RT-PCR analyses identify an additional upstream G50 exon. **(A)** RACE analyses were performed using cDNA generated from G50pKO-infected 3T12s or A20-HE2s 24hours following treatment with TPA. The 5' end of E0 was mapped using the primer located in exon 2 (indicated at nt 68071) for 3T12 analyses (top), and the splice-junction spanning primer II for A20-A20-HE2 analyses (bottom). Both experiments identified the 5' terminus for E0 at nucleotide position 65909. The E0-E1-E2 spliced product is depicted. **(B)** RT-PCR analyses of A20-HE2 cells treated with TPA. cDNA was prepared from A20-HE2 cells either untreated or at the indicated time following TPA treatment and used in PCR analyses to detect E0-containing transcripts generated upon reactivation. The positions of the forward and reverse primers used in each of the three panels are indicated. Products a and e represent unspliced transcripts, and product c represents a partially spliced transcript containing unspliced E0-E1 sequence and spliced E1-E2; the spliced transcripts are indicated by asterisks. Products b, d, and f are artifacts of the amplification reaction and represent hybrid species (heteroduplexes) formed between RT-PCR products arising from spliced and unspliced/partially-spliced transcripts (verified in separate PCR reactions using purified plasmids containing either the fully spliced and/or unspliced/partially-spliced templates; data not shown). Note that these transcripts are derived from a wild-type G50 locus with both distal and proximal promoter intact.

Figure 5. Promoter activity in region immediately 5' to MHV68 E0. NIH 3T12 or RAW 264.7 cells were co-transfected with phRL-Luc (Renilla luciferase) and pGL4.10[luc] luciferase reporter constructs containing either 100, 250, 500, or 1000bp fragments

immediately upstream of E0. RAW 264.7 cells were stimulated 24 hours after transfection with LPS (5 ug/mL). Luciferase assays were performed 48 hours after transfection and data presented as fold difference in the ratio of firefly:renilla over an empty vector control. Data are representative of three independent transfections.

Figure 6. Quantitative RT-PCR analysis of distal versus proximal promoter-driven transcripts. Relative copy numbers of E1-E2 versus E0-E1-E2 transcripts in cDNA from TPA-treated A20-HE2s or 3T12s infected with wild-type MHV68. Mean copy number was calculated from 2 independent experiments comprised of at least 2 independent cDNA synthesis reactions. Each qRT-PCR reaction was performed in triplicate and data is presented as average mean for at least 4 independent cDNA preparations with calculated SEM. n.d, not detected.

Figure 7. Identification of upstream-initiated transcripts from treated EBV or KSHV latent cell lines. **(A)** Strategy to identify putative E0-containing transcripts from EBV and KSHV latent cell lines. To detect putative E0-containing transcripts, RNA was prepared from untreated cells or cells treated with reactivating stimuli for the indicated time. cDNA was generated and amplified with a forward primer positioned upstream of the G50/Rta/BRLF1 Exon1-proximal promoter and reverse primer in E1 or E2. The indicated products were cloned and sequenced to confirm the identity of spliced upstream-initiated transcripts. **(B)** cDNA generated from Akata cells treated with anti-IgG was used for PCR with the indicated primers. The indicated products are schematically represented. **(C)** cDNA generated from

BCBL-1 cells treated with TPA for the indicated times was used for PCR with the indicated primers. The exon structures of the amplified products are schematically represented.

Figure 8. Exon 0 extends the EBV and KSHV G50 reading frames. **(A)** Translation of the observed EBV transcript using an ATG in exon 0 (gray) provides an additional 31 amino acids to the N-terminus of the EBV BRLF1 Exon2 reading frame (black). **B)** Translation of the observed KSHV exon 0-containing transcript A. Exon 0 and exon1 (gray) both extend the Rta exon2 reading frame (black).

Figure 9. G50pKO virus establishes latency *in vivo* but exhibits a severe reactivation defect. **(A)** Real-time PCR analysis of splenocytes from mice at day 16 following infection with the indicated virus. Establishment of latent infection is determined by quantification of relative G50 copy number (compared to GAPDH) in splenocytes from infected animals. **(B)** Ex vivo reactivation analysis to determine the frequency of cells reactivating from latency upon explant to MEF monolayers. Reactivation is scored by the presence of CPE.

Figure 10. Bisulfite PCR analysis of CpG methylation in regions containing the proximal and distal G50 promoters. Bisulfite-treated DNA from MHV68-infected splenocytes at the indicated times post-infection or from MHV68-positive latent cell lines was amplified, cloned, and sequenced to determine the frequency of methylated CpGs in the distal versus proximal promoter regions. A circle represents a CpG dinucleotide and the genomic position indicated above each column. Open circles represent unmethylated cytosines, and filled

circles represent methylated cytosines. Each row represents the sequence of an individual clone.

Figure 11. G50pKO virus reactivates from peritoneal exudate cells following intraperitoneal infection. Female C57BL/6 mice 6-8 weeks of age were infected with 1000pfu G50pKO or G50pKO.MR virus by intraperitoneal injection. Splenocytes and PECs were harvested at day 18 following infection and assessed for establishment of and reactivation from latency by limiting-dilution assays. **A)** Splenocytes and PECs were plated in serial dilutions and subjected to nested PCR to detect G50. The percentage of genome positive cells in each dilution was used to calculate the frequency of genome-positive cells as in Ref.45. **B)** Splenocytes and PECs were plated in serial dilutions onto MEF monolayers as in Fig.9. The percentage of wells exhibiting cytopathic effect in each dilution was used to calculate the frequency of cells reactivating from latency. Mechanically disrupted cells were plated in parallel for each virus and cell type and verified the absence of preformed infectious virus (data not shown). Data are representative of at least two independent experiments with at least four mice per group, and error bars were generated using SEM.

2.VII FIGURES

1. Conservation of G50/BRLF1/Rta coding region among gammaherpesviruses
2. Generation and confirmation of MHV68.G50pKO and MHV68.G50pKO-MR viruses
3. MHV68.G50pKO virus replicates *in vitro*
4. RACE and RT-PCR analyses identify an additional upstream G50 exon
5. Promoter activity in region immediately 5' to MHV68 E0
6. Quantitative RT-PCR analysis of distal versus proximal promoter-driven transcripts
7. Identification of upstream-initiated transcripts from treated EBV or KSHV latent cell lines
8. Exon 0 extends the EBV and KSHV G50 reading frames
9. G50pKO virus establishes latency *in vivo* but exhibits severe reactivation defect
10. Bisulfite PCR analysis of CpG methylation in regions containing the proximal and distal G50 promoters
11. G50pKO virus reactivates from peritoneal exudate cells following intraperitoneal infection

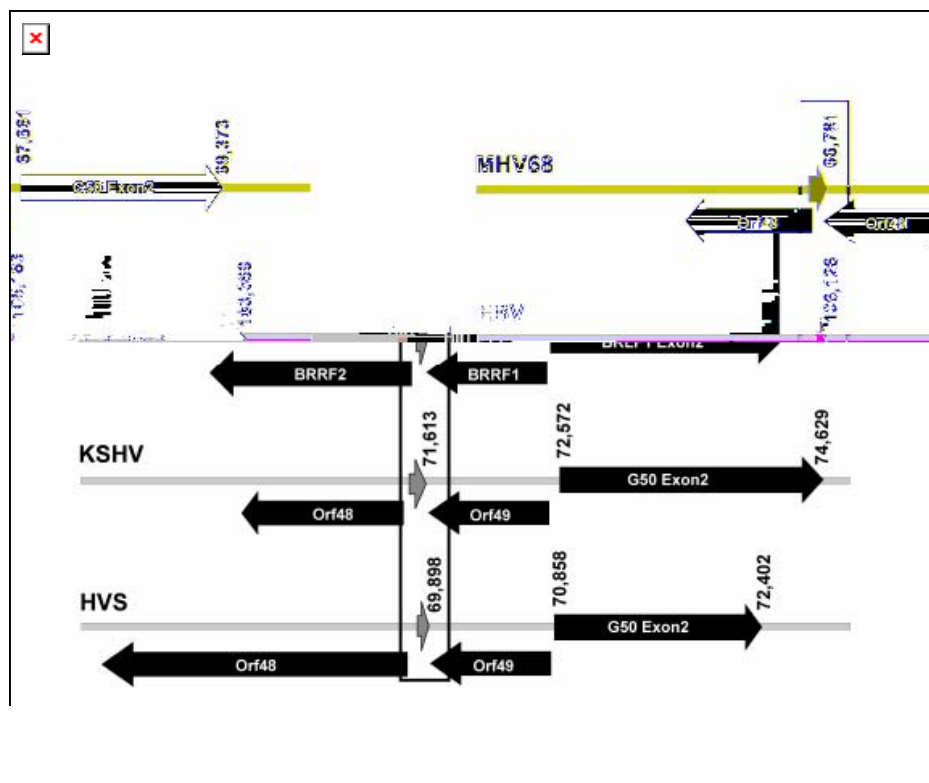


Figure 1

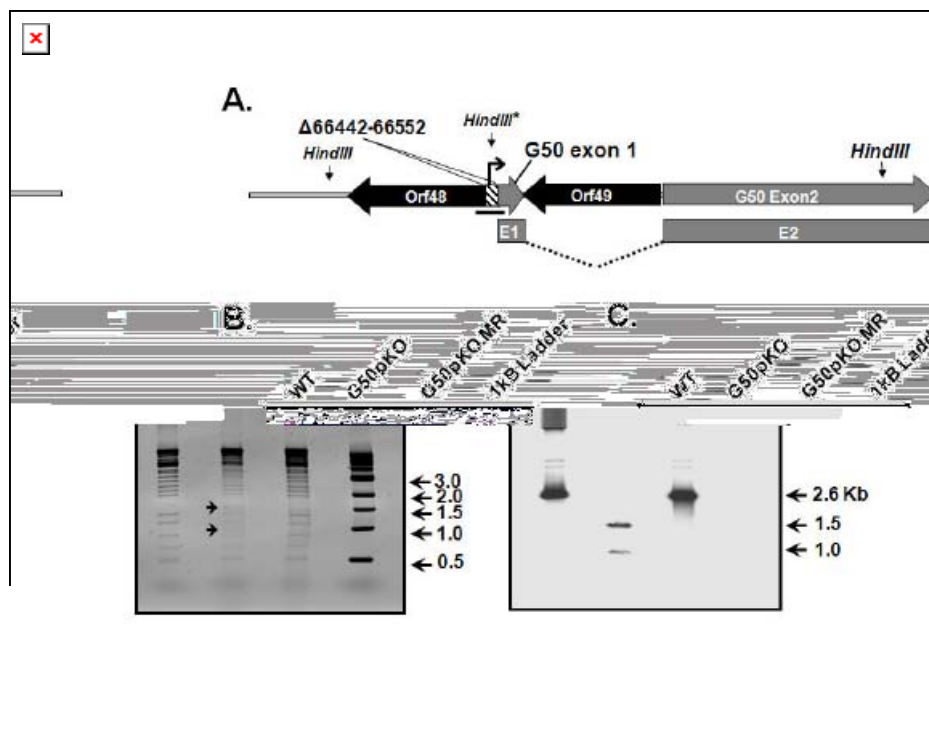


Figure 2

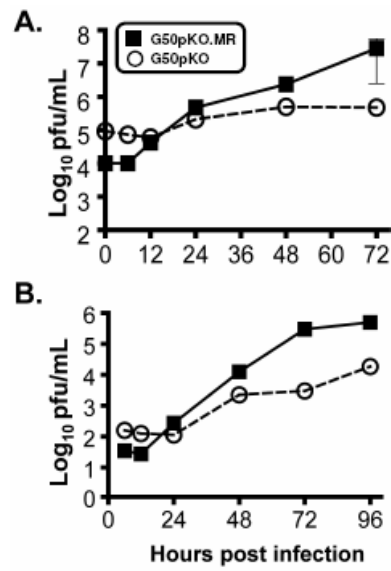


Figure 3

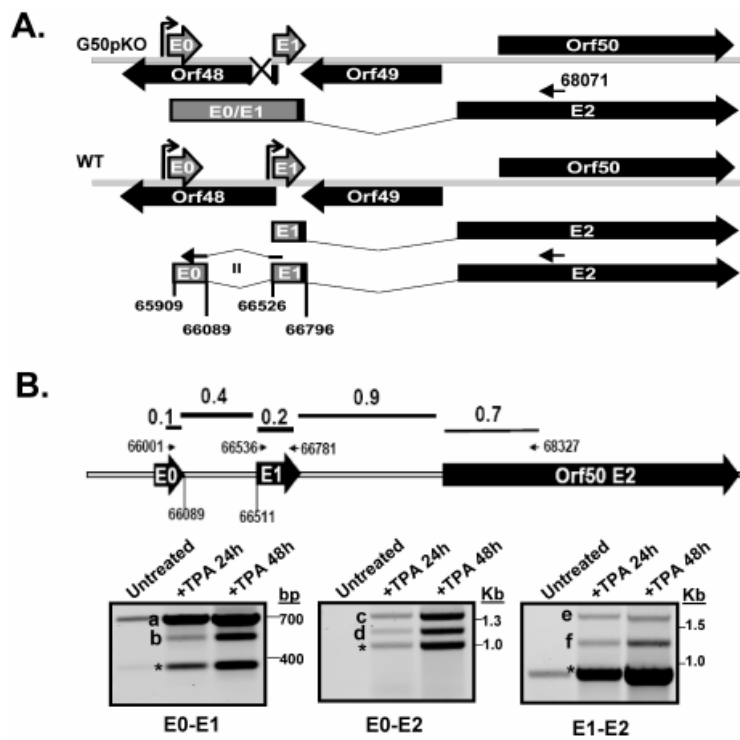


Figure 4

Figure 5

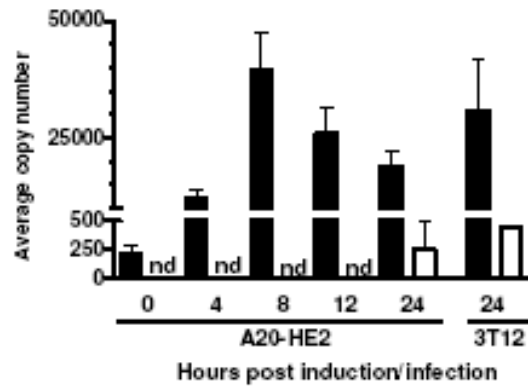
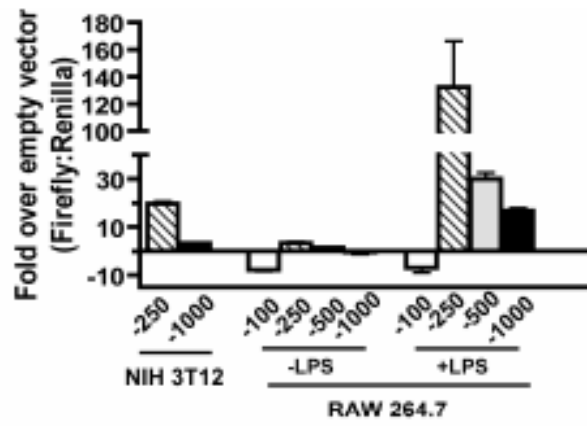


Figure 6

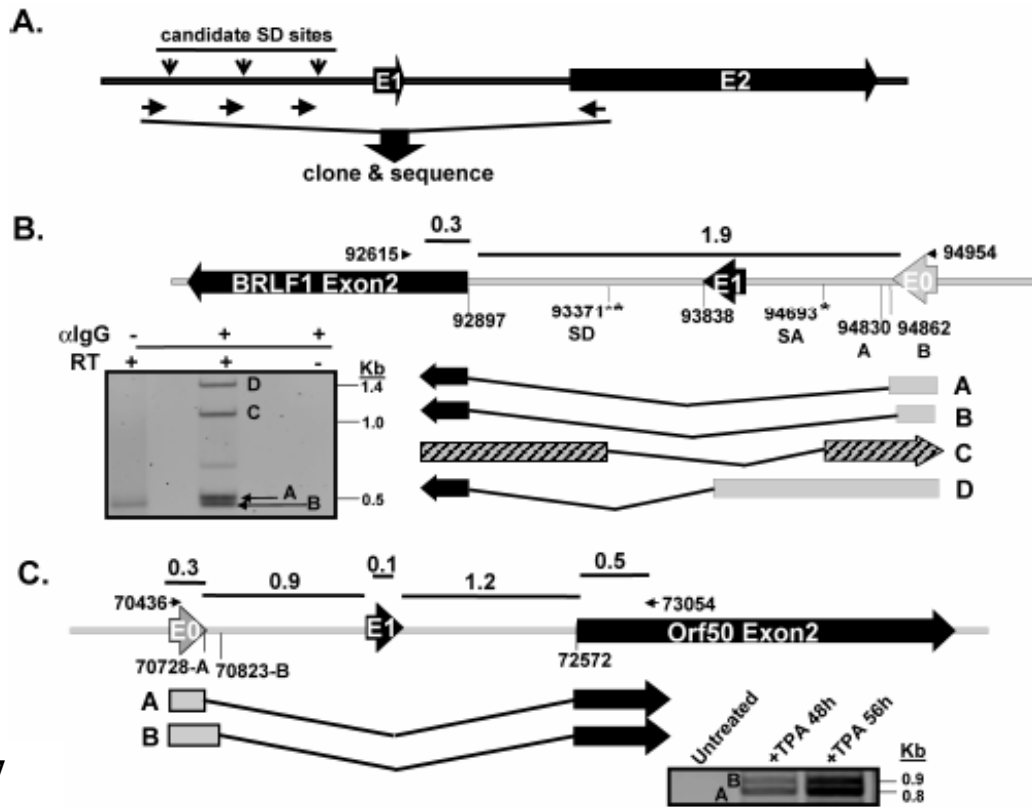


Figure 7

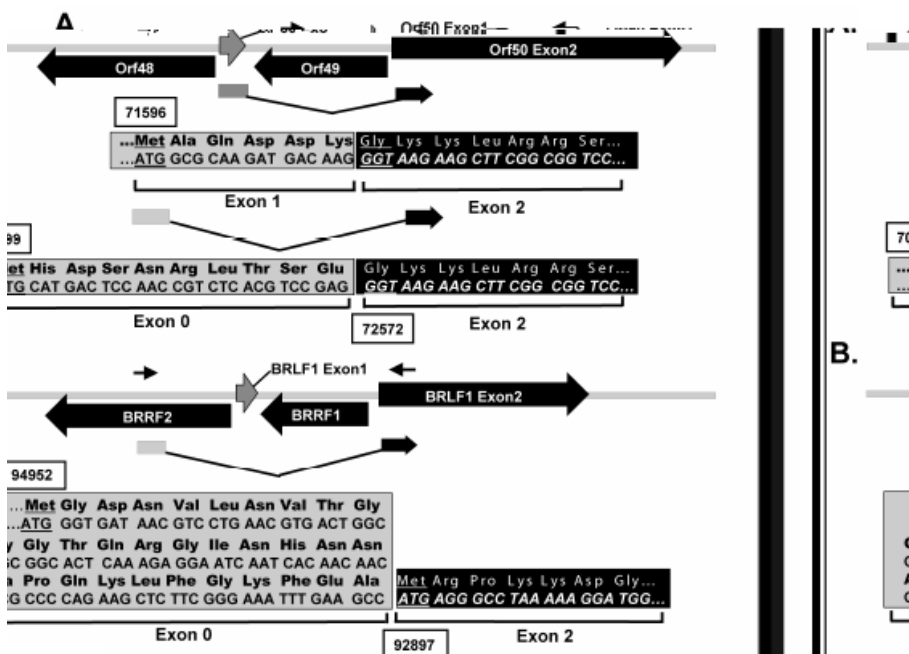


Figure 8

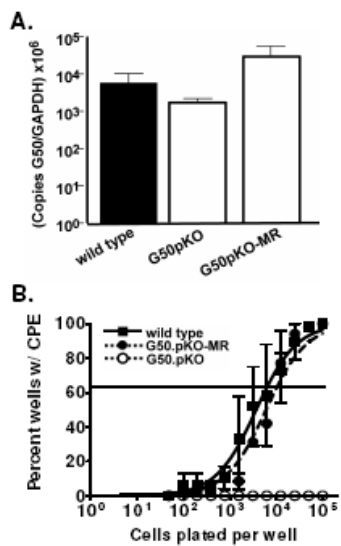


Figure 9

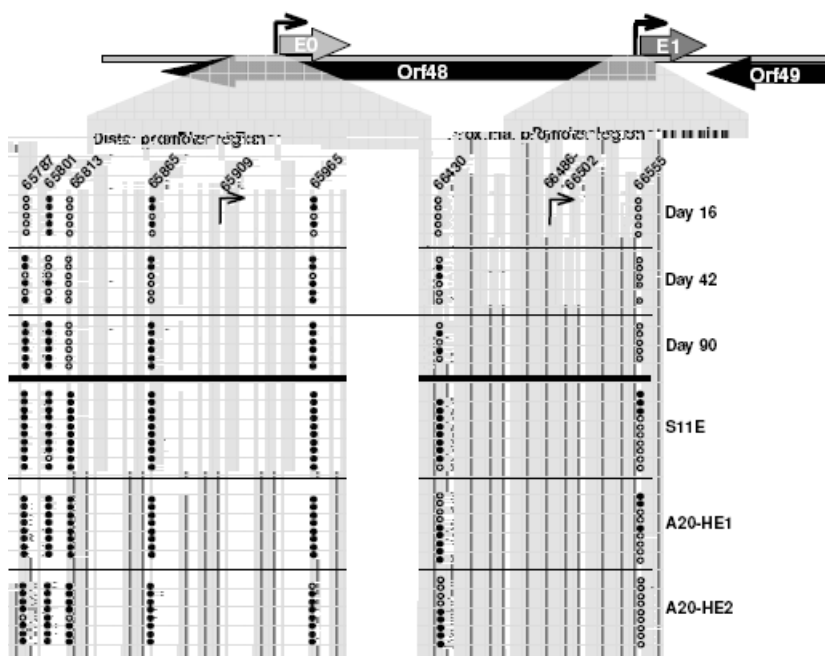


Figure 10

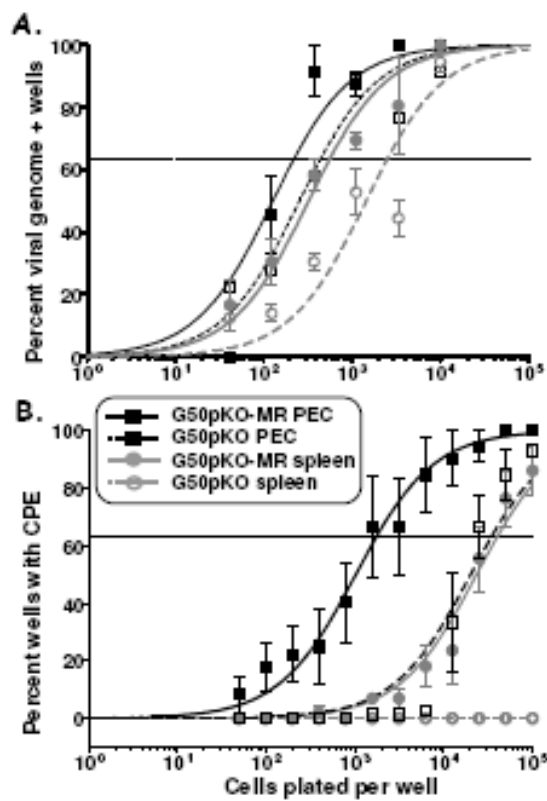


Figure 11

Chapter 3: Deregulated murine gammaherpesvirus gene 50/Rta transcription in vivo in the absence of the de novo methyltransferases DNMT3a and DNMT3b

3.I. Abstract

3.II. Introduction

3.III. Results

3.IV. Discussion

3.V. Materials and Methods

3.IV. Figures

1. Methyltransferase inhibitor treatment induces MHV68 reactivation
2. In vitro methylation reduces distal Gene 50 promoter activity
3. Rearrangement of *Dnmt3a* and *Dnmt3b* alleles in *CD19^{+/Cre} Dnmt3a^{2loxP/2loxP} Dnmt3b^{2loxP/2loxP}* splenocytes
4. Evidence of ongoing lytic replication in CD19+/Cre mice during early latency
5. Gene 50 transcripts are elevated in CD19+/Cre mice at day 18
6. Bisulfite PCR analysis of the distal Gene 50 promoter region at day 18
7. Genome frequency at day 42 post-infection
8. Bisulfite PCR analysis of the distal Gene 50 promoter region at day 42 post-infection
9. Bisulfite PCR analysis of the v-cyclin and v-bcl2 promoter region at days 18 and 42 post-infection

3.VII. Figure legends

3.I. ABSTRACT

The role of epigenetic modifications in the regulation of gammaherpesvirus latency has been a subject of active study for more than 20 years. DNA methylation, associated with transcriptional silencing in mammalian genomes, has been shown to be an important mechanism in the transcriptional control of several key gammaherpesvirus genes. In particular, DNA methylation of the functionally conserved immediate-early replication and transcription activator (RTA) has been shown to regulate Epstein-Barr virus and Kaposi's Sarcoma-associated herpesvirus Rta expression. Here we demonstrate that the murine gammaherpesvirus (MHV68) homolog, encoded by gene 50, is also subject to direct repression by DNA methylation, both in vitro and in vivo. We observed that treatment of MHV68 latently B cell lines with a methyltransferase inhibitor induced virus reactivation. In addition, we show that methylation of the recently characterized distal gene 50 promoter represses activity in a murine macrophage cell line. To evaluate the role of de novo methyltransferases (DNMTs) in the establishment of these methylation marks, we infected mice in which conditional DNMT3a and DNMT3b alleles were selectively deleted in B lymphocytes. Mice lacking functional DNMT3a/3b in B cells exhibited hallmarks of deregulated lytic virus replication, including increased splenomegaly and the presence of infectious virus in the spleen at day 18 following infection. In addition, total gene 50 transcripts were elevated in the spleens of these mice at day 18 - which correlated with hypomethylation of the distal gene 50 promoter. However, by day 42 post-infection aberrant virus replication was resolved and we observed wild-type frequencies of viral genome positive splenocytes in mice lacking functional DNMT3a/3b in B lymphocytes. The latter correlated with increased CpG methylation in the distal gene 50 promoter, which was

restored to levels similar to littermate controls harboring functional DNMT3a/b alleles in B lymphocytes - suggesting the existence of an alternative mechanism for de novo methylation of the MHV68 genome. Importantly, this DNMT3a/DNMT3b-independent methylation appeared to be specifically targeted to the gene 50 promoter, as we observed that the promoters for MHV68 gene 72 (v-cyclin) and M11 (v-bcl2) remained hypomethylated at day 42 post-infection. Taken together these data provide the first evidence of the importance of DNA methylation in regulating gammaherpesvirus RTA/gene 50 transcription during virus infection in vivo, and provide insight into the hierarchy of host machinery required to establish this modification.

3.II. INTRODUCTION

Herpesviruses are large, double-stranded DNA viruses characterized by distinct lytic and latent stages. Upon initial infection the virus undergoes several rounds of lytic replication, after which it establishes a latent infection in which viral gene transcription is limited and tightly controlled. Intimately associated with the lytic-latent cycle is virus reactivation, the process by which lytic replication is reinitiated from a latent viral genome. The mechanisms leading to virus reactivation are only partially understood, but probably involve a combination of extrinsic cellular signals and a complicated intrinsic cellular and viral protein milieu. It is clear, however, that regulation of lytic replication and therefore virus reactivation is key to herpesvirus biology, as the ability to establish a quiescent latent infection is essential to herpesvirus survival in the host.

Among the three families of herpesviruses, (alpha, beta, and gamma), the gammaherpesviruses share the propensity to infect lymphocytes. In the case of the human gammaherpesviruses, Epstein-Barr virus (EBV) and Kaposi's Sarcoma-Associated Herpesvirus (KSHV), B cells are the primary reservoir for long-term latency (4). Although *in vitro* infections and transformed cell lines from patients have been valuable tools in the study of gammaherpesvirus biology, the field is limited by the inability to thoroughly study viral pathogenesis in the context of its natural human host. The development of murine herpesvirus 68 (MHV68) as a model system has provided the opportunity to study a naturally-occurring gammaherpesvirus in laboratory mice. MHV68 shares significant sequence homology with other gammaherpesviruses, and infection with MHV68 recapitulates many important aspects of human gammaherpesvirus infection, including B-cell

tropism, periodic reactivation, and an association with lymphomagenesis in immunocompromised mice (120, 167, 184).

Although KSHV, EBV, and MHV68 encode several unique proteins, one of the most conserved regions in gammaherpesviruses is that encompassing gene 50 in MHV68, also known as Rta (KSHV and EBV). The immediate-early gene 50/Rta protein is a potent transcriptional activator of both viral and cellular genes, and has a key role in lytic replication (151). Gene 50/Rta is required for lytic replication of MHV68, KSHV and EBV, and its expression is sufficient to induce reactivation in latently infected cell lines (97, 128, 158, 188, 189). Due to its potent ability to drive lytic viral gene transcription, gene 50/Rta expression must be tightly regulated for gammaherpesvirus latency to be established and maintained. There are several mechanisms by which this is accomplished, and evidence exists to support a strong epigenetic component in the regulation of gene 50/Rta transcription (8, 19, 22, 29, 56, 57, 95). DNA methylation in particular has been demonstrated to be an important gammaherpesvirus regulatory mechanism for both lytic and latent genes (8, 22). The Rta promoter have been shown to be methylated in KSHV and EBV latently infected B cells, and treatment with methyltransferase inhibitors initiates reactivation in some latently-infected cell lines (6, 22).

DNA methylation, originally characterized in bacteria as a means to protect endogenous bacterial genetic material from self-digestion by restriction endonucleases, can occur at several dinucleotide sequences. In mammals however, the primary modification is methylation of cytosines coupled with guanines, commonly called CpG dinucleotides. The addition of methyl groups to cytosines is accomplished by mammalian DNA methyltransferases (DNMTs). Five DNMTs have been characterized in mammals, but only

three have been shown to have catalytic DNA methyltransferase activity: DNMT1, DNMT3a, and DNMT3b (70). Although DNMT1 has been shown to have the ability to modify unmethylated DNA (known as “de novo” methylation), its primary role is thought to be the maintenance of pre-existing methylation marks present on hemi-methylated DNA following semi-conservative replication. DNMT3a and DNMT3b have therefore been largely classified as the “de novo” methyltransferases, and are crucial to the establishment of methylation patterns during embryonic development following the massive wave of demethylation post-implantation (90). DNA methylation is a crucial regulatory mechanism in mammalian cells and in promoter regions is associated with transcriptional repression. It plays a key role in differentiation, and aberrant DNA methylation is strongly associated with tumorigenesis and disease, therefore making it a subject of intense study in the field of cancer genetics.

We have recently described an additional gene 50 exon and promoter in MHV68, and provided evidence that this additional transcriptional unit is conserved in KSHV and EBV (53). The newly-identified MHV68 “distal” promoter is progressively methylated in splenocytes throughout latent infection. Since virion DNA is unmethylated upon entry into the cell (163), we wished to examine the role of DNMT3a and DNMT3b in establishing methylation patterns at the MHV68 distal gene 50 promoter following infection of B lymphocytes. Using conditional deletion of *Dnmt3a* and *Dnmt3b* alleles specifically in B cells, we demonstrate that the absence of de novo methyltransferases is associated with aberrant lytic replication and hypomethylation of lytic gene promoters during early latent infection. By later times post-infection, lytic replication is resolved and normal latency is established, accompanied by the restoration of methylation at the distal gene 50 promoter,

but not at other lytic gene promoters. These observations suggest a role for DNMT3a and DNMT3b activity during early latent infection, but also demonstrate the existence of alternative de novo methylation mechanisms, highlighting the importance of specifically methylating the distal gene 50 promoter to establish long-term latency.

3.III. RESULTS

Methyltransferase inhibitor treatment reactivates latent MHV68

It has been demonstrated that reactivation can be induced in some EBV and KSHV latently infected B cell lines following treatment with the methyltransferase inhibitor 5-aza-2-deoxycytidine (5azaCdR), presumably due to passive demethylation of the viral genome resulting from inhibition of the maintenance methyltransferase DNMT1 during cell division. To determine the effects of 5azaCdR treatment on latent MHV68 infection, we used murine A20 cell lines latently harboring MHV68 as an *in vitro* latency model (12). The A20-HE1 and A20-HE2 cell lines were cultured for 72 hours either with or without 5azaCdR treatment and analyzed for evidence of lytic antigen expression. Probing with a rabbit anti-MHV68 antisera revealed induction of virus replication-associated antigens in both A20-HE cell lines (Fig.1A). The specificity of this induction was confirmed using an antibody specific for the viral DNA polymerase processivity factor encoded by Orf59 - untreated cells expressed little or no detectable Orf59 protein, while cells treated with either TPA or 5azaCdR expressed the Orf59 protein (Fig.1B). Notably, following treatment with 5 μ M 5azaCdR resulted in levels of Orf59 protein comparable to that observed following TPA treatment. 5azaCdR-induced reactivation was accompanied by expression of distal gene 50 promoter-generated transcripts containing the newly characterized gene 50 E0 exon (data not shown). We recently demonstrated that this promoter is methylated in the latently infected A20-HE cell lines, as well as in the MHV68 latently-infected S11 B lymphoma cell line and in latently-infected splenocytes recovered from MHV68 infected mice (14). Treatment of latent MHV68 with methyltransferase inhibitors may therefore induce reactivation in part by facilitating demethylation of the distal gene 50 promoter.

Distal gene 50 promoter activity is repressed by methylation

Methylation of promoters is associated with transcriptional repression, and is often targeted to promoter regions containing dense CpG distribution. The core region of the proximal gene 50 promoter, defined in murine RAW264.7 macrophages (92), contains no CpGs and thus is unlikely to be regulated by DNA methylation. However, the distal gene 50 promoter contains several CpGs that are targeted for methylation *in vivo* (14). In the murine RAW macrophage cell line, the 250 bp region upstream of the gene 50 exon 0 conveys the greatest promoter activity and contains only 4 CpGs (Fig.2A). To determine if methylation of these few sites could repress distal gene 50 promoter activity, we performed reporter assays using the pCpG luciferase vector containing the 250bp distal gene 50 promoter region following *in vitro* methylation with M.SssI methyltransferase. The pCpG-Basic vectors are devoid of CpGs (82), thus allowing targeted methylation of cloned promoter sequences *in vitro* using the bacterial CpG methyltransferase M.SssI treatment followed by transfection of target cells. This approach eliminates arduous and inefficient patch-methylation techniques (e.g., methylation cassette assay) necessary with reporter vectors containing CpGs to avoid the repressive effects of a methylated vector backbone (82). Mock-methylation (in the absence of M.SssI) did not alter either basal or LPS-induced promoter activity from that of the un-manipulated vector. M.SssI-treatment reduced basal distal gene 50 promoter activity, and also repressed the strong induction seen following LPS treatment of transfected cells. This suggests that despite the sparse distribution of CpGs within the distal gene 50 promoter region, DNA methylation is still capable of repressing gene 50 promoter activity.

Deletion of the de novo methyltransferases DNMT3a and DNMT3b in B cells results in persistent MHV68 replication

Our laboratory has studied MHV68 infection in several conditional animals using a recombinant virus expressing Cre-recombinase from a CMV promoter-driven expression cassette introduced into a phenotypically “neutral” locus of the viral genome located between Orf27 and Orf29b. Since deletion of *Dnmt3a* or *Dnmt3b* results in either early-postnatal or embryonic lethality respectively, we had originally intended to study the effect of de novo methyltransferase deletion in *Dnmt3a*^{2loxP/2loxP} or *Dnmt3b*^{2loxP/2loxP} animals infected with MHV68-Cre which would result in deletion of these methyltransferases only in MHV68 infected cells. However, RT-PCR experiments on sorted splenocyte populations revealed that these enzymes are expressed in naïve B cells (data not shown). We therefore reasoned that pre-existing DNMT3a and DNMT3b may be present at sufficient levels to methylate the MHV68 genome, rendering Cre-mediated deletion of the *Dnmt3a* and *Dnmt3b* genes ineffective in blocking methylation of the viral genome. In order to eliminate DNMT3A and DNMT3B in naïve B cells prior to infection, we crossed *Dnmt3a*^{2loxP/2loxP}, *Dnmt3b*^{2loxP/2loxP}, or *Dnmt3a*^{2loxP/2loxP}*3b*^{2loxP/2loxP} conditional mice (35, 75) to knock-in mice expressing Cre recombinase under the control of the *CD19* promoter from one allele (*CD19*^{+/*Cre*}). *CD19* is a cell surface co-receptor maintained from the early pro-B cell stage through plasma cell differentiation, and is therefore used as a prototypical B cell marker. Genotyping confirmed the presence of rearranged *Dnmt3a* and *Dnmt3b* alleles in *CD19*^{+/*Cre*}*Dnmt3a*^{2loxP/2loxP}*3b*^{2loxP/2loxP} mice, while only the intact, unmodified 2loxP alleles were detected in *CD19*^{+/+}*Dnmt3a*^{2loxP/2loxP}*3b*^{2loxP/2loxP} (*CD19*^{+/+}) littermate controls (Fig.3).

Single deletion of either *Dnmt3a* or *Dnmt3b* in B cells had no impact on establishment of latency or reactivation from latently-infected splenocytes at day 18 following MHV68 infection (data not shown). However, upon harvest of spleens from *Dnmt3a/Dnmt3b* double-conditionals crossed to CD19-Cre expressing mice ($CD19^{+/Cre}Dnmt3a^{2loxP/2loxP}3b^{2loxP/2loxP}$) resulted in a dramatic increase in splenomegaly relative to the $CD19^{+/+}$ littermate controls (Fig.4A). Splenomegaly is a common feature of EBV-induced infectious mononucleosis, as well as early MHV68 infection, and is associated with inflammatory viral infection and a demand for increased antigen clearance and antibody production. Analysis of MHV68-genome frequency in splenocytes revealed a 5-fold increase in viral genome-positive cells in splenocytes from $CD19^{+/Cre}$ mice relative to $CD19^{+/+}$ controls, from approximately 1/200 to 1/40 viral genome-positive cells (Fig.4B). Frequency of reactivation was also augmented about 7-fold in $CD19^{+/Cre}$ mice (Fig.4C). In this assay, mechanically-disrupted cells were plated in parallel with intact cells to control for the presence of pre-formed infectious virus, which is largely absent in the spleen by day 16 post-infection in wild type mice. As expected, in the $CD19^{+/+}$ littermate control splenocytes there was little or no preformed infectious virus detected, whereas disrupted splenocytes from $CD19^{+/Cre}$ mice contained significant levels of preformed infectious virus (Fig.4C). This abnormally high level of pre-formed infectious virus most likely contributes to both the increased frequency of reactivation and viral genome-positive splenocytes in the $CD19^{+/Cre}Dnmt3a^{2loxP/2loxP}3b^{2loxP/2loxP}$ splenocytes, as well as increased splenomegaly, and suggests that the cessation of MHV68 replication is altered in the absence of DNMT3A and DNMT3B.

The distal gene 50 promoter is hypomethylated in $CD19^{+/Cre}Dnmt3a^{2loxP/2loxP}Dnmt3b^{2loxP/2loxP}$ splenocytes during early latency

Since gene 50 encodes the primary protein required for induction of virus replication, we used qRT-PCR to examine splenocytes for evidence of increased gene 50 transcription in $CD19^{+/Cre}Dnmt3a^{2loxP/2loxP}3b^{2loxP/2loxP}$ mice compared to littermate controls. Total gene 50 transcripts were elevated in $CD19^{+/Cre}$ mice relative $CD19^{+/+}$ littermate controls (Fig.5), suggesting that in the absence of DNMT3a and DNMT3b the distal gene 50 promoter is more transcriptionally active at day 18 post-infection.

We next wished to determine if the presence of infectious virus and increased gene 50 transcripts in the spleens of $CD19^{+/Cre}Dnmt3a^{2loxP/2loxP}3b^{2loxP/2loxP}$ mice at day 18 post-infection was a consequence of compromised methylation in $Dnmt3a/Dnmt3b$ -null B cells. We used bisulfite PCR to assess the methylation status of the 4 CpGs within the distal gene 50 promoter, as well as the single CpG immediately within Exon 0, in $CD19^{+}$ splenocytes from $CD19^{+/Cre}Dnmt3a^{2loxP/2loxP}3b^{2loxP/2loxP}$ mice and $CD19^{+/+}Dnmt3a^{2loxP/2loxP}3b^{2loxP/2loxP}$ littermate control mice (Fig.2A). Nearly half of all CpGs in the distal gene 50 promoter were methylated in B cells recovered from littermate control mice, while less than 4% of these sites were methylated in B cells recovered from the $CD19$ -*Cre* expressing mice (Fig.6). The presence of one or two methylated CpGs in several clones, versus 2 or more sites in clones from $CD19^{+/+}$ mice, suggests that these amplicons are derived from hypomethylated viral genomes within infected cells, rather than pre-formed virions within the cell which would be devoid of any CpG methylation.

Restoration of wild-type infection and distal gene 50 methylation at later times post-infection

Previous studies with transgenic mice and recombinant MHV68 over-expressing gene 50 have demonstrated that overexpression of the gene 50 protein, or failure to properly control lytic replication, results in either a failure to establish long-term MHV68 latency or persistent, high-level viral replication and associated pathologies (26, 36, 101). We therefore analyzed MHV68 genome loads and reactivation at day 42 post-infection to determine if increased lytic replication at day 18 in *CD19^{+Cre}* mice had compromised aspects of latent infection, as well as to determine if aberrant lytic replication was still present. Notably, there was little or no evidence of MHV68 reactivation from splenocytes of either *CD19^{+Cre}* or *CD19^{+/+}* mice at day 42 post-infection, indicating that lytic replication had been largely silenced from that seen in *CD19^{+Cre}* mice at day 18 post-infection (data not shown). Furthermore, by day 42 post-infection the frequency of viral genome-positive cells in splenocytes from *CD19^{+Cre}* mice was equivalent to that of *CD19^{+/+}* littermate controls (Fig.7). This suggested that at some point between day 18 and day 42, transcription of gene 50 had been controlled in such a way that allowed for the efficient establishment and maintenance of MHV68 latent infection, even in the absence of DNMT3a and DNMT3b.

To determine if methylation was still capable of contributing to distal gene 50 promoter silencing, we again performed bisulfite PCR on CD19⁺ splenocytes from mice 42 days post-infection. Surprisingly, the extent of methylation of the distal gene 50 promoter was nearly equivalent between *CD19^{+Cre}* mice and littermate controls, with the exception of a single *CD19^{+Cre}* infected mouse (mouse #3) (Fig.8). This is interesting in that it supports the existence of a DNMT3a/DNMT3b-independent mechanism of de novo DNA methylation

(perhaps mediated by the maintenance methyltransferase Dnmt1). It also further strengthens the hypothesis that this epigenetic mechanism play an important role in regulating MHV68 gene 50 promoter activity, such that selective pressure exists to methylate and thus silence gene 50 expression to allow for the establishment of latent infection.

Dnmt3a/3b-independent methylation is specifically targeted to the distal gene 50 promoter

As discussed previously, the area encompassing MHV68 lytic genes, particularly gene 50, is dramatically CpG-suppressed, suggesting that these regions or the viral genome have been subjected to intense DNA methylation over the course of MHV68 evolution resulting in the loss of CpGs. In an effort to further investigate the importance of methylation in the gene 50 promoter region, we examined the promoter region of two other lytic genes, Orf72 and M11, encoding the viral D-type cyclin and bcl-2, respectively. We have confirmed the promoter activity of this region in the context of v-cyclin (1), and unpublished observations have suggested that v-bcl-2, encoded on the opposite strand of the genome, shares this promoter located between the 5' ends of the two genes (Fig. 9). At day 18 post infection, this region is extensively methylated in *CD19^{+/+}* mice, and much like the distal gene 50 promoter, is hypomethylated in *CD19^{+Cre}* mice and extensively methylated in *CD19^{+/+}* littermate control mice (Fig.9A). However, while the extent of methylation in the gene 50 promoter increases with ongoing latent infection, the methylation pattern of the intergenic region between Orf72 and M11 in *CD19^{+/+}* littermate control mice remains largely unchanged at day 42 (Fig. 9B). Interestingly, this region remains hypomethylated in *CD19^{+Cre}* mice at day 42, suggesting that, unlike the distal gene 50 promoter, methylation of this region does not appear to be required for efficient establishment of long-term latency.

3.IV. DISCUSSION

These studies have demonstrated that DNA methylation plays an important role in the regulation of MHV68 gene 50 promoter activity. Demethylation of the viral genome is associated with reactivation from latently-infected cells, and concomitantly, methylation is associated with distal gene 50 promoter silencing and reduced transcriptional activity both in vitro and in vivo. Because DNA in infectious virions has been shown to be unmethylated, we hypothesized that methylation of the MHV68 genome would require the action of the de novo methyltransferases DNMT3a and DNMT3b. Global deletion of either *Dnmt3a* or *Dnmt3b* results in embryonic lethality or death soon after birth. We therefore sought to examine the effect of deleting the de novo methyltransferases in B cells, the primary targets of MHV68 latency, by *CD19* promoter-driven Cre-recombinase mediated deletion of *Dnmt3a* and *Dnmt3b*. We found evidence of aberrant lytic replication in splenocytes from mice with conditional deletion of these enzymes, as evidenced by splenomegaly, the presence of ongoing persistent virus replication, and increased gene 50 transcription during the early stages of latent infection (day 18 post-infection). The distal gene 50 promoter, which has been shown to be methylated throughout latent infection, was hypomethylated in B cells lacking DNMT3a/3b, supporting the in vitro data demonstrating that DNA methylation can repress distal gene 50 promoter activity. Importantly, aberrant lytic replication was resolved in these animals by day 42 post-infection, accompanied by restoration of distal gene 50 promoter methylation to wild-type levels. The latter observation indicates that there is a DNMT3A/3B-independent mechanism for methylating the distal gene 50 promoter. In contrast, the promoters for two other lytic viral genes (v-cyclin and v-bcl2) remained hypomethylated at both days 18 and 42 post-infection. These data suggest that DNA

methylation is an important mechanism to regulate gene 50 expression, and that alternative mechanisms exist to specifically target de novo methylation to the distal gene 50 promoter in the absence of DNMT3A and DNMT3B.

Loss of DNMT3a/3b expression in B cells does not alter global B cell responses during primary immunization

Upon the initiation of the $CD19^{+/Cre}Dnmt3a^{2loxP}Dnmt3b^{2loxP}$ infections, we had speculated that the hyper-lytic MHV68 phenotype was a result of some perturbation in normal B cell function arising from the deletion of *Dnmt3a* and *Dnmt3b* in these cells. Several studies have demonstrated the importance of B cells in the control of MHV68 infection (26, 36, 47, 179). A previous study using Cre-retrovirus-mediated deletion of *Dnmt3a* and *Dnmt3b* in hematopoietic stem cells (HSCs) revealed a requirement for either DNMT3a or DNMT3b (but not DNMT3a or DNMT3b alone) in maintaining self-renewal capacity (164). This study, however, was examining the effect of deleting *Dnmt3a* and *Dnmt3b* at an early stage of differentiation. In $CD19^{+/Cre}$ mice, the *Dnmt3* alleles would be deleted at the pro-B-cell stage, prior to the migration of B cells from the bone marrow to the periphery. However, it was formally possible that deletion of *Dnmt3a* or *Dnmt3b* would affect some aspect of mature B cell development or function, and that this might result in a failure to properly control MHV68 infection. To ensure that the MHV68 hyper-lytic phenotype was a direct consequence of compromised DNA methylation in the context of MHV68 infection, we examined global B cell responses in $CD19^{+/Cre}$ mice to several non-MHV68 immunogens. Primary immunizations with both OVA-CFA and sheep red blood cells (SRBCs) revealed no gross alterations in either B cell activation, germinal center

formation, or class switching compared to littermate controls (data not shown). Total B cell numbers were also unaltered, and ELISpot assays revealed no overt differences in total numbers of antibody-secreting cells in the spleen. Infection with the arenavirus lymphocytic choriomeningitis (LCMV) also failed to reveal any gross alterations in B cell responses, and also did not induce the augmented splenomegaly seen with MHV68 infection (data not shown). Thus, these control studies indicate that the phenotype observed upon MHV68 infection of *CD19^{+Cre}* mice arises from a direct requirement for DNMT3a and DNMT3b function in the context of MHV68 infection, rather than a compromised or otherwise-altered B cell response.

Relative importance of methylation in regulating gene 50 transcription

The splenomegaly, increased gene 50 transcription, presence of infectious virus, and hypomethylation of the distal gene 50 promoter at day 18 all support an important role for DNMT3a and DNMT3b-mediated methylation of the viral genome. We were surprised, however, to find that distal gene 50 promoter methylation was restored at later time points, and is associated with the resolution of aberrant persistent virus replication. Two possible explanations for this are: (1) the MHV68 genome is targeted for methylation by a DNMT3a/3b-independent mechanism (perhaps mediated by DNMT1), or (2) the observed methylation of the MHV68 genome at late times post-infection arises in cells in which Cre-mediated deletion of the *Dnmt3a* and *Dnmt3b* has been inefficient (i.e., not all alleles have been deleted in an appropriate time frame). We favor the former explanation since the intergenic region between the v-cyclin and v-bcl2 genes remained hypomethylated at day 42

post-infection, indicating the absence of de novo methyltransferase activity in MHV68 infected B cells.

What evidence exists for selective pressure to methylate the gene 50 promoter? As previously discussed, the MHV68 genome is highly CpG suppressed overall. However, the gene 50 locus is even more so, indicating that this region has been subjected to methylation as the virus has evolved, leading to an eventual loss of CpG dinucleotides through mutagenesis of CpGs to TpGs (53). Also, we demonstrate that the distal gene 50, v-cyclin, and v-bcl2 promoter regions are hypomethylated at d18 in DNMT3a/DNMT3b-deficient mice. However, while gene 50 promoter methylation is restored to near wild-type levels by d.42, v-cyclin/v-bcl2 methylation status is not, suggesting that methylation and transcriptional repression of this locus is not the primary means of negative regulation; other cellular or viral factors will suffice. Also, the intergenic region between v-cyclin and v-bcl2 is more CpG-dense, perhaps suggesting that methylation of this segment of the genome has been less aggressive as MHV68 has evolved relative to the gene 50 region. This targeted repression is logical, as expression of gene 50 alone is necessary and sufficient for MHV68 reactivation, while v-cyclin and v-bcl2 have less influential roles in terms of driving virus replication.

Gene 50/Rta/Rp promoter methylation and reactivation--similarities and differences

The role of gene 50 promoter methylation may serve another purpose distinct from transcriptional repression in the context of MHV68 reactivation. Recent intriguing studies have demonstrated that the Z protein of EBV is not only capable of activating a methylated viral promoter, but actually in some cases appears to preferentially do so (8, 60, 79). These

studies are particularly enlightening given a study addressing the role of DNMT3B in EBV promoter methylation. Tao et al demonstrated hypomethylation of both latent and lytic viral promoters in LCLs generated from cells of patients with ICF syndrome, a rare disorder arising from deleterious mutations in the *Dnmt3b* gene (165). The authors were surprised to find that, despite relative hypermethylation of the Rp promoter, LCLs generated from normal cells produced higher levels of Rp-driven transcripts than those generated from ICF patients. Recent studies demonstrating that methylation actually enhances Z-mediated transactivation of Rp help to explain these observations. Our observations are similar to those of Tao et al in that lack of functional DNMT3s results in hypomethylation of the MHV68 distal gene 50 promoter. However, they are strikingly dissimilar in that this hypomethylation is associated with increased gene 50 transcription. In addition, there was no observable phenotype in the single conditional-deletion mice, which may simply reflect the moderate Dnmt3 redundancy that has been observed in other murine methyltransferase studies (122). Unlike KSHV and EBV, a Zta/bZIP protein homologue has not been identified in MHV68. Yet the highly CpG-suppressed MHV68 genome (relative to KSHV and EBV) suggests that the virus has been extensively methylated over time, therefore requiring the evolution of a methylation-resistant reactivation mechanism similar to its human counterparts. We have demonstrated that the proximal gene 50 promoter, which lacks any CpGs in the core promoter sequences, drives gene 50 transcription first during MHV68 reactivation (53), but the precise cellular signals initiating this process are currently unknown. Is the gene 50 product encoded by the proximal-promoter-driven transcript capable of transactivating the methylated distal 50 promoter? Or does it induce sufficient viral replication to overwhelm host methylation machinery and thus passively dilute methylation such that the distal promoter is once again

rendered active? Further characterization of the distal gene 50 promoter will partially answer these questions and is currently being pursued.

Another interesting question addresses the effect of reactivation on methylation status throughout the duration of latent infection. We demonstrated that methylation accumulates in the MHV68 distal 50 promoter region over time. Studies with EBV and KSHV have also described methylated latent genomes in both normal and tumor cells (22, 38, 121, 125, 126). One model proposes that gammaherpesviruses infect naïve B lymphocytes, and thus are exposed to the unique environment of the germinal center following B cell activation. Germinal center B cells express high levels of AID; DNA in these cells is therefore highly susceptible to mutagenesis, especially at methylated cytosines. In the context of an actual infection, it could be that periodic reactivation serves as a “reset” mechanism for viral methylation patterns to avoid potentially deleterious mutations that may result from repeated activation of latently-infected memory B cells. If key regulatory CpGs in the MHV68 distal gene 50 promoter were methylated in this setting, either during establishment of latency or during a reactivation episode, it could lead to a deleterious loss of what appears to be an important gene 50 regulatory mechanism. It would be interesting to determine if a reactivation-incompetent MHV68 virus would accumulate C to T mutations in the context of serial episodes of exogenous B cell activation or other reactivation stimuli, and if these mutations would have crippling effects on normal viral gene regulation.

In summary, these studies have demonstrated that DNA methylation is an important mechanism in regulating MHV68 gene 50 promoter activity. There is a role for DNMT3a and DNMT3b in establishing methylation patterns during early latency, but an alternative mechanism exists to allow for restoration of gene 50 distal promoter methylation and

resolution of lytic replication, facilitating the establishment of long-term latency. Further studies are required to elucidate the contribution of other epigenetic mechanisms to the regulation of this key lytic gene.

3.V. MATERIALS AND METHODS

Ethics statement

All animal experiments were carried out with approval of the Emory University Institutional Animal Care and Use Committee (IACUC).

Viruses, tissue culture, and cell treatments

Wild-type MHV68 (ATCC VR-1465) was propagated in 3T12 fibroblasts and titers determined by plaque assay. Mouse embryonic fibroblasts (MEFs) derived from C57BL/6 embryos, RAW264.7 murine macrophages, and NIH 3T12 fibroblasts were maintained in Dulbecco's modified Eagle's medium supplemented with 10% fetal calf serum, 2 mM L-glutamine, 100 U penicillin per ml, and 100 mg streptomycin per ml. A20-HE1 and A20-HE2 cell lines were maintained in RPMI 1640 medium supplemented with 10% fetal calf serum, 2 mM L-glutamine, 100 U penicillin per ml, and 100 mg streptomycin per ml. A20-HE1 and A20-HE2 cells were maintained under hygromycin selection as previously described (44). All tissue culture was performed in a 5% CO₂ tissue culture incubator at 37°C.

Methyltransferase inhibitor treatments and western blots

Cells were treated with 5-aza-2-deoxycytidine (Sigma) (initially dissolved in DMSO and diluted with distilled, deionized water) for 72 hours at the indicated concentration. Cell equivalents were pelleted and resuspended in radioimmunoprecipitation buffer (50 mM Tris-HCl pH 7.4, 150 mM NaCl, 1 mM EDTA), supplemented with EDTA-free protease inhibitor Mini-Tabs (Roche). Cell lysates were frozen at -20°C. Membranes were blocked for one hour 5% milk/PBS/1% Tween then probed overnight with either rabbit MHV68-lytic antisera or

chicken-derived Orf59 antibody diluted in 5% milk/PBS/1%Tween. After washing, membranes were again blocked, and probed for one hour with horseradish-peroxidase-conjugated donkey-anti-rabbit or donkey-anti-chicken antibodies. Chemiluminescence was induced with ECL Western Blotting Reagents (Pierce) and visualized on film.

In vitro methylation, transfections, and reporter assays

The -250bp of the distal promoter region was amplified using the primers previously described (53), but instead incorporating *PstI* and *HindIII* restriction sites. The insert was cloned into the pCpG reporter vector and propagated in Pir1 chemically competent cells (Stratagene) with Zeocin selection. Vectors were methylated or mock-methylated in the presence (2.5U/ μ g) or absence of M.SssI (2.5U/ μ g) (NEB) in Buffer 2 and 160 μ M S-adenosylmethionine (SAM) at 37C for 4 hours. After 2 hours, additional SAM was added to 160 μ M. DNA was ethanol-precipitated and resuspended in endotoxin-free water. RAW264.7 macrophages were plated at 1.5E6 cells per well in CMEM and transfected the next day (at 75% confluency) with the indicated vector and 5ng of a renilla control plasmid using the LT-1 TransIT reagent (Mirus) according to manufacturer's instructions. Cells were treated with media or LPS (5 μ g/mL) at 24 hours and harvested at 48 hours. Firefly and renilla luciferase activity were read using the Dual Luciferase Kit (Promega) as previously described (53).

Infections, organ harvest, and preparation

See below for generation of *CD19-CreDnmt3a-Dnmt3b* conditional knockout mice. All infections were performed by intranasal inoculation of mice (between 6 and 12 weeks of

age) with 20uL of a 5E4 pfu/mL viral stock (1000pfu) diluted in CMEM. Mice were anesthetized by isoflurane inhalation prior to infection. Mice were sacrificed by isoflurane inhalation and cervical dislocation. Spleens were harvested and splenocytes prepared by homogenization and treated with Tris-ammonium chloride for red blood cell elimination as described previously (179). Splenocytes were immediately used for reactivation analyses, genomic DNA isolation, or stored in cMEM-10% dimethyl sulfoxide at -80°C until prepared for quantitative or limiting dilution PCR analyses.

Generation of $CD19^{+/Cre} Dnmt3a^{2loxP/2loxP} Dnmt3b^{2loxP/2loxP}$ conditional knockout mice

$Dnmt3a^{2loxP/2loxP}$ (75) and $Dnmt3b^{2loxP/2loxP}$ (35) conditional knockout mice (C57BL/6 background) were obtained from Taiping Chen at Novartis and housed at the Yerkes or Whitehead vivarium in accordance with university and federal guidelines. $Dnmt3a^{2loxP/2loxP}$ and $Dnmt3b^{2loxP/2loxP}$ mice were interbred, and the F1 generation bred to obtain $Dnmt3a^{2loxP/2loxP} Dnmt3b^{2loxP/2loxP}$ double-conditional knockouts. Double-conditional knockout mice were bred to $CD19^{+/Cre}$ mice (C57BL/6 background), a kind gift from Klaus Rajewsky (138), to obtain $CD19^{+/Cre} Dnmt3a^{2loxP/2loxP} Dnmt3b^{2loxP/2loxP}$ mice. Colonies were maintained by breeding $CD19^{+/Cre} Dnmt3a^{2loxP/2loxP} Dnmt3b^{2loxP/2loxP}$ mice to $Dnmt3a^{2loxP/2loxP} Dnmt3b^{2loxP/2loxP}$ mice and screening offspring for the *CD19-Cre* transgene using primers 5'-ACGAACCTGGTCGAAATCAGTGCG-3' and 5'-CGGTCGATGCAACGAGTGATGAG-3'. $CD19^{+/+} Dnmt3a^{2loxP/2loxP} Dnmt3b^{2loxP/2loxP}$ offspring (Cre-negative) were used as littermate controls. Mice were screened using DNA extracted from tail biopsies using the Qiagen Blood and Tissue Kit (Qiagen). Genotyping for the non-rearranged *Dnmt3a* locus was performed using the primers 5'-TGCAATGACCTCTCCATTGTCAAC-3' and 5'-GGTAGAACTCAA

AGAAGAGGCGGC-3' and for *Dnmt3b* using the primers 5'-AGAGCACTGCACCACTA CTGCTGGA-3' and 5'-CAGGTCAGACCTCTCTGGTGACAAG-3'. The rearranged, 1loxP *Dnmt3a* allele was detected using the primers 5'-CTGTGGCATCTCAGGGTGATGAGC-3' and 5'-GGTAGAACTCAAAGAAGAGGCGGC-3' and the rearranged 1loxP allele with primers 5'-GAGCTGCTATATGTGCCTCCCTCAG-3' and 5'-CAGGTCAGACCTCTCTGGTGACAAG-3'. PCR was performed using GoFlexiTaq polymerase (Promega) according to manufacturer's instructions with the following parameters: 95C for 5 minutes, 35 cycles of 94C for 30 seconds, 58C for 30 seconds, and 72C for 30 seconds, and 72C for 7 minutes.

Ex vivo limiting dilution assays

To determine the frequency of genome-positive cells in preparations of splenocytes, serially diluted cells were subjected to nested PCR using primers to detect gene 50 as previously described (180). To determine the frequency of cells reactivating from latency, single-cell suspensions of splenocytes from mice at day 18 postinfection were plated in twofold serial dilutions onto MEFs in 96-well plates as previously described (180). At day 21 postplating, each well was assessed for the presence of cytopathic effect (CPE). To determine the frequency of cells reactivating, the percentage of wells with CPE at each dilution was used in a nonlinear regression analysis to calculate the frequency of reactivation per cell by Poisson distribution. Disrupted splenocytes and PECs were also plated in parallel as previously described to determine the contribution of preformed infectious virus to reactivation (179).

Quantitative RT-PCR

RNA from total splenocytes (prepared as above) was isolated using Trizol reagent (Invitrogen). Three or five micrograms of RNA was treated with DNase I (Invitrogen) according to the manufacturer's instructions in a total volume of 50 μ l. Twenty microliters of DNase-treated RNA was subsequently used in first-strand cDNA synthesis using SuperScript II reverse transcriptase (Invitrogen). Five microliters of the cDNA reaction mixture was used in each quantitative amplification reaction mixture. Quantitative PCR was performed using iQ Supermix (Bio-Rad) with the forward primer (5'-GGAATTTCTGCAGCGATGGCCTCT-3') and reverse primer (5'-CCTCTTTTGTTCAGCAGAGACTCCA-3') at 900nM. Taqman probe was used (at 250nM; 5'-6-carboxyfluorescein-CTGGCACGGATCGAAGCAGGTCTAC-6-carboxytetramethyl-rhodamine-3'). PCR was performed with the following cycle parameters: 95°C for 3 min, 40 cycles at 95°C for 30 seconds, 58°C for 30 seconds, and 72°C for 30 seconds, and then 95°C for 1 min. A standard curve was generated using a spliced E0-E1-E2 PCR product amplified from TPA-treated A20-HE2 cDNA under the conditions described below for MHV68 E0-E2 reverse transcription-PCR (RT-PCR) cloned into the pGEMT-Easy vector (Promega). Quantitative RT-PCR (qRT-PCR) was performed in a Becton-Dickinson iCycler and analyzed using Bio-Rad iCycler software.

Bisulfite PCR analyses

Splenocytes from infected mice at day 18 or day 42 post-infection were prepared as above and the CD19⁺ population enriched by magnetic-bead sorting using the B cell isolation kit (Miltenyi Biotech) and the AutoMACS cell separation system (Miltenyi

Biotech). CD19⁺-enrichment was verified by staining with CD19-PE antibody and analyzing by flow cytometry; CD19⁺ cells comprised >85% total cells following magnetic cell separation. Total genomic DNA was prepared from the enriched CD19⁺ fraction by phenol-chloroform extraction following overnight proteinase K digestion. Five hundred nanograms of genomic DNA was bisulfite modified using the EZ-DNA Methylation Kit (Zymo Research) according to manufacturer's instructions. Bisulfite-modified DNA was amplified using AmpliTaqGold DNA polymerase (Applied Biosystems). Each nested and heminested PCR mixture contained 1x AmpliTaq Gold buffer, 3 mM MgCl₂, deoxynucleoside triphosphates (0.2 mM each), and forward and reverse primers (0.2 μM each). All reactions were performed in a Becton Dickinson iCycler with the following parameters: 95°C for 10 min (hot start); 30 cycles of 95°C for 30 seconds, annealing at the indicated temperature for 30 seconds, and 72°C for 1 min; followed by a final extension at 72°C for 7 min. For round 1, 2 μl of bisulfite-modified DNA was used in each 25-μl reaction mixture. One μl of round 1 product was used as the template for the round 2 reaction. For the distal promoter region round 1, the forward primer 5'-ATGATGATTTATTAAAGAATTATGTTTT AGGT-3' and reverse primer 5'-CAACCTCACCAACTTTTACAATAAATA-3' were used. Round 1 annealing was performed at 49C. For gene 50 round 2, the forward primer was the same as for round 1 and the reverse primer was 5' CCCTTAATAACCTAATAAAAAACC CAATA-3'. Round 2 annealing was performed at 50°C with 30 cycles. For the v-cyclin/v-bcl2 promoter round 1, the forward primer 5'-GAGATAATGGTAATATTTATTAAATTATAATAT-3' and reverse primer 5'-CCCACAACATTCCACCTTCAACAAA-3' primers were used for set A at an annealing temperature of 48C, and the forward primer 5'-

GGTGTAGTTTGTAGATTGTAGGTTGTT-3' and reverse primer 5'-CCACAAAATCACCTAAATCTAATCCAAA-3' were used for set B at an annealing temperature of 50C. For round 2, the forward primer 5'-GGTTTATAGTTAAGTGTA TATAGGTTAGTGTGAT-3' and reverse primer 5'-CAACCTACAATCTACAACTACACC-3' were used for set A, and the forward primer 5'-GGTGGAATGTTGTGGGGTGT-3' and reverse primer 5'-CCACAAAATCACCTAAATCTAATCCAAA-3' were used for set B. Annealing temperature for both v-cyclin/v-bcl2 set A and B round 2 was 55C. PCR products were visualized by ethidium gel electrophoresis, purified using the GeneCleanII system as above, and ligated into the pGEMT-Easy vector (Promega). Plasmid DNA was sequenced by MacroGen USA (Rockville, MD) and analyzed using SeqMan alignment software (Lasergene).

3.VI. FIGURES

1. Methyltransferase inhibitor treatment induces MHV68 reactivation
 2. In vitro methylation reduces distal Gene 50 promoter activity
3. Rearrangement of *Dnmt3a* and *Dnmt3b* alleles in *CD19^{+/-Cre} Dnmt3a^{2loxP/2loxP} Dnmt3b^{2loxP/2loxP}* splenocytes
4. Evidence of ongoing lytic replication in CD19+/Cre mice during early latency
5. Gene 50 transcripts are elevated in CD19+/Cre mice at day 18
6. Bisulfite PCR analysis of the distal Gene 50 promoter region at day 18
7. Genome frequency at day 42 post-infection
8. Bisulfite PCR analysis of the distal Gene 50 promoter region at day 42 post-infection
9. Bisulfite PCR analysis of the v-cyclin and v-bcl2 promoter region at days 18 and 42 post-infection

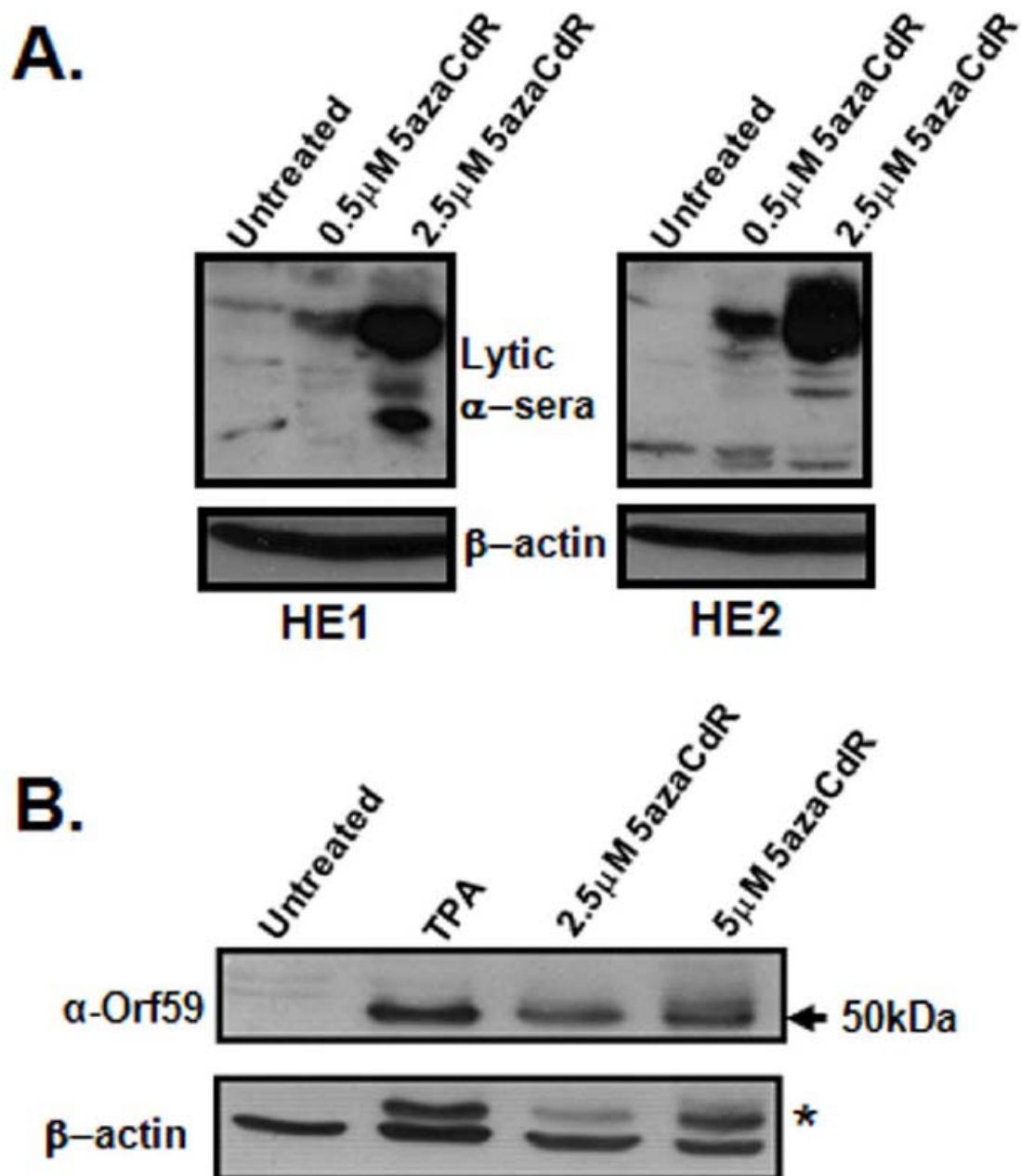


Figure 1

A.

65550
 |
 tatgatgattcatcaaagaactatgccccaggct
 atgctttacctgtcactatagtgctgtcagaaag
 ccataaccaactatgattctgcccaaggacca
 tggcaactagtctctttaatcctatatggagatctt
 ccttaaaggcctctgtgtagaattcctgatcatga
 cttctagtcatatcctgtacacaaacatcatggg
 atgttctatgacttccttttcagcaatacgggctgct
 ggccacgcccagggtactcgaagtgtccagctgg
 agtccattattctttgcaccctctgaatacaatcc
 cgaagcagagctgttggtgagacatgcagtc
 aagattatcttcacaaccagcacatgttcaaac
 atgtgacatgctcagcaaattctcctaattg
 ctttcatagccttgaagactactgggtcctccac
 caggtcatcaagg

66014
 |

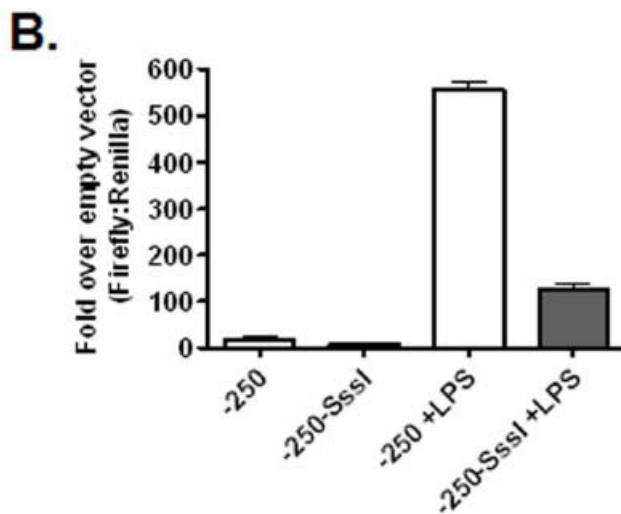


Figure 2

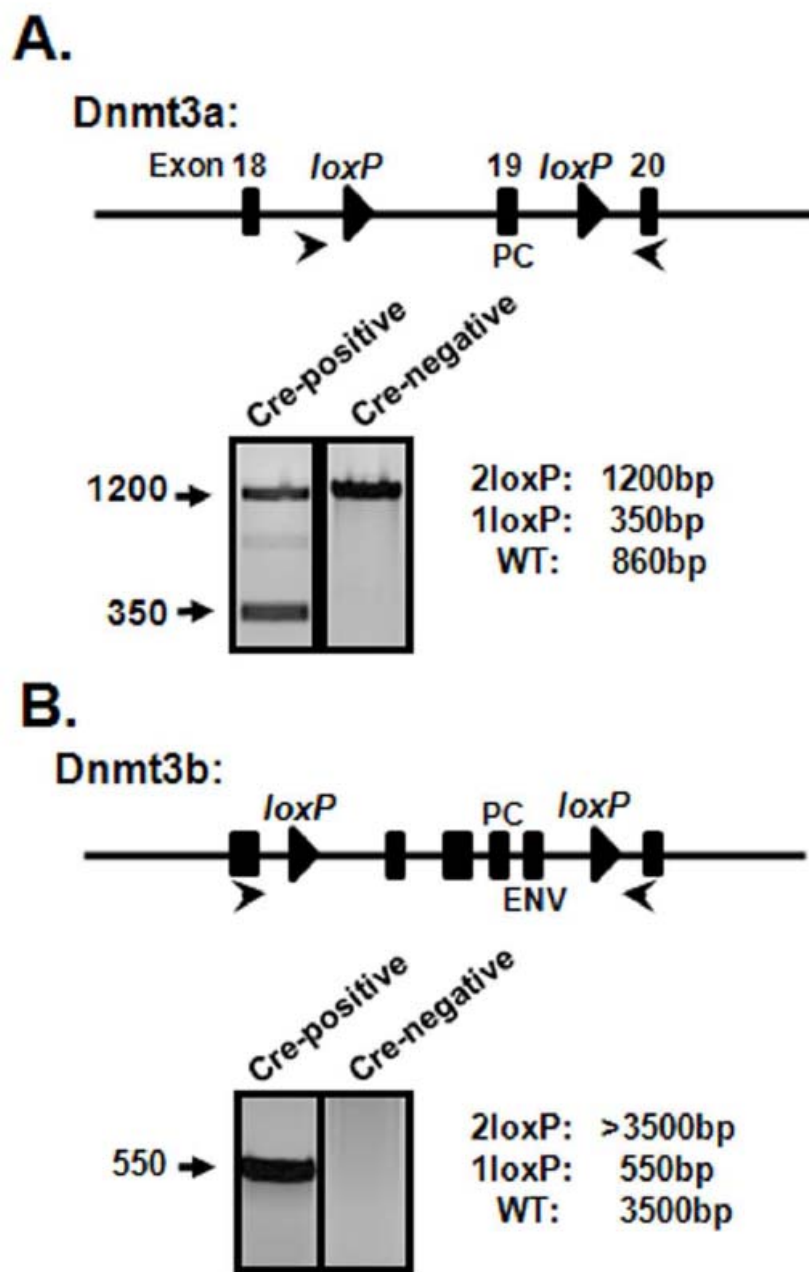


Figure 3

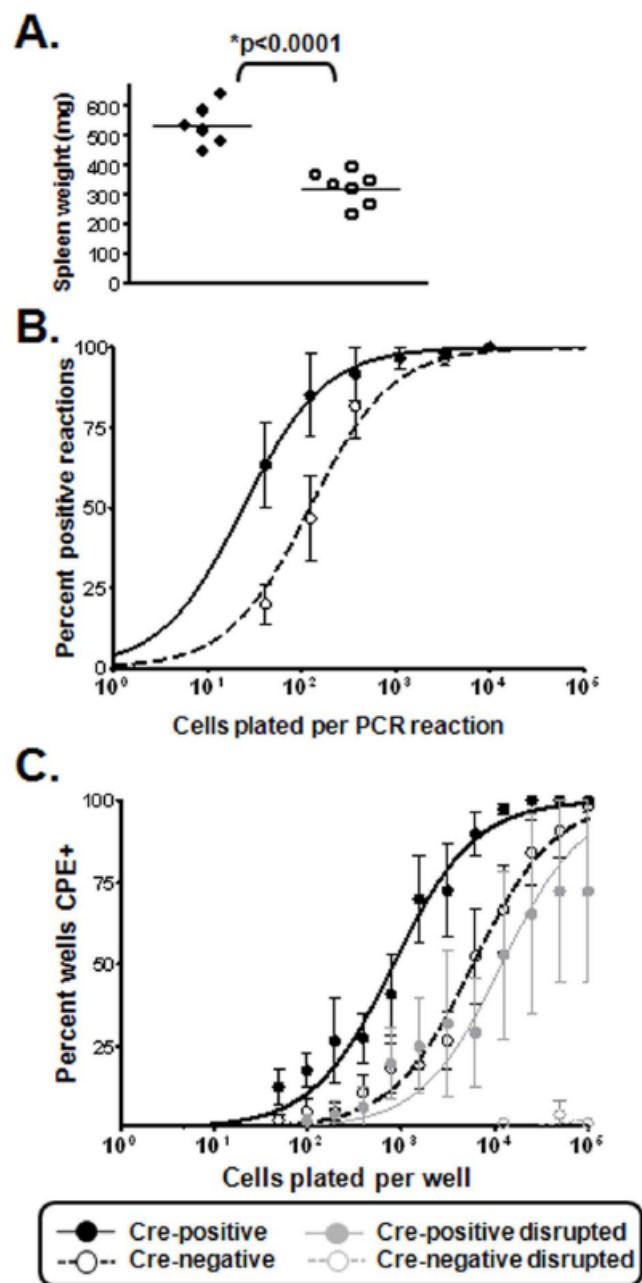


Figure 4

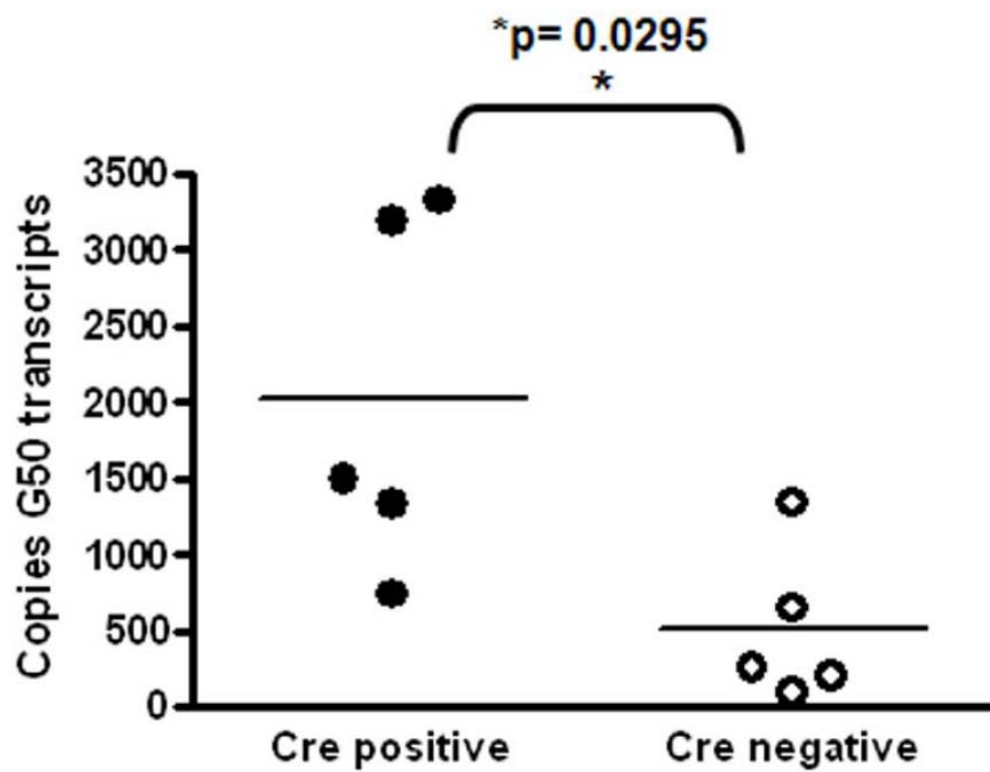


Figure 5

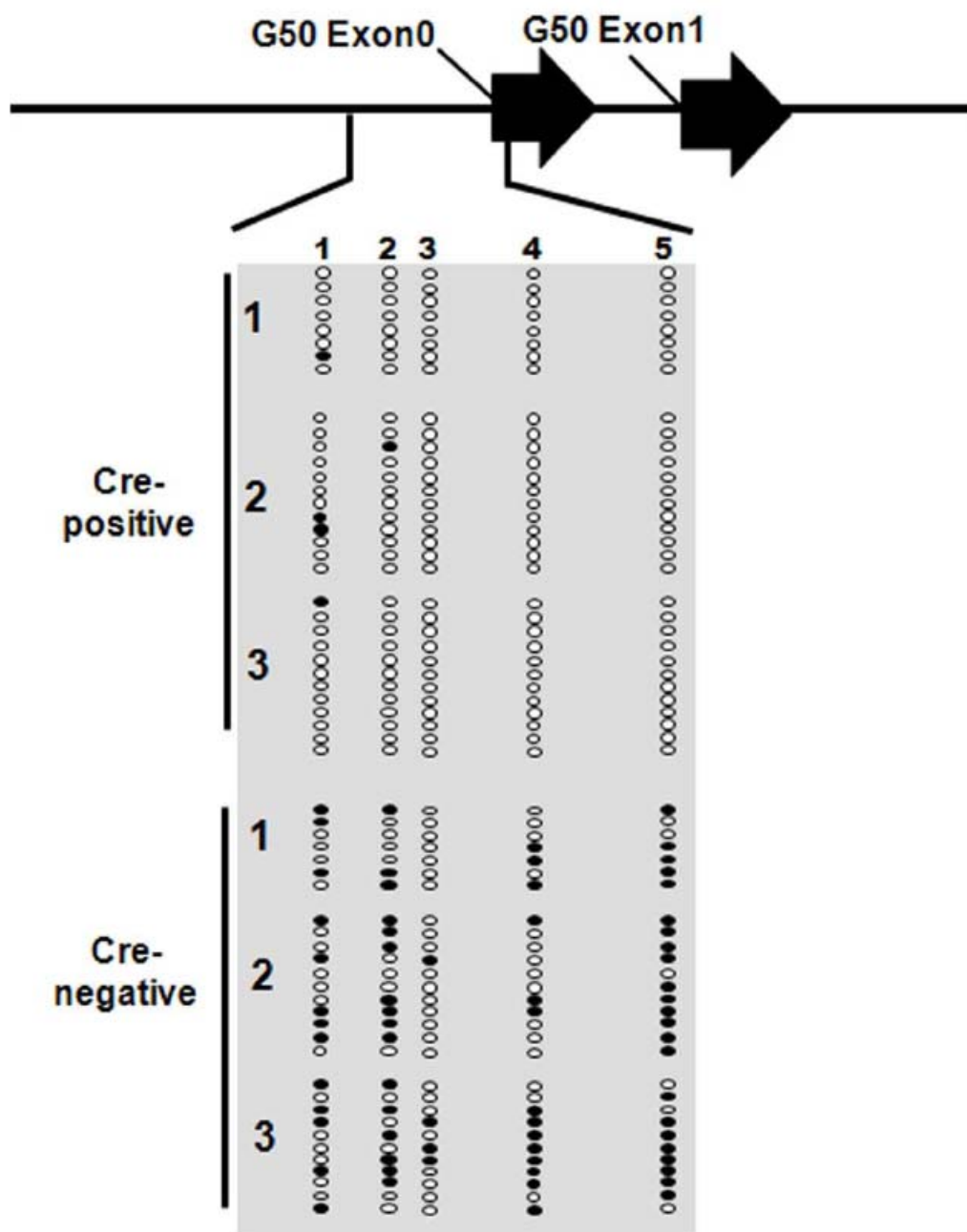


Figure 6

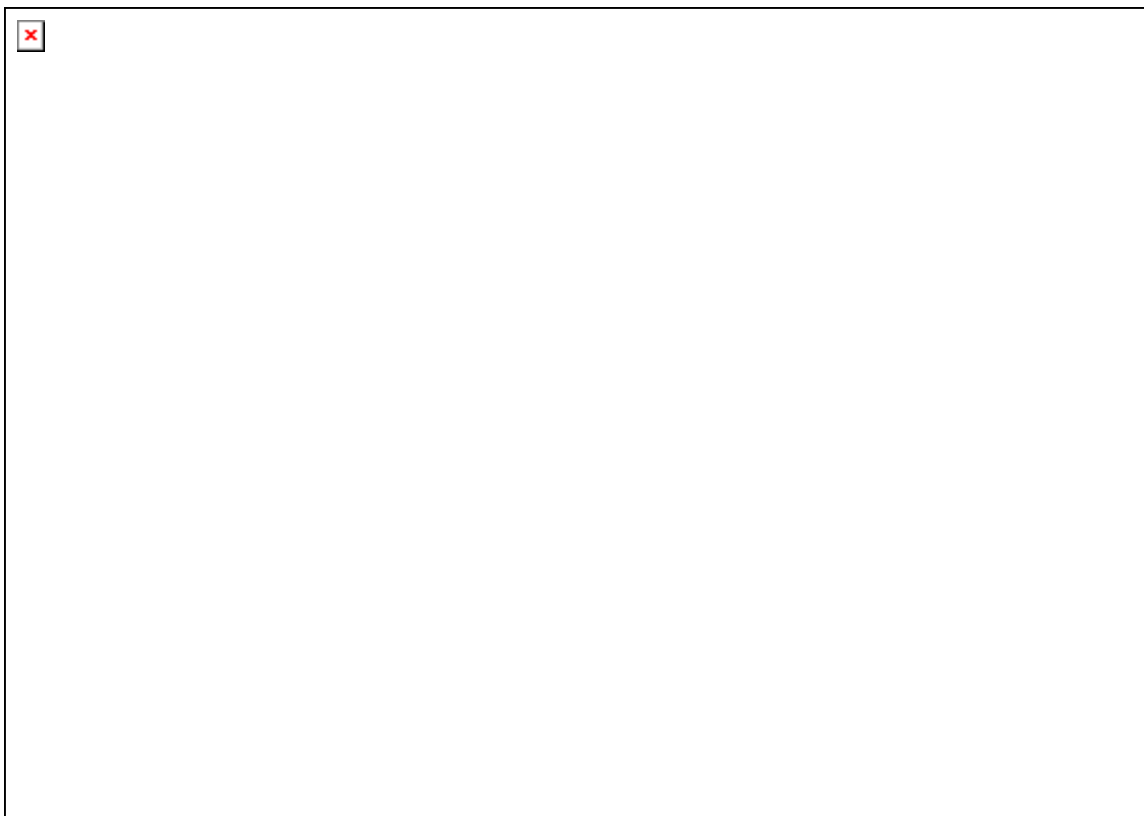


Figure 7

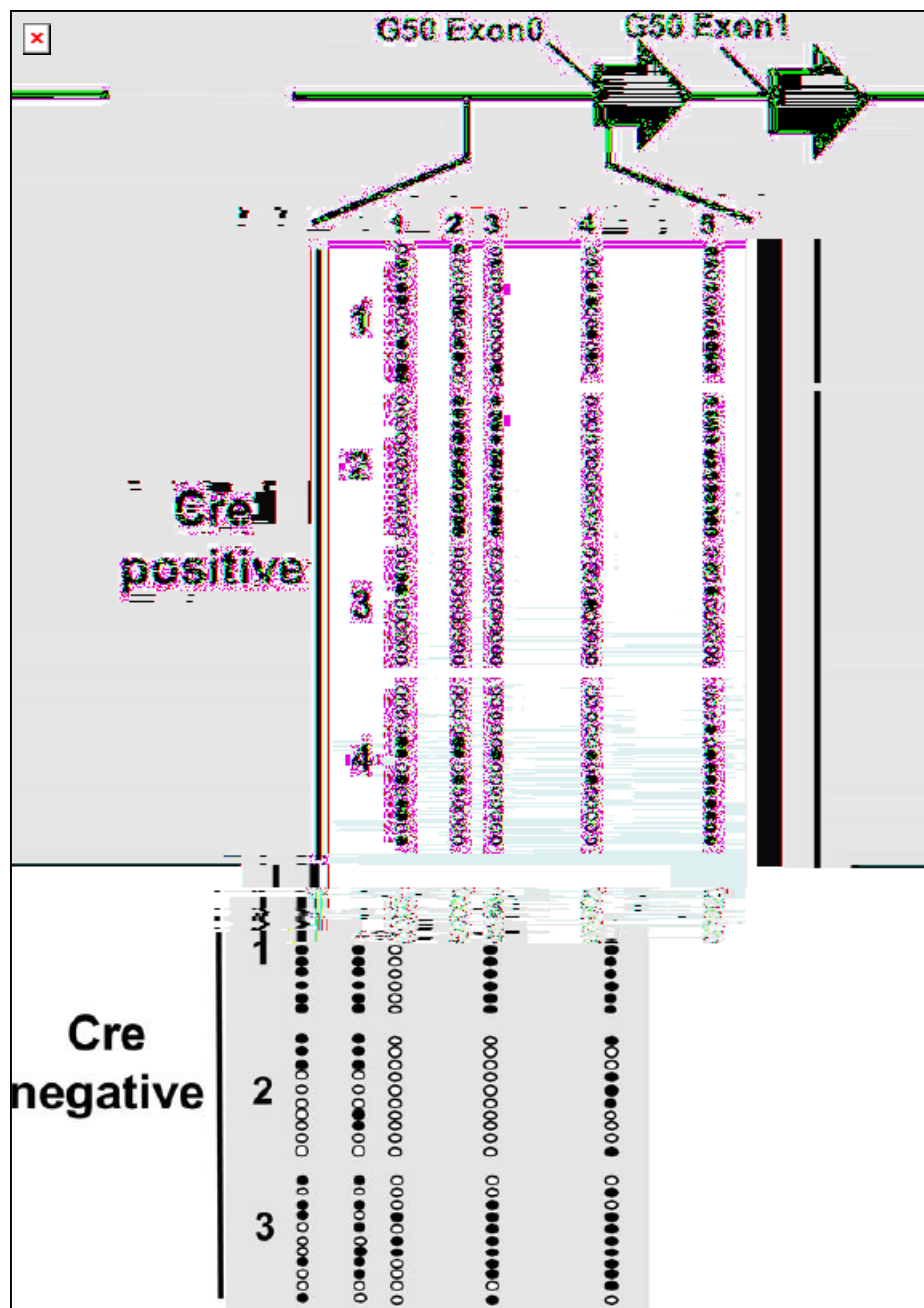


Figure8

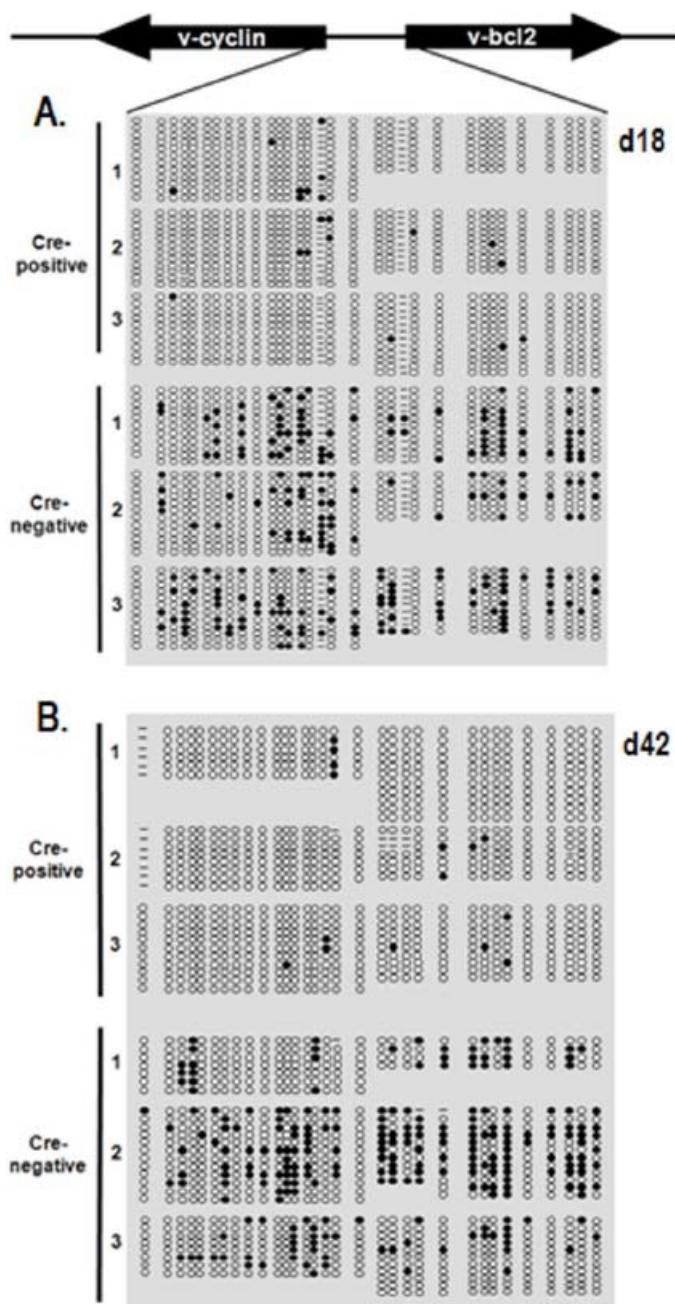


Figure 9

3.VII. FIGURE LEGENDS

Figure 1. Methyltransferase inhibitor treatment induces MHV68 reactivation. (A)

Whole cell extracts from A20-HE1 or A20-HE2 cells treated for 72 hours with 5azaCdR at the indicated concentration and probed with rabbit-derived MHV68-lytic antisera. **(B)** Whole cell extracts from A20-HE2 cells treated for 72 hours with 5azaCdR at the indicated concentration and probed with Orf59 antibody. The asterisk in the beta-actin blot indicates residual Orf59 antibody that was not efficiently stripped prior to β -actin antibody hybridization.

Figure 2. In vitro methylation reduces distal GENE 50 promoter activity. (A)

Sequence of distal gene 50 promoter from bp 65550 to bp 66014. The CpGs examined by bisulfite analysis are indicated (1-5). Exon0 is underlined and the shaded region represents the -250 promoter region examined in B. **(B)** Reporter assay for distal GENE 50 promoter activity in RAW264.7 murine macrophages +/- LPS (5ug/mL), following M.SssI-treatment or mock-methylated. Data are representative of at least three independent transfections from two independent M.SssI treatments.

Figure 3. Rearrangement of *Dnmt3a* and *Dnmt3b* alleles in *CD19^{+/Cre}*Dnmt3a*^{2loxP/2loxP}*

***Dnmt3b*^{2loxP/2loxP} splenocytes. (A & B)** Total genomic DNA was prepared from CD19-enriched splenocytes (see Materials and Methods) from CD19^{+/Cre} (Cre positive) mice or littermate controls (Cre negative). Schematic indicates the location of *Dnmt3a* or *Dnmt3b* exons (rectangles), and loxP sites (triangles). Cre-mediated rearrangement deletes exons

encoding key DNMT catalytic domains; PC (Pro-Cys) and ENV (Glu-Asn-Val). PCR was performed with the primers indicated (arrows), and representative reactions shown.

Figure 4. Evidence of ongoing lytic replication in CD19⁺/Cre mice during early latency.

(A) Increased splenomegaly in Cre-positive mice relative to littermate controls. (B) Limiting-dilution PCR analysis to determine frequency of genome-positive cells. (C) Limiting-dilution analysis of intact and disrupted cells plated onto MEF monolayers to determine the frequency of cells reactivating from latency, and to assess the contribution of preformed infectious virus to CPE. Genome and reactivation frequencies are elevated in Cre-positive mice, and the CPE observed upon plating of disrupted cells indicates ongoing lytic replication.

Figure 5. GENE 50 transcripts are elevated in CD19⁺/Cre mice at day 18. Quantitative RT-PCR for total gene 50 (exon 2) transcripts on cDNA generated from total splenocyte RNA. Transcript levels are elevated in Cre-positive mice relative to Cre-negative littermate controls.

Figure 6. Bisulfite PCR analysis of the distal GENE 50 promoter region at day 18. Total genomic DNA was extracted from purified CD19⁺ splenocytes from mice at day 18 post-infection and subjected to bisulfite PCR analysis. The region analyzed corresponds to bp 65550-66014, upstream of GENE 50 Exon0 (see Fig.2). Each column represents an individual CpG dinucleotide, and each row represents an individual PCR clone. Filled circles

represent methylated cytosines, while open circles represent unmethylated cytosines. Three individual mice were analyzed for Cre-positive and Cre-negative groups.

Figure 7. Genome frequency at day 42 post-infection. Limiting-dilution analysis to determine frequency of genome-positive cells in Cre-positive and Cre-negative mice. Reactivation was negligible in both groups at this time.

Figure 8. Bisulfite PCR analysis of the distal GENE 50 promoter region at day 42 post-infection. Total genomic DNA was extracted from purified CD19⁺ splenocytes isolated from mice at day 42 post-infection and subjected to bisulfite PCR analysis as described in the legend to figure 6.

Figure 9. Bisulfite PCR analysis of the v-cyclin and v-bcl2 promoter region at days 18 and 42 post-infection. Total genomic DNA was extracted from purified CD19⁺ splenocytes from mice at day 18 (A) or day 42 (B) post-infection and subjected to bisulfite PCR analysis. The region analyzed corresponds to bp 102548 to 103915, between the 5' ends of each gene. Each column represents an individual CpG dinucleotide, and each row represents an individual PCR clone. Filled circles represent methylated cytosines, while open circles represent unmethylated cytosines. Dashes represent CpGs whose methylation status was indeterminate upon sequence analysis. Three individual mice were analyzed for Cre-positive and Cre-negative groups.

Chapter 4: CONCLUSIONS & FUTURE DIRECTIONS

Pathologies related to EBV and KSHV infection make understanding these viruses a necessity, yet their strict human tropism severely restricts their study. The development of MHV68 as a model system has the potential to allow insights into gammaherpesvirus pathogenesis which may be otherwise inaccessible. The high degree of homology between MHV68 and its human counterparts lends confidence that those phenomena observed in MHV68 can be translated into KSHV and EBV pathogenesis as well. In the same vein, the recapitulation of well-documented aspects of EBV and KSHV infection in the MHV68 system reinforces its use as a model system. In the first part of this dissertation, the opportunity to genetically manipulate MHV68 and assess the consequences in its natural host led to the identification of an additional transcriptional unit controlling expression of a key lytic protein. These observations led to the identification of a similar element in the human gammaherpesviruses, and emphasize the value of the MHV68 system as a tool for making new discoveries with respect to EBV and KSHV. At the end of Chapter 2, we verified that MHV68, like EBV and KSHV, uses DNA methylation to regulate Rta transcription. With this commonality established, in Chapter 3 we were able to extend these analyses to study how these methylation marks are established, and deduced a role for DNMT3A and DNMT3B in the initial establishment of Rta promoter methylation. Although the usefulness as MHV68 as a model system may still fall under occasional criticism, either due to disparities in sequence homology or relevance to EBV or KSHV biology, these studies demonstrate that study of the mouse virus can help to identify aspects of EBV and KSHV pathogenesis that have previously gone unnoticed. The alternative Rta coding exon and

promoter were identified only upon characterization of a virus which was readily generated following simple homologous recombination using the MHV68 BAC system, and characterized in the context of a naturally permissive infection in murine fibroblasts. Generation of recombinant EBV and KSHV is much more laborious, and lack of a truly permissive system for EBV infection make it unlikely that study of the human gammaherpesviruses would have led to the identification of E0 and the alternative Rta promoter. Likewise, it would be nearly impossible to study the effects of Dnmt3a and Dnmt3b deletion on lytic replication in human cells. Naturally-occurring mutations in these enzymes are extremely rare, and even if Dnmt3a/Dnmt3b-null B cells were isolated, study of KSHV or EBV lytic infection would require that these cells lack endogenous gammaherpesviruses, not likely given the ubiquitous nature of EBV infection. Therefore, MHV68 has been a useful tool for studying both Rta transcription and viral DNA methylation in vivo, and will hopefully provide further insight into the understanding of both these aspects of gammaherpesvirus pathogenesis.

4.I. Rta

4.I.i *Rta transcription, splicing, and the function of Exon0*

All previous work characterizing Rta transcription in EBV, KSHV, and MHV68 has provided the basis for a model in which a short exon (Exon1) splices to a long downstream exon (Exon2); expression of this transcript is driven by the action of a single promoter upstream of Exon1. We generated a virus in which this Exon1-proximal promoter was deleted, and since this was the only known promoter for Rta, expected the virus to have an Rta-null phenotype (i.e. no lytic replication). We were surprised to find that the virus was fit

for lytic growth in fibroblasts and only slightly attenuated compared to wild-type virus. RACE analyses and reporter assays led to the identification of an additional Rta-coding exon (Exon0) and an associated second promoter. In vivo analysis of the proximal-promoter deletion virus showed little to no defect in its ability to establish latency following intranasal or intraperitoneal infection. However, while reactivation from PECs was only slightly affected, this virus was incapable of reactivating from splenocytes, suggesting that the distal promoter may be regulated in a cell-type specific manner (53).

Dual promoters driving Rta transcription has been documented for another gammaherpesvirus, herpesvirus saimiri (HVS) (182). This study demonstrates that in addition to the major promoter upstream of Exon1, which transcribes the spliced product (50a), there is an additional promoter located within the Rta coding region. This promoter drives expression of a shorter, unspliced transcript of unknown function (50b), containing only Exon 2 coding sequence. This promoter appears to be temporally regulated, active later during lytic infection than the upstream promoter. Our studies reveal similarities to HVS Rta transcription in that the distal and proximal promoter also appear to be temporally regulated, as transcripts originating from the distal promoter appear much later and at lower abundance than those from the proximal promoter during reactivation of A20.HE cells. The major difference, however, between the MHV68 and HVS Rta dual promoters is that the MHV68 distal promoter appears to give rise to a functional spliced Rta product which can sufficiently drive lytic replication during both permissive infection and reactivation from latency in PECs.

Complex transcription and splicing in the Rta locus has been observed in human gammaherpesviruses as well. In EBV lytic replication, Zta can be transcribed from a

monocistronic transcript generated from the Zp promoter, or from a polycistronic transcript generated from the Rp promoter and containing both Zta and Rta coding exons (99)--Zta and Rta proteins are generated from this transcript by alternative splicing. In addition, EBV encodes a transcript called RAZ, which is a hybrid containing the c-terminus of Zta and the N-terminus of Rta; this protein inhibits Z transactivation by forming RAZ:Z heterodimers that are unable to bind to Zta-responsive elements (ZREs) (46). In KSHV, the KSHV K8 bZIP protein sharing limited homology with Zta is also transcribed from a multicistronic message containing Rta coding material. This transcript is generated from the Rta promoter and contains the coding exons for the Rta, K8, K8.1a and K8.1b proteins, two variants of a surface glycoprotein. The transcripts encoding these proteins are differentially spliced, but all use a common polyA signal (199). The role of antisense transcription in this region is less well-characterized, but most likely also contributes to regulation of Rta expression. Studies from our laboratory have noted the existence of especially long transcripts hybridizing to antisense probes from the Rta locus (92). This supports the possibility that in addition to encoding the Orf48 and Orf49 proteins, transcripts antisense relative to Rta may serve an additional function by interfering with lytic transcription in this area.

In Chapter 2, we discuss the possible function of Exon0. In EBV, the entire Rta open reading frame lies within Exon2, yet Exon1 and Exon0 are retained as transcriptionally viable units. It is therefore possible that these exons serve a purpose as 5'UTRs and somehow regulate Rta transcription. In the case of KSHV and MHV68, the first ATG in Exon2 is located well within Exon2; using the ATG in Exon1 to translate the spliced Exon1-Exon2 transcript significantly extends the Rta open reading frame, and adds an additional ~60 amino acids to the full-length protein (92, 158). In EBV and KSHV, only the E1-E2 and E0-E2

transcripts were detected, while in MHV68, only E1-E2 and E0-E1-E2 transcripts were detected. Translating the KSHV E0-E2 product using an ATG in Exon0 shows that this transcript is capable of encoding a protein that splices in the same frame as that generated by translation of the E1-E2 transcript. In MHV68, translating the E0-E1-E2 product using an ATG in Exon0 cannot generate in-frame transcripts predicted to give rise to a full-length Rta protein. However, when E1 is removed, the hypothetical E0-E2 transcript encodes a full-length protein splicing in-frame with Exon2 as for KSHV (Fig.1a,b). Although the E0-E2 species was not detected in MHV68 lytic replication or reactivation, it seems unlikely that these observations are without some meaning in the context of E0 function. Switching out E1 for E0 in the Rta transcript alters the amino terminus of the protein, the region encompassing the DNA binding domain in KSHV Rta. Analysis using structure-prediction software predicts that the region encoded by E1 forms a series of alpha-helices, while the substitution with E0 alters the structure to include several beta-strands (Fig.1c). It is therefore tempting to speculate that the function of E0 is to provide some type of alteration in Rta-DNA interactions, perhaps acting as a dominant-negative inhibitor of E1-E2 Rta, or enabling interactions with an alternative set of auxiliary trans-factors.

Attempts to generate and analyze the E0-E2 hypothetical protein are already underway. We have cloned the artificially-spliced E0-E2 transcript into the pCMV-Tag2B overexpression vector, enabling us to express the protein in many cell types and detect its expression using an N-terminal FLAG tag. We plan to use previously established parameters of Rta function to assess whether the E0-E2 protein shares similar abilities with the E1-E2 protein. We will co-transfect the E0-E2 plasmid into 3T12 fibroblasts and RAW 264.7 murine macrophages along with an Orf57 promoter luciferase vector to assess E0-E2s ability

to transactivate the Orf57 promoter (92). We will also nucleofect A20.HE cells to determine if ectopic expression of E0-E2 can induce reactivation from latency analogous to KSHV and EBV Rta. All these studies will be done in parallel with the E1-E2 transcript in pCMV-Tag2B as a control. If we determine that E0-E2 does in fact encode a stable protein, but does not share the same transactivating capabilities as E1-E2, we will further explore the possibility of E0-E2 as a dominant-negative inhibitor of Rta function (analogous to RAZ inhibiting Zta function) by co-expressing both transcripts in the above assays at various ratios. Finally, reporter assays using M.SssI-methylated Orf57 promoter constructs suggest that MHV68 Rta is also capable of transactivating methylated promoters (Fig.2) Therefore, we will explore the possibility that the N-terminus of Rta is involved in the ability of Rta to bind to and activate methylated promoters analogous to EBV Zta by performing the reporter assays mentioned above with E0-E2 and E1-E2 plasmids and a methylated Orf57 promoter luciferase vector (92).

4.I.ii *Transcription factors regulating the Rta distal promoter*

The proximal MHV68 Rta promoter was mapped in murine macrophages and human DG75 B cells (92); it was not performed in murine B cells because the promoter had little or no activity in these cells. This is not surprising, as murine B cells are the primary latency reservoir and are most likely not conducive to lytic replication except in the context of highly specific reactivation cues. It is interesting, however, that the distal promoter has basal activity in macrophages as well, yet no activity in B cells, and the proximal-promoter-deletion virus can reactivate from PECs (primarily macrophages infected) (181) but not splenocytes (primarily B cells infected) (28). This evidence together suggests that the distal and proximal

promoters may in fact have different cellular tropism, and that this cell-specific activity may serve some role in the maintenance of latent infection. Transcriptional Element Search Software (TESS) analysis of proximal and distal MHV68 Rta promoters to identify consensus transcription factor binding sites revealed several interesting candidates for promoter regulation. While the proximal promoter contains Sp1, MEF-2, and GATA-1 binding sites (92), many of which are shared with the KSHV and EBV Rta promoters, the distal promoter contains several consensus binding sites for factors induced during cellular stress. Two notable sites lie within the core 250-bp region with the most promoter activity in macrophages; a hypoxia-inducible factor (HIF) binding site at 65785, and a metal-regulatory transcription factor 1 (MTF-1) site at 65843). The ability of hypoxia to induce gammaherpesvirus reactivation has been reported for KSHV and EBV, and recently for MHV68 as well. Our preliminary data indicates that chemically-induced hypoxia, as well as HIF-overexpression, can induce distal promoter activity (Fig.3). Cells in the mouse peritoneum are hypoxic, and infected PECs hyper-reactivate relative to infected splenocytes (153, 154, 180). We therefore hypothesize that hypoxia helps to activate the distal Rta promoter in PECs, and may contribute to the increased frequency of reactivating cells from this anatomical site. Further studies are underway to determine in detail the role of hypoxia in regulating Rta expression and will include the generation and characterization of a HIF-binding site mutant virus in the context of the proximal-promoter deletion, and also the effects of hypoxia on the kinetics of distal promoter-driven E0-containing transcripts in vivo. Inflammation-induced oxidative stress induces the expression of both HIF-1 and MTF-1, which serves to activate genes involved in zinc transport and stabilize intracellular metal concentration. Several studies have reported cross-talk between the metal-overload and

hypoxia- response (116-119). Consensus HIF and MTF-1 sites are also present in the KSHV Rta promoters (58), and may therefore represent a potential conserved mechanism for induction of Rta transcription in oxygen-stressed cells. In addition to the MTF-1 and HIF sites, there are also strong consensus sites in the distal promoter for C/EBP family members, as well as Blimp-1, a transcription factor induced upon B cell differentiation and involved in plasma cell maintenance (144, 145). The latter is of particular interest given the association between plasma cell differentiation and gammaherpesvirus reactivation (86, 185). Until the involvement of these factors in MHV68 Rta expression is confirmed with molecular and biochemical assays, their predicted binding sites are only material for speculation as to how the distal Rta promoter is regulated. However, as has been seen with HIF-mediated activation, transcription element search programs are useful in providing a starting point for identifying potential cis-regulatory elements.

4.II. DNA methylation in MHV68 infection

4.II.i *Role of de novo DNMTs in B cells*

As discussed in Chapter 3, our initial experimental approach to examine the effects of Dnmt3a and Dnmt3b deletion on MHV68 infection was to infect conditional mice with recombinant MHV68 expressing Cre recombinase. This virus was generated to include a CMV promoter-driven Cre expression cassette cloned into a phenotypically “neutral” locus in the MHV68 genome (111). Lack of any significant phenotype prompted us to examine the expression of Dnmt3a and Dnmt3b in naïve B cells, the assumed initial target for the establishment of latent infection. Although Dnmt3a and Dnmt3b activity is normally downregulated in differentiated cells (123), we found that Dnmt3a and Dnmt3b are

transcribed in naïve B cells but were not readily detected (Fig.4). This may not be surprising, given that 1) naïve lymphocytes represent cells at an intermediate, not terminal, stage of differentiation and 2) Dnmt3a has been reported to retain de novo methyltransferase activity in human 293 epithelial cells (64). We hypothesized that pre-existing DNMT3A and DNMT3B would be sufficient to methylate incoming MHV68 DNA before Cre could even be synthesized from the viral genome, thus masking any phenotype arising from subsequent deletion of the Dnmt3a and Dnmt3b loci. We therefore switched approaches and generated CD19-Cre-Dnmt3aDnmt3b conditional mice to examine MHV68 infection in which the de novo methyltransferases were deleted specifically in naive B cells. As discussed previously, DNA methylation has been shown to play an integral role in regulating several aspects of normal B cell physiology (113). DNA methylation is not only profoundly important during the generation of diverse BCRs during lymphocyte development, but also plays a key role during the life of a mature B cell. This epigenetic modification may have the ability to influence B cell effector function via aberrant silencing or activation of cytokine genes (such as IL-4 or IFN γ), shaping splenic B cell development, or regulating aspects of B cell migration and homing (40, 84, 178). Therefore, the lack of any apparent defect in normal B cell responses in the context of viral infection (MHV68 or LCMV), or following immunization with OVA-CFA or SRBCs was surprising, but strengthened the likelihood that aberrant lytic MHV68 replication was a specific consequence of suboptimal methylation of the Rta promoter.

Given the role of DNA methylation in immunoglobulin receptor rearrangement, and since primary immunizations revealed no apparent defects, we wondered if perhaps Dnmt3a/Dnm3b-null B cells may be compromised for secondary immune responses. To test

this, we used the well-characterized NP-CGG system to assess NP-specific antibody secretion following secondary immunization. Mice were injected intraperitoneally with NP-CGG in alum, and after 30 or more days, received secondary immunizations with NP-CGG via tail vein injection. Four days following secondary immunization, splenocytes and bone marrow were analyzed by flow cytometry and ELISpot to determine if B cell secondary antibody responses were altered in CD19^{Cre/+} mice versus littermate controls. Cells from both compartments in both groups were similar by FACS analysis, as were numbers of NP-specific antibody secreting cells (ASCs) in the spleen (Fig.5a). Serum ELISAs for day 30 following primary immunization and day 4 following secondary immunization were performed to validate these results. Although Cre-positive mice seemed to produce lower quantities of NP-specific IgG than Cre-negative littermates, these differences were not statistically significant (Fig.5b and c). Nevertheless, these results prompted us to evaluate the MHV68-specific IgG response in infected animals at day 150 post-infection, when serum IgG should be maintained at a steady-state concentration. A limited number of animals were readily available for this experiment, but those analyzed did not reveal a failure of Cre-positive mice to elicit an MHV68-specific IgG response (Fig.6a). Further experiments are obviously required to further clarify any potential differences in antibody responses in Cre-positive versus Cre-negative mice.

If there should prove to be differences in antibody production to NP versus MHV68, this could potentially reflect differences in light chain usage between antibody responses to NP and MHV68. Traditional mouse immunoglobulins are composed of κ -light chains (10), but the NP-antibody response relies heavily on λ -light chain usage (93). As previously mentioned, DNA methylation has been shown to regulate κ -chain allelic exclusion (113-

115); therefore, alterations in antibody production may result during responses requiring λ -chain usage in the context of deregulated κ -chain expression. Based on the small sample number of mice analyzed, we cannot formally exclude the possibility that the MHV68 antibody response is somehow altered in Cre-positive mice, and antibody does appear to play a role in limiting viral lytic replication and latency control (47). However, aberrant lytic replication is seen in Cre-positive mice at day 18, before the onset of a detectable MHV68-specific humoral immune response (141). The role of nonspecific antibody generated from polyclonal B cell activation may play a role in controlling lytic replication during early latency (141), but since total IgG and IgM are equivalent in Cre-positive and Cre-negative mice at day 18, it is unlikely that defects in non-specific Ig contribute to the lytic replication phenotype (Fig.6b). We therefore conclude that the increased lytic replication seen in Cre-positive mice is primarily due to hypomethylation of the Rta promoter and not compromised B cell antibody production in the absence of DNMT3A and DNMT3B.

It is still a possibility that cytokine secretion or some other aspect of B cell function is altered in these mice and was not detectable with the assays used. To fully characterize the role of DNMT3A and DNMT3B in mature B cell physiology, it would be interesting to perform cytokine or transcriptional array analyses to determine if B cells from CD19^{Cre/+} mice exhibited any aberrant expression patterns. It may also be interesting to compare their global DNA methylation levels to those of normal mice as a possible reflection of de novo DNMT activity during the developmental stages subsequent to CD19 expression.

Although the role of DNA methylation in B cells was not the primary focus of this dissertation, it is nonetheless relevant to MHV68 infection and the B cell field in general. In the context of gammaherpesvirus infection, in Chapter 3 we reference studies performed

using EBV to generate LCLs from B cells isolated from ICF patients (165). This disease results from a genetic alteration in the *Dnmt3b* gene rendering the enzyme dysfunctional and is associated with severe immune system defects, including a hyper-IgM-like syndrome apparently resulting from a failure of ICF B cells to undergo isotype switching (37). We had originally speculated as to whether $CD19^{Cre/+}$ B cells would also display this defect, which would be detrimental to the control of MHV68 infection as most MHV68-specific antibody is of the IgG2a subtype. Indeed, the $Dnmt3b^{2loxP/2loxP}$ mice used to generate the mice used in this study have been adapted for use in an animal model of ICF syndrome (170). However, as discussed above, we did not observe an obvious class-switching defect in Cre-positive mice in our limited analyses. This may be due to the fact that deletion of *Dnmt3a* and *Dnmt3b* occurs later during B cell development than the germline mutation in ICF patients. Detailed analyses of antibody responses in $CD19^{Cre/+}$ mice would be required to answer these questions with confidence.

4.II.iii. *De novo methyltransferases and human gammaherpesviruses*

With regards to methylation of viral DNA sequences in the study by Tao et al (165), the authors observed hypomethylation of several viral gene promoters, including Rp. In contrast to our observations of hyper-lytic replication, the study noted reduced expression of Rta (but not Zta). As previously discussed, this may be explained by the recent studies demonstrating the Zta-mediated activation of Rp is enhanced by DNA methylation. This mechanism further illustrates differences in how the γ -1 and γ -2 herpesviruses overcome the hurdle of reactivation from latent infection. As discussed in Chapter 2, MHV68 encodes no known homolog of Zta, and while KSHV encodes a bZIP protein, it is not functionally

homologous to Zta. Therefore, while Zta apparently confers EBV's ability to reactivate methylated latent virus, the source of MHV68 and KSHV's ability to do so is less evident. It may lie not in the action of a specific viral protein, but in the sequence composition itself. The proximal promoter in MHV68 does not contain CpGs; therefore, transcription of the E1-E2 Rta form from the proximal promoter in response to some extracellular stimulus may provide the methylation-insensitive lytic switch. In the EBV-ICF study, the Zp promoter does not become methylated in either normal or ICF cells, which supports the hypothesis that transcription of the lytic switch protein itself must be insensitive to methylation, while it uniquely possesses the ability to transactivate methylated promoters. That the Rta encoded by E1-E2 can activate a methylated Orf57 promoter (as discussed above) supports its potential Zta-like role during MHV68 reactivation.

The Tao et al study showed evidence that the EBV latency promoters Wp and Cp were also hypomethylated in LCLs generated from ICF cells. The subject of DNA methylation in MHV68 latent gene transcription was not addressed in our study, but is nevertheless an area of great interest. Previous work from our lab has demonstrated that transcription of the EBNA-1 homologue mLANA is regulated by the action of at least two distinct promoters located in or near the MHV68 terminal repeats (2) (Fig.7a). The placement of these promoters is very much like that of Wp and Cp, and it is therefore tempting to speculate that MHV68 also has distinct latency transcriptional programs, and that DNA methylation plays some role in their regulation. We have data from latent MHV68 cell lines demonstrating that extensive DNA methylation occurs in p2 promoter region, which would be analogous to the Wp promoter, while little to no methylation was detected in the p1 region (Fig.7b). Further analyses are required to more fully determine methylation patterns in this

region, but it is likely that DNA methylation regulates MHV68 latent gene transcription as well. No observable defects or alterations in MHV68 latency were seen by day 42 in CD19^{Cre/+} mice, but detailed transcriptional analyses may reveal changes in latent gene expression that would support this hypothesis.

In addition to its effects on transcription factor binding, DNA methylation plays a key role in shaping overall chromatin structure. Methyl-binding domain proteins (MBDs) have been called the “readers” of DNA methylation because they bind methylated DNA and bring associated proteins to those methylated regions. MBDs interact with chromatin remodeling machinery such as histone deacetyltransferases (HDACs) and histone demethylases that lead to the perpetuation of the transcriptional silencing initiated by DNA methylation (174, 175). In contrast, recent evidence has suggested that MBD-containing complexes may also be involved in relieving transcriptional repression by bringing HDACs and methyltransferases (HMTs) to heterochromatin (192). These multi-protein complexes are often cell-specific, and perform different chromatin-altering functions depending on their components, yet they still retain a MBD protein to facilitate interaction with methylated DNA. The effect of histone modifications on gammaherpesvirus gene transcription is a field of active study, and much effort has been made to understand the role of chromatin in regulating latency (104). In chapter 2, we proposed that the reactivation phenotype seen in splenocytes infected with the proximal-promoter-deletion virus is due to methylation of the distal promoter in these cells (53). However, we have recently performed bisulfite PCR analyses which revealed the same degree of methylation in infected PECs, which are capable of reactivation (Fig.8). Therefore, it seems that DNA methylation alone is not fully responsible for regulating distal Rta promoter activity. Given that DNA methylation patterns are the same in PECs and

splenocytes, yet their proximal-promoter-deletion virus phenotypes are so disparate, it is possible that in addition to regulation by cell-specific transcription factors, there is also cell-specific epigenetic machinery that either A) establishes a more repressed chromatin conformation in splenocytes than PECs, thus creating the block in splenocyte reactivation, or B) more efficiently facilitates the “re-opening” of accessible chromatin in PECs, perhaps mediated by MBDs. Elucidation of chromatin status at the Rta promoters in different cell types may provide some enlightenment. A recent study by Yang et al reports that histone acetylation at the Rta promoter region is sufficient for reactivation from latency in both infected MHV68+ cell lines and in vivo (191). That histone modifications and higher-order chromatin organization play a role in MHV68 infection is undeniable, and will need to be further addressed in future studies.

4.II.iv. *Role of methylation in regulating gammaherpesvirus Rta: Relevance*

From the standpoint of human disease, the study of gammaherpesvirus DNA methylation is important for several reasons. Most apparent is the use of DNA methyltransferase inhibitors (MTIs) such as AZA as treatment for pathologies related to latent EBV infection. When lytic cycle-inducing agents, such as TPA, valproic acid, or AZA are administered in the presence of antiherpesviral agents such as cidofovir, cells undergoing lytic transcription die. This approach has been termed “lytic induction therapy,” and AZA has had moderate success in a clinical setting in the treatment of EBV+ nasopharyngeal carcinoma (18). Understanding of the underlying mechanism and subsequent application of this treatment regimen was only possible given the preceding studies designed to characterize EBV DNA methylation in various cell types and settings.

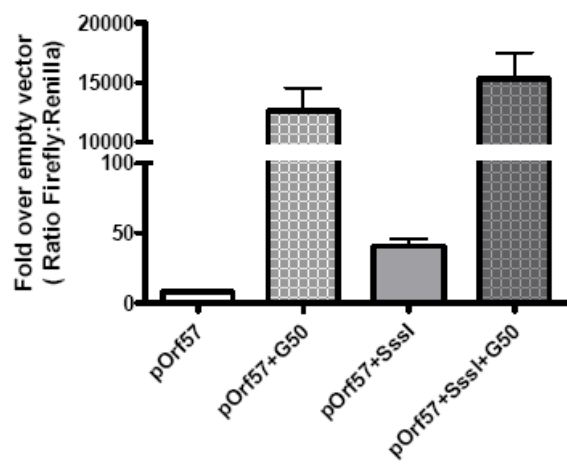
Secondly, the recent studies identifying Zta as a “methylation-enhanced” transcription factor is of relevance to not just the herpesvirus field, but to the field of transcriptional regulation in general (8, 9). Elucidation of the domains which confer this unique ability may lead to the discovery of mammalian transcription factors which also preferentially bind to and activate methylated promoters. Such a discovery could have great implications to pathologies associated with epigenetic deregulation, such as cancer, lupus, and other developmental disorders. That this factor was first described in the context of EBV further emphasizes the value of viruses as tools to understand and highlight important aspects of cell biology.

4.III. Summary

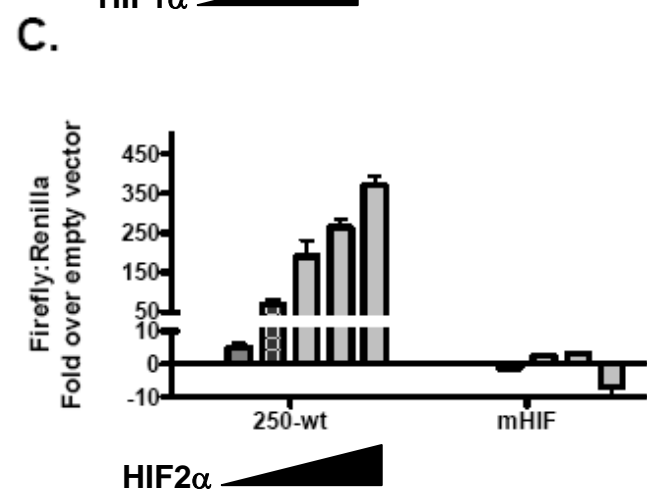
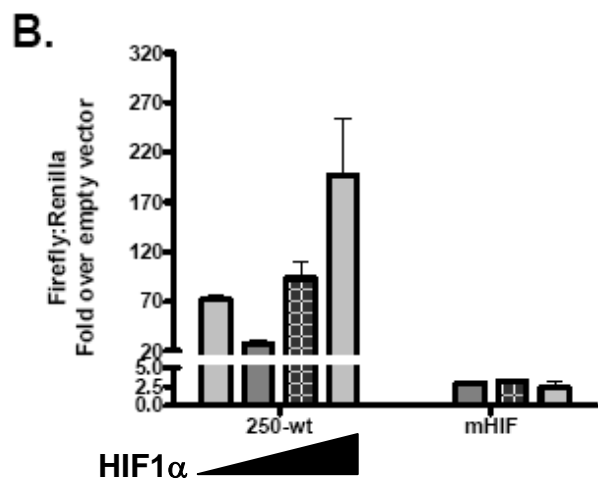
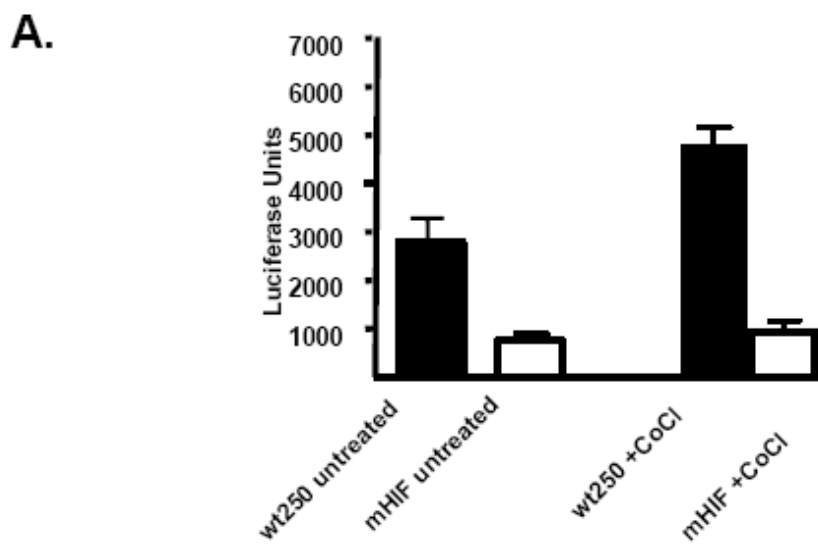
This work has identified a novel transcriptional component of a conserved essential gammaherpesvirus gene, Rta. The newly defined Rta promoter is targeted for DNA methylation during the establishment of latency, and this is associated with transcriptional silencing of Rta transcription. We also demonstrate a role for DNMT3A and DNMT3B in the transcriptional repression of Rta and the establishment of gammaherpesvirus latency *in vivo*. The specific targeting of the Rta distal promoter by a DNMT3-independent process accentuates the importance of DNA methylation in regulating lytic gene expression and provides insight into the mechanism of how this key modification is achieved in B cells, the primary reservoir for long-term gammaherpesvirus latency.

4.IV. FIGURES

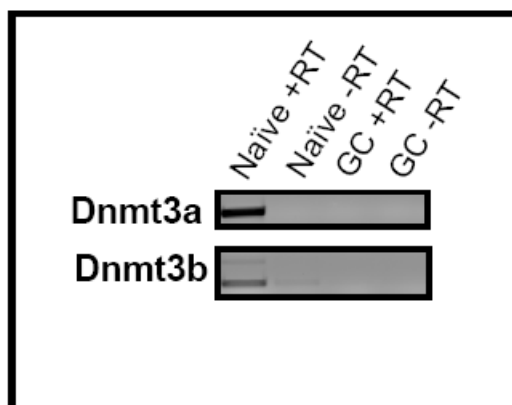
1. A. Translation of N-terminus of hypothetical MHV68 E0-E2 protein
B. Summary of detected gammaherpesvirus Rta transcripts and translations
C. Results of structural prediction analysis of E0 vs E1-containing proteins
2. Rta can transactivate a methylated Orf57 promoter
3. A. Hypoxia-induced activation of the distal Rta promoter is dependent on a HIF binding site
B. HIF1 α activates the distal Rta promoter
C. HIF2 α activates the distal Rta promoter
4. Dnmt3a and Dnm3b transcripts are detectable in naïve B cells
5. Analysis of NP-specific antibody response in CD19⁺/Cre mice versus littermate controls:
 - A. ELISpot analysis of secondary antibody response following secondary immunization with NP-CGG
 - B. NP-specific antibody response following primary immunization
 - C. NP-specific antibody response following secondary immunization
6. Analysis of antibody response in MHV68-infected CD19⁺/Cre mice versus littermate controls:
 - A. MHV68-specific antibody response
 - B. ELISpot analysis of total IgM and IgG ASCs
7. A. Alternative splicing and promoter usage in transcription of MHV68-LANA
B. Bisulfite sequence analysis of LANA latent promoter region



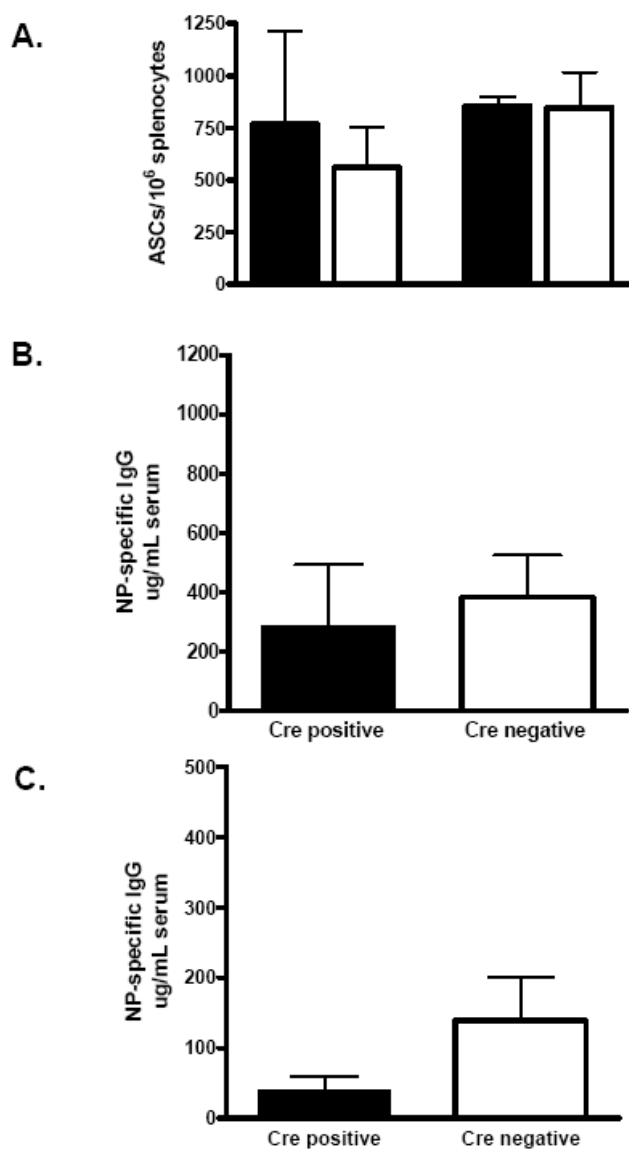
Summary-Figure 2



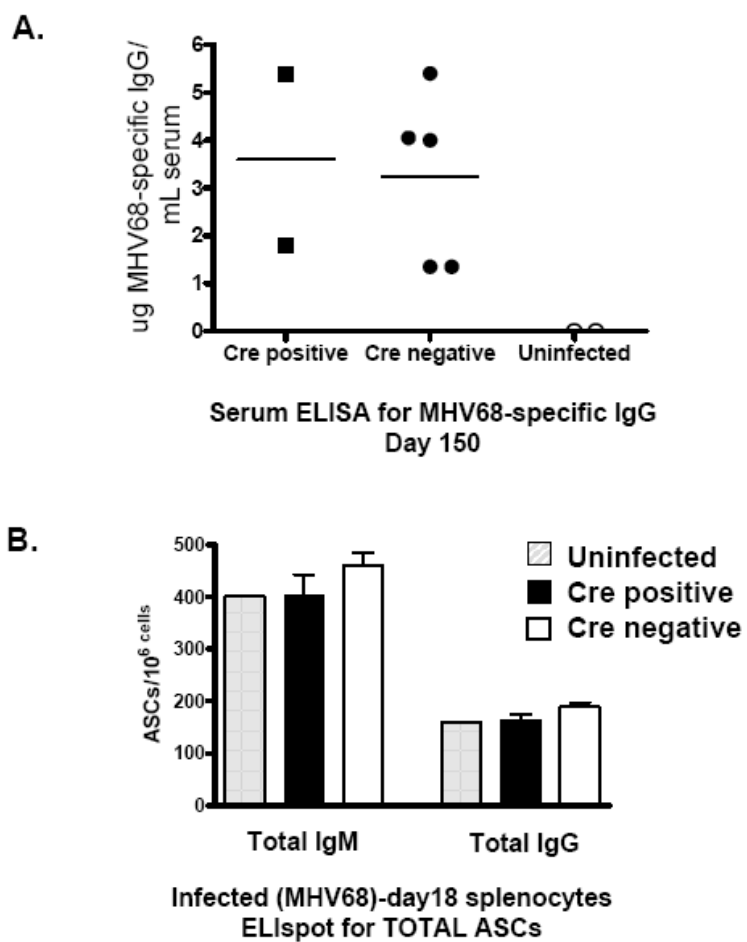
Summary- Figure 3



Summary- Figure 4

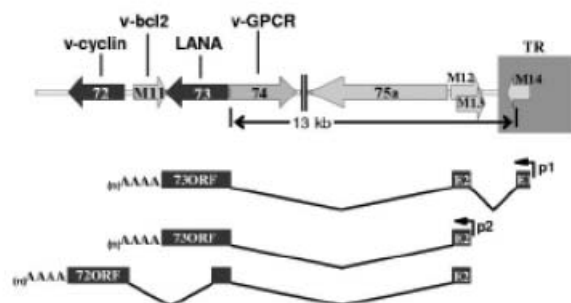


Summary- Figure 5

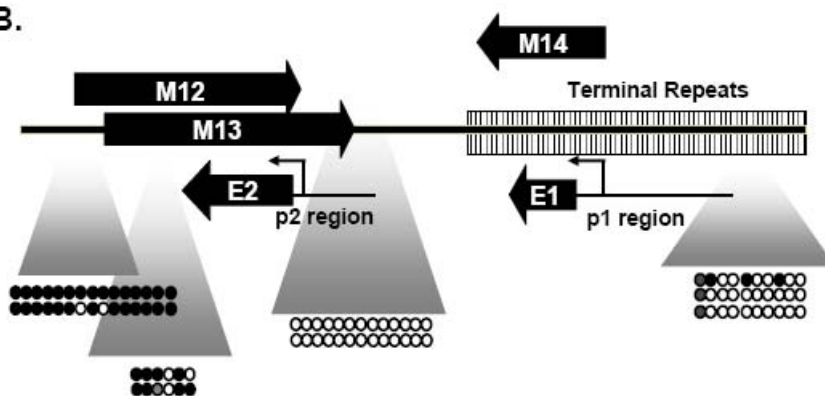


Summary- Figure 6

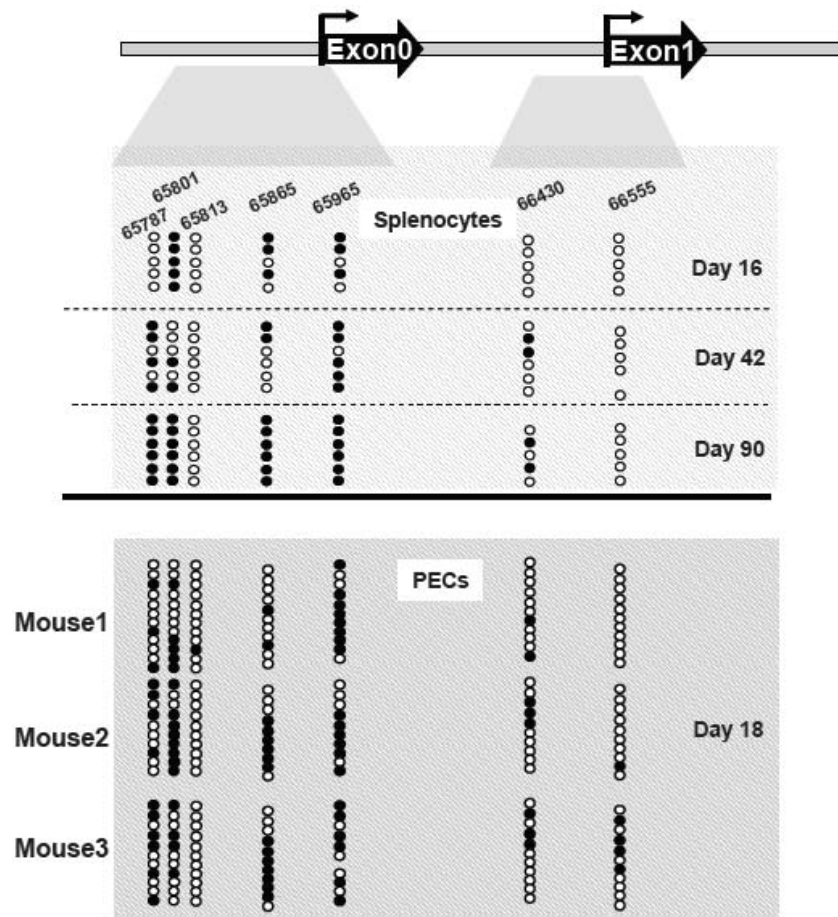
A.



B.



Summary- Figure 7



Summary- Figure 8

4.V. FIGURE LEGENDS

Figure 1. A hypothetical MHV68 E0-E2 spliced transcript encodes a full-length Rta protein. A) Exon1 encodes 12 amino acids using an ATG start at 66761; Exon0 encodes 14 amino acids using an ATG start at 66048. Using the splice donor site previously characterized, Exon0 splices in-frame with Exon2 to encode an Rta protein with an alternative N-terminus. B) E1-E2 transcripts were detected by RT-PCR from reactivated latent MHV68, KSHV, and EBV cell lines (using TPA or anti-IgG as described in Chapter 2). The E0-E2 transcript was detected in KSHV and EBV, but non MHV68, yet it is predicted to encode the protein in A. C) Hypothetical E0 and E1 N-termini have different predicted secondary structure. Regions conferred by E0 or E1 are indicated by the orange boxes. c=alpha helix, e=beta strand. Structural prediction performed using PHYRE analysis program (<http://www.sbg.bio.ic.ac.uk/phyre/>).

Figure 2. Methylation does not alter ability of Rta to activate Orf57 promoter. The Orf57 promoter (92) was cloned into the pCpG vector and methylated in vitro using M.SssI as in Chapter 3. Full-length E1-E2 Rta in pCMV-Tag2B or empty vector was co-transfected with the Orf57 promoter into RAW264.7 macrophages as in Chapter 2.

Figure 3. Hypoxia induces distal Rta promoter activity. A) RAW264.7 macrophages were transfected with the wild-type 250-bp distal Rta promoter (as in Chapter 2) or a plasmid in which the predicted HIF binding site was mutated (mHIF). Cells were transfected and treated with 100 μ M cobalt chloride (CoCl₂), a chemical inducer of hypoxia. Cells were co-transfected with increasing amounts of a HIF1 α (B) or HIF2 α expression plasmid (C).

Figure 4. Naïve B cells express Dnmt3a and Dnmt3b transcripts. Mouse splenocytes were sorted into naïve (IgD⁺) and germinal center (GL7+Fas^{hi}) populations and mRNA used to prepare cDNA. RT-PCR was performed for Dnmt3a or Dnmt3b.

Figure 5. CD19Cre/+ mice do not display a defect in the NP-specific antibody response.

Mice were immunized with 50µg NP-CGG in alum by intraperitoneal injection; secondary immunization was performed by tail vein administration of NP in PBS at day 50. A) Total splenocytes were assessed for NP-specific antibody-secreting cells (ASCs) at day 4 following secondary immunization by ELIspot. CD19Cre/+, black bars; CD19+/+, white bars. NP-specific serum IgG levels were determined by ELISA at day 30 following primary immunization (pre-secondary) (B) or day 4 following secondary immunization (C).

Figure 6. CD19Cre/+ mice do not display a defect in the MHV68-specific antibody response. A) MHV68-specific serum IgG levels were determined by ELISA at day 150 post-infection. B) Total splenocytes were assessed for total IgM or IgG ASCs at day 18 following infection (Note that this is prior to the generation of appreciate MHV68-specific antibodies).

Figure 7. Evidence of DNA methylation in MHV68 latency region. A) Schematic depicting the generation of mLANA transcripts from two promoters in or near the terminal repeats (From Allen, R. D., 3rd, S. Dickerson, and S. H. Speck. 2006. *J Virol* **80**:2055-62.(2)) B) Bisulfite sequence analysis of S11E cells (an MHV68-positive mouse B cell lymphoma cell lines). Circles represent CpGs in areas indicated; open circles represent

unmethylated sites, closed circles represent methylated sites, gray circles indicate ambiguous sequencing results.

Figure 8. The distal and proximal Rta promoters are methylated in PECs at day 18.

Data from splenocytes (Chapter 2, Figure 10) is provided for comparison. Bisulfite sequencing reveals that PECs have a similar methylation pattern to that of latently-infected splenocytes.

LITERATURE CITED

1. **Allen, R. D., 3rd, M. N. DeZalia, and S. H. Speck.** 2007. Identification of an Rta responsive promoter involved in driving gammaHV68 v-cyclin expression during virus replication. *Virology* **365**:250-9.
2. **Allen, R. D., 3rd, S. Dickerson, and S. H. Speck.** 2006. Identification of spliced gammaherpesvirus 68 LANA and v-cyclin transcripts and analysis of their expression in vivo during latent infection. *J Virol* **80**:2055-62.
3. **Balada, E., J. Ordi-Ros, and M. Vilardell-Tarres.** 2007. DNA methylation and systemic lupus erythematosus. *Ann N Y Acad Sci* **1108**:127-36.
4. **Barozzi, P., L. Potenza, G. Riva, D. Vallerini, C. Quadrelli, R. Bosco, F. Forghieri, G. Torelli, and M. Luppi.** 2007. B cells and herpesviruses: a model of lymphoproliferation. *Autoimmun Rev* **7**:132-6.
5. **Bechtel, J. T., Y. Liang, J. Hvidding, and D. Ganem.** 2003. Host range of Kaposi's sarcoma-associated herpesvirus in cultured cells. *J Virol* **77**:6474-81.
6. **Ben-Sasson, S. A., and G. Klein.** 1981. Activation of the Epstein-Barr virus genome by 5-aza-cytidine in latently infected human lymphoid lines. *Int J Cancer* **28**:131-5.
7. **Bhende, P. M., S. J. Dickerson, X. Sun, W. H. Feng, and S. C. Kenney.** 2007. X-box-binding protein 1 activates lytic Epstein-Barr virus gene expression in combination with protein kinase D. *J Virol* **81**:7363-70.
8. **Bhende, P. M., W. T. Seaman, H. J. Delecluse, and S. C. Kenney.** 2005. BZLF1 activation of the methylated form of the BRLF1 immediate-early promoter is regulated by BZLF1 residue 186. *J Virol* **79**:7338-48.
9. **Bhende, P. M., W. T. Seaman, H. J. Delecluse, and S. C. Kenney.** 2004. The EBV lytic switch protein, Z, preferentially binds to and activates the methylated viral genome. *Nat Genet* **36**:1099-104.
10. **Blaser, K., and H. N. Eisen.** 1978. Lambda2 light chains in normal mouse immunoglobulins. *Proc Natl Acad Sci U S A* **75**:1495-9.
11. **Blaskovic, D., M. Stancekova, J. Svobodova, and J. Mistrikova.** 1980. Isolation of five strains of herpesviruses from two species of free living small rodents. *Acta Virol* **24**:468.
12. **Bortz, E., J. P. Whitelegge, Q. Jia, Z. H. Zhou, J. P. Stewart, T. T. Wu, and R. Sun.** 2003. Identification of proteins associated with murine gammaherpesvirus 68 virions. *J Virol* **77**:13425-32.
13. **Cai, Q., K. Lan, S. C. Verma, H. Si, D. Lin, and E. S. Robertson.** 2006. Kaposi's sarcoma-associated herpesvirus latent protein LANA interacts with HIF-1 alpha to upregulate RTA expression during hypoxia: Latency control under low oxygen conditions. *J Virol* **80**:7965-75.
14. **Callan, M. F.** 2003. The evolution of antigen-specific CD8+ T cell responses after natural primary infection of humans with Epstein-Barr virus. *Viral Immunol* **16**:3-16.
15. **Callan, M. F., N. Steven, P. Krausa, J. D. Wilson, P. A. Moss, G. M. Gillespie, J. I. Bell, A. B. Rickinson, and A. J. McMichael.** 1996. Large clonal expansions of CD8+ T cells in acute infectious mononucleosis. *Nat Med* **2**:906-11.
16. **Carbone, A., E. Cesarman, M. Spina, A. Gloghini, and T. F. Schulz.** 2009. HIV-associated lymphomas and gamma-herpesviruses. *Blood* **113**:1213-24.

17. **Cardin, R. D., J. W. Brooks, S. R. Sarawar, and P. C. Doherty.** 1996. Progressive loss of CD8+ T cell-mediated control of a gamma-herpesvirus in the absence of CD4+ T cells. *J Exp Med* **184**:863-71.
18. **Chan, A. T., Q. Tao, K. D. Robertson, I. W. Flinn, R. B. Mann, B. Klencke, W. H. Kwan, T. W. Leung, P. J. Johnson, and R. F. Ambinder.** 2004. Azacitidine induces demethylation of the Epstein-Barr virus genome in tumors. *J Clin Oncol* **22**:1373-81.
19. **Chang, L. K., and S. T. Liu.** 2000. Activation of the BRLF1 promoter and lytic cycle of Epstein-Barr virus by histone acetylation. *Nucleic Acids Res* **28**:3918-25.
20. **Chang, Y., E. Cesarman, M. S. Pessin, F. Lee, J. Culpepper, D. M. Knowles, and P. S. Moore.** 1994. Identification of herpesvirus-like DNA sequences in AIDS-associated Kaposi's sarcoma. *Science* **266**:1865-9.
21. **Chedin, F., M. R. Lieber, and C. L. Hsieh.** 2002. The DNA methyltransferase-like protein DNMT3L stimulates de novo methylation by Dnmt3a. *Proc Natl Acad Sci U S A* **99**:16916-21.
22. **Chen, J., K. Ueda, S. Sakakibara, T. Okuno, C. Parravicini, M. Corbellino, and K. Yamanishi.** 2001. Activation of latent Kaposi's sarcoma-associated herpesvirus by demethylation of the promoter of the lytic transactivator. *Proc Natl Acad Sci U S A* **98**:4119-24.
23. **Chen, J., F. Ye, J. Xie, K. Kuhne, and S. J. Gao.** 2009. Genome-wide identification of binding sites for Kaposi's sarcoma-associated herpesvirus lytic switch protein, RTA. *Virology* **386**:290-302.
24. **Cheng, X.** 1995. DNA modification by methyltransferases. *Curr Opin Struct Biol* **5**:4-10.
25. **Cheng, X., and R. M. Blumenthal.** 2008. Mammalian DNA methyltransferases: a structural perspective. *Structure* **16**:341-50.
26. **Christensen, J. P., R. D. Cardin, K. C. Branum, and P. C. Doherty.** 1999. CD4(+) T cell-mediated control of a gamma-herpesvirus in B cell-deficient mice is mediated by IFN-gamma. *Proc Natl Acad Sci U S A* **96**:5135-40.
27. **Clemens, M. J.** 1993. The small RNAs of Epstein-Barr virus. *Mol Biol Rep* **17**:81-92.
28. **Collins, C. M., J. M. Boss, and S. H. Speck.** 2009. Identification of infected B-cell populations by using a recombinant murine gammaherpesvirus 68 expressing a fluorescent protein. *J Virol* **83**:6484-93.
29. **Countryman, J. K., L. Gradoville, and G. Miller.** 2008. Histone hyperacetylation occurs on promoters of lytic cycle regulatory genes in Epstein-Barr virus-infected cell lines which are refractory to disruption of latency by histone deacetylase inhibitors. *J Virol* **82**:4706-19.
30. **Dalton-Griffin, L., S. J. Wilson, and P. Kellam.** 2009. X-box binding protein 1 contributes to induction of the Kaposi's sarcoma-associated herpesvirus lytic cycle under hypoxic conditions. *J Virol* **83**:7202-9.
31. **Davis, D. A., A. S. Rinderknecht, J. P. Zoetewij, Y. Aoki, E. L. Read-Connole, G. Tosato, A. Blauvelt, and R. Yarchoan.** 2001. Hypoxia induces lytic replication of Kaposi sarcoma-associated herpesvirus. *Blood* **97**:3244-50.
32. **Deng, H., Y. Liang, and R. Sun.** 2007. Regulation of KSHV lytic gene expression. *Curr Top Microbiol Immunol* **312**:157-83.

33. **Dezalia, M., and S. H. Speck.** 2008. Identification of closely spaced, but distinct transcription initiation sites for the murine gammaherpesvirus 68 latency-associated M2 gene. *J Virol*.
34. **Dickerson, S. J., Y. Xing, A. R. Robinson, W. T. Seaman, H. Gruffat, and S. C. Kenney.** 2009. Methylation-dependent binding of the Epstein-Barr virus BZLF1 protein to viral promoters. *PLoS Pathog* **5**:e1000356.
35. **Dodge, J. E., M. Okano, F. Dick, N. Tsujimoto, T. Chen, S. Wang, Y. Ueda, N. Dyson, and E. Li.** 2005. Inactivation of Dnmt3b in mouse embryonic fibroblasts results in DNA hypomethylation, chromosomal instability, and spontaneous immortalization. *J Biol Chem* **280**:17986-91.
36. **Dutia, B. M., C. J. Clarke, D. J. Allen, and A. A. Nash.** 1997. Pathological changes in the spleens of gamma interferon receptor-deficient mice infected with murine gammaherpesvirus: a role for CD8 T cells. *J Virol* **71**:4278-83.
37. **Ehrlich, M., C. Sanchez, C. Shao, R. Nishiyama, J. Kehrl, R. Kuick, T. Kubota, and S. M. Hanash.** 2008. ICF, an immunodeficiency syndrome: DNA methyltransferase 3B involvement, chromosome anomalies, and gene dysregulation. *Autoimmunity* **41**:253-71.
38. **Elliott, J., E. B. Goodhew, L. T. Krug, N. Shakhnovsky, L. Yoo, and S. H. Speck.** 2004. Variable methylation of the Epstein-Barr virus Wp EBNA gene promoter in B-lymphoblastoid cell lines. *J Virol* **78**:14062-5.
39. **Faggioni, A., C. Zompetta, S. Grimaldi, G. Barile, L. Frati, and J. Lazdins.** 1986. Calcium modulation activates Epstein-Barr virus genome in latently infected cells. *Science* **232**:1554-6.
40. **Falek, P. R., S. Z. Ben-Sasson, and M. Ariel.** 2000. Correlation between DNA methylation and murine IFN-gamma and IL-4 expression. *Cytokine* **12**:198-206.
41. **Fejer, G., A. Koroknai, F. Banati, I. Gyory, D. Salamon, H. Wolf, H. H. Niller, and J. Minarovits.** 2008. Latency type-specific distribution of epigenetic marks at the alternative promoters Cp and Qp of Epstein-Barr virus. *J Gen Virol* **89**:1364-70.
42. **Flano, E., S. M. Husain, J. T. Sample, D. L. Woodland, and M. A. Blackman.** 2000. Latent murine gamma-herpesvirus infection is established in activated B cells, dendritic cells, and macrophages. *J Immunol* **165**:1074-81.
43. **Flemington, E., and S. H. Speck.** 1990. Identification of phorbol ester response elements in the promoter of Epstein-Barr virus putative lytic switch gene BZLF1. *J Virol* **64**:1217-26.
44. **Forrest, J. C., and S. H. Speck.** 2008. Establishment of B-cell lines latently infected with reactivation-competent murine gammaherpesvirus 68 provides evidence for viral alteration of a DNA damage-signaling cascade. *J Virol* **82**:7688-99.
45. **Forrest, J. C., and S. H. Speck.** 2008. Establishment of reactivation competent murine gammaherpesvirus-68 latently infected B cell lines provides evidence for viral alteration of a DNA damage signaling cascade. *J Virol*.
46. **Furnari, F. B., V. Zacny, E. B. Quinlivan, S. Kenney, and J. S. Pagano.** 1994. RAZ, an Epstein-Barr virus transdominant repressor that modulates the viral reactivation mechanism. *J Virol* **68**:1827-36.
47. **Gangappa, S., S. B. Kapadia, S. H. Speck, and H. W. t. Virgin.** 2002. Antibody to a lytic cycle viral protein decreases gammaherpesvirus latency in B-cell-deficient mice. *J Virol* **76**:11460-8.

48. **Gargano, L. M., J. C. Forrest, and S. H. Speck.** 2009. Signaling through Toll-like receptors induces murine gammaherpesvirus 68 reactivation in vivo. *J Virol* **83**:1474-82.
49. **Gerle, B., A. Koroknai, G. Fejer, A. Bakos, F. Banati, K. Szenthe, H. Wolf, H. H. Niller, J. Minarovits, and D. Salamon.** 2007. Acetylated histone H3 and H4 mark the upregulated LMP2A promoter of Epstein-Barr virus in lymphoid cells. *J Virol* **81**:13242-7.
50. **Golden, H. D., R. S. Chang, W. Prescott, E. Simpson, and T. Y. Cooper.** 1973. Leukocyte-transforming agent: prolonged excretion by patients with mononucleosis and excretion by normal individuals. *J Infect Dis* **127**:471-3.
51. **Goll, M. G., and T. H. Bestor.** 2005. Eukaryotic cytosine methyltransferases. *Annu Rev Biochem* **74**:481-514.
52. **Goll, M. G., F. Kirpekar, K. A. Maggert, J. A. Yoder, C. L. Hsieh, X. Zhang, K. G. Golic, S. E. Jacobsen, and T. H. Bestor.** 2006. Methylation of tRNA^{Asp} by the DNA methyltransferase homolog Dnmt2. *Science* **311**:395-8.
53. **Gray, K. S., R. D. Allen, 3rd, M. L. Farrell, J. C. Forrest, and S. H. Speck.** 2009. Alternatively initiated gene 50/RTA transcripts expressed during murine and human gammaherpesvirus reactivation from latency. *J Virol* **83**:314-28.
54. **Grogan, E., H. Jenson, J. Countryman, L. Heston, L. Gradoville, and G. Miller.** 1987. Transfection of a rearranged viral DNA fragment, WZhet, stably converts latent Epstein-Barr viral infection to productive infection in lymphoid cells. *Proc Natl Acad Sci U S A* **84**:1332-6.
55. **Gwack, Y., H. J. Baek, H. Nakamura, S. H. Lee, M. Meisterernst, R. G. Roeder, and J. U. Jung.** 2003. Principal role of TRAP/mediator and SWI/SNF complexes in Kaposi's sarcoma-associated herpesvirus RTA-mediated lytic reactivation. *Mol Cell Biol* **23**:2055-67.
56. **Gwack, Y., H. Byun, S. Hwang, C. Lim, and J. Choe.** 2001. CREB-binding protein and histone deacetylase regulate the transcriptional activity of Kaposi's sarcoma-associated herpesvirus open reading frame 50. *J Virol* **75**:1909-17.
57. **Gwack, Y., S. Hwang, C. Lim, Y. S. Won, C. H. Lee, and J. Choe.** 2002. Kaposi's Sarcoma-associated herpesvirus open reading frame 50 stimulates the transcriptional activity of STAT3. *J Biol Chem* **277**:6438-42.
58. **Haque, M., D. A. Davis, V. Wang, I. Widmer, and R. Yarchoan.** 2003. Kaposi's sarcoma-associated herpesvirus (human herpesvirus 8) contains hypoxia response elements: relevance to lytic induction by hypoxia. *J Virol* **77**:6761-8.
59. **Hata, K., M. Okano, H. Lei, and E. Li.** 2002. Dnmt3L cooperates with the Dnmt3 family of de novo DNA methyltransferases to establish maternal imprints in mice. *Development* **129**:1983-93.
60. **Heather, J., K. Flower, S. Isaac, and A. J. Sinclair.** 2009. The Epstein-Barr virus lytic cycle activator Zta interacts with methylated ZRE in the promoter of host target gene *egr1*. *J Gen Virol* **90**:1450-4.
61. **Henikoff, S., T. Furuyama, and K. Ahmad.** 2004. Histone variants, nucleosome assembly and epigenetic inheritance. *Trends Genet* **20**:320-6.
62. **Herskowitz, J., M. A. Jacoby, and S. H. Speck.** 2005. The murine gammaherpesvirus 68 M2 gene is required for efficient reactivation from latently infected B cells. *J Virol* **79**:2261-73.

63. **Honess, R. W., U. A. Gompels, B. G. Barrell, M. Craxton, K. R. Cameron, R. Staden, Y. N. Chang, and G. S. Hayward.** 1989. Deviations from expected frequencies of CpG dinucleotides in herpesvirus DNAs may be diagnostic of differences in the states of their latent genomes. *J Gen Virol* **70 (Pt 4):**837-55.
64. **Hsieh, C. L.** 1999. In vivo activity of murine de novo methyltransferases, Dnmt3a and Dnmt3b. *Mol Cell Biol* **19:**8211-8.
65. **Hsieh, C. L., G. Gauss, and M. R. Lieber.** 1992. Replication, transcription, CpG methylation and DNA topology in V(D)J recombination. *Curr Top Microbiol Immunol* **182:**125-35.
66. **Hsieh, C. L., and M. R. Lieber.** 1992. CpG methylated minichromosomes become inaccessible for V(D)J recombination after undergoing replication. *Embo J* **11:**315-25.
67. **Hwang, S., T. T. Wu, L. M. Tong, K. S. Kim, D. Martinez-Guzman, A. D. Colantonio, C. H. Uittenbogaart, and R. Sun.** 2008. Persistent gammaherpesvirus replication and dynamic interaction with the host in vivo. *J Virol* **82:**12498-509.
68. **Idesawa, M., N. Sugano, K. Ikeda, M. Oshikawa, M. Takane, K. Seki, and K. Ito.** 2004. Detection of Epstein-Barr virus in saliva by real-time PCR. *Oral Microbiol Immunol* **19:**230-2.
69. **Jacoby, M. A., H. W. t. Virgin, and S. H. Speck.** 2002. Disruption of the M2 gene of murine gammaherpesvirus 68 alters splenic latency following intranasal, but not intraperitoneal, inoculation. *J Virol* **76:**1790-801.
70. **Jeltsch, A.** 2006. Molecular enzymology of mammalian DNA methyltransferases. *Curr Top Microbiol Immunol* **301:**203-25.
71. **Jia, D., R. Z. Jurkowska, X. Zhang, A. Jeltsch, and X. Cheng.** 2007. Structure of Dnmt3a bound to Dnmt3L suggests a model for de novo DNA methylation. *Nature* **449:**248-51.
72. **Jiang, J. H., N. Wang, A. Li, W. T. Liao, Z. G. Pan, S. J. Mai, D. J. Li, M. S. Zeng, J. M. Wen, and Y. X. Zeng.** 2006. Hypoxia can contribute to the induction of the Epstein-Barr virus (EBV) lytic cycle. *J Clin Virol* **37:**98-103.
73. **Jung, E. J., Y. M. Lee, B. L. Lee, M. S. Chang, and W. H. Kim.** 2007. Lytic induction and apoptosis of Epstein-Barr virus-associated gastric cancer cell line with epigenetic modifiers and ganciclovir. *Cancer Lett* **247:**77-83.
74. **Kafri, T., M. Ariel, M. Brandeis, R. Shemer, L. Urven, J. McCarrey, H. Cedar, and A. Razin.** 1992. Developmental pattern of gene-specific DNA methylation in the mouse embryo and germ line. *Genes Dev* **6:**705-14.
75. **Kaneda, M., M. Okano, K. Hata, T. Sado, N. Tsujimoto, E. Li, and H. Sasaki.** 2004. Essential role for de novo DNA methyltransferase Dnmt3a in paternal and maternal imprinting. *Nature* **429:**900-3.
76. **Kaneda, M., T. Sado, K. Hata, M. Okano, N. Tsujimoto, E. Li, and H. Sasaki.** 2004. Role of de novo DNA methyltransferases in initiation of genomic imprinting and X-chromosome inactivation. *Cold Spring Harb Symp Quant Biol* **69:**125-9.
77. **Kang, H., and P. M. Lieberman.** 2009. Cell cycle control of Kaposi's sarcoma-associated herpesvirus latency transcription by CTCF-cohesin interactions. *J Virol* **83:**6199-210.

78. **Karlin, S., W. Doerfler, and L. R. Cardon.** 1994. Why is CpG suppressed in the genomes of virtually all small eukaryotic viruses but not in those of large eukaryotic viruses? *J Virol* **68**:2889-97.
79. **Karlsson, Q. H., C. Schelcher, E. Verrall, C. Petosa, and A. J. Sinclair.** 2008. Methylated DNA recognition during the reversal of epigenetic silencing is regulated by cysteine and serine residues in the Epstein-Barr virus lytic switch protein. *PLoS Pathog* **4**:e1000005.
80. **Kenney, S., E. Holley-Guthrie, E. C. Mar, and M. Smith.** 1989. The Epstein-Barr virus BMLF1 promoter contains an enhancer element that is responsive to the BZLF1 and BRLF1 transactivators. *J Virol* **63**:3878-83.
81. **Kersh, E. N., D. R. Fitzpatrick, K. Murali-Krishna, J. Shires, S. H. Speck, J. M. Boss, and R. Ahmed.** 2006. Rapid demethylation of the IFN-gamma gene occurs in memory but not naive CD8 T cells. *J Immunol* **176**:4083-93.
82. **Klug, M., and M. Rehli.** 2006. Functional analysis of promoter CpG methylation using a CpG-free luciferase reporter vector. *Epigenetics* **1**:127-30.
83. **Krug, L. T., C. M. Collins, L. M. Gargano, and S. H. Speck.** 2009. NF-kappaB p50 plays distinct roles in the establishment and control of murine gammaherpesvirus 68 latency. *J Virol* **83**:4732-48.
84. **Kubarek, L., A. Kozłowska, M. Przybylski, M. Lianeri, and P. P. Jagodzinski.** 2009. Down-regulation of CXCR4 expression by tamoxifen is associated with DNA methyltransferase 3B up-regulation in MCF-7 breast cancer cells. *Biomed Pharmacother* **63**:586-91.
85. **Kutok, J. L., and F. Wang.** 2006. Spectrum of Epstein-Barr virus-associated diseases. *Annu Rev Pathol* **1**:375-404.
86. **Laichalk, L. L., and D. A. Thorley-Lawson.** 2005. Terminal differentiation into plasma cells initiates the replicative cycle of Epstein-Barr virus in vivo. *J Virol* **79**:1296-307.
87. **Laman, H., and C. Boshoff.** 2001. Is KSHV lytic growth induced by a methylation-sensitive switch? *Trends Microbiol* **9**:464-6.
88. **Levitskaya, J., M. Coram, V. Levitsky, S. Imreh, P. M. Steigerwald-Mullen, G. Klein, M. G. Kurilla, and M. G. Masucci.** 1995. Inhibition of antigen processing by the internal repeat region of the Epstein-Barr virus nuclear antigen-1. *Nature* **375**:685-8.
89. **Levitskaya, J., A. Sharipo, A. Leonchiks, A. Ciechanover, and M. G. Masucci.** 1997. Inhibition of ubiquitin/proteasome-dependent protein degradation by the Gly-Ala repeat domain of the Epstein-Barr virus nuclear antigen 1. *Proc Natl Acad Sci U S A* **94**:12616-21.
90. **Li, E.** 2002. Chromatin modification and epigenetic reprogramming in mammalian development. *Nat Rev Genet* **3**:662-73.
91. **Liu, P., and S. H. Speck.** 2003. Synergistic autoactivation of the Epstein-Barr virus immediate-early BRLF1 promoter by Rta and Zta. *Virology* **310**:199-206.
92. **Liu, S., I. V. Pavlova, H. W. t. Virgin, and S. H. Speck.** 2000. Characterization of gammaherpesvirus 68 gene 50 transcription. *J Virol* **74**:2029-37.
93. **Liu, T., E. B. Reilly, C. B. Zhang, and H. N. Eisen.** 1984. Frequency of lambda light chain subtypes in mouse antibodies to the 2,4-dinitrophenyl (DNP) group. *Eur J Immunol* **14**:667-72.

94. **Liu, Y., Y. Cao, D. Liang, Y. Gao, T. Xia, E. S. Robertson, and K. Lan.** 2008. Kaposi's sarcoma-associated herpesvirus RTA activates the processivity factor ORF59 through interaction with RBP-Jkappa and a cis-acting RTA responsive element. *Virology* **380**:264-75.
95. **Luka, J., B. Kallin, and G. Klein.** 1979. Induction of the Epstein-Barr virus (EBV) cycle in latently infected cells by n-butyrate. *Virology* **94**:228-31.
96. **Lukac, D. M., J. R. Kirshner, and D. Ganem.** 1999. Transcriptional activation by the product of open reading frame 50 of Kaposi's sarcoma-associated herpesvirus is required for lytic viral reactivation in B cells. *J Virol* **73**:9348-61.
97. **Lukac, D. M., R. Renne, J. R. Kirshner, and D. Ganem.** 1998. Reactivation of Kaposi's sarcoma-associated herpesvirus infection from latency by expression of the ORF 50 transactivator, a homolog of the EBV R protein. *Virology* **252**:304-12.
98. **Lyon, A. B., and S. R. Sarawar.** 2006. Differential requirement for CD28 and CD80/86 pathways of costimulation in the long-term control of murine gammaherpesvirus-68. *Virology* **356**:50-6.
99. **Manet, E., H. Gruffat, M. C. Trescol-Biemont, N. Moreno, P. Chambard, J. F. Giot, and A. Sergeant.** 1989. Epstein-Barr virus bicistronic mRNAs generated by facultative splicing code for two transcriptional trans-activators. *Embo J* **8**:1819-26.
100. **Masucci, M. G., B. Contreras-Salazar, E. Ragnar, K. Falk, J. Minarovits, I. Ernberg, and G. Klein.** 1989. 5-Azacytidine up regulates the expression of Epstein-Barr virus nuclear antigen 2 (EBNA-2) through EBNA-6 and latent membrane protein in the Burkitt's lymphoma line rael. *J Virol* **63**:3135-41.
101. **May, J. S., H. M. Coleman, B. Smillie, S. Efstathiou, and P. G. Stevenson.** 2004. Forced lytic replication impairs host colonization by a latency-deficient mutant of murine gammaherpesvirus-68. *J Gen Virol* **85**:137-46.
102. **Melvin, A. J., M. E. McGurn, S. J. Bort, C. Gibson, and D. B. Lewis.** 1995. Hypomethylation of the interferon-gamma gene correlates with its expression by primary T-lineage cells. *Eur J Immunol* **25**:426-30.
103. **Milho, R., C. M. Smith, S. Marques, M. Alenquer, J. S. May, L. Gillet, M. Gaspar, S. Efstathiou, J. P. Simas, and P. G. Stevenson.** 2009. In vivo imaging of murid herpesvirus-4 infection. *J Gen Virol* **90**:21-32.
104. **Minarovits, J.** 2006. Epigenotypes of latent herpesvirus genomes. *Curr Top Microbiol Immunol* **310**:61-80.
105. **Miranda, T. B., and P. A. Jones.** 2007. DNA methylation: the nuts and bolts of repression. *J Cell Physiol* **213**:384-90.
106. **Monk, M., M. Boubelik, and S. Lehnert.** 1987. Temporal and regional changes in DNA methylation in the embryonic, extraembryonic and germ cell lineages during mouse embryo development. *Development* **99**:371-82.
107. **Moorman, N. J., C. Y. Lin, and S. H. Speck.** 2004. Identification of candidate gammaherpesvirus 68 genes required for virus replication by signature-tagged transposon mutagenesis. *J Virol* **78**:10282-90.
108. **Moorman, N. J., D. O. Willer, and S. H. Speck.** 2003. The gammaherpesvirus 68 latency-associated nuclear antigen homolog is critical for the establishment of splenic latency. *J Virol* **77**:10295-303.
109. **Morris, S. A., B. Rao, B. A. Garcia, S. B. Hake, R. L. Diaz, J. Shabanowitz, D. F. Hunt, C. D. Allis, J. D. Lieb, and B. D. Strahl.** 2007. Identification of histone H3

- lysine 36 acetylation as a highly conserved histone modification. *J Biol Chem* **282**:7632-40.
110. Moser, J. M., M. L. Farrell, L. T. Krug, J. W. Upton, and S. H. Speck. 2006. A gammaherpesvirus 68 gene 50 null mutant establishes long-term latency in the lung but fails to vaccinate against a wild-type virus challenge. *J Virol* **80**:1592-8.
 111. Moser, J. M., J. W. Upton, R. D. Allen, 3rd, C. B. Wilson, and S. H. Speck. 2005. Role of B-cell proliferation in the establishment of gammaherpesvirus latency. *J Virol* **79**:9480-91.
 112. Moser, J. M., J. W. Upton, K. S. Gray, and S. H. Speck. 2005. Ex vivo stimulation of B cells latently infected with gammaherpesvirus 68 triggers reactivation from latency. *J Virol* **79**:5227-31.
 113. Mostoslavsky, R., and Y. Bergman. 1997. DNA methylation: regulation of gene expression and role in the immune system. *Biochim Biophys Acta* **1333**:F29-50.
 114. Mostoslavsky, R., A. Kirillov, Y. H. Ji, M. Goldmit, M. Holzmann, T. Wirth, H. Cedar, and Y. Bergman. 1999. Demethylation and the establishment of kappa allelic exclusion. *Cold Spring Harb Symp Quant Biol* **64**:197-206.
 115. Mostoslavsky, R., N. Singh, A. Kirillov, R. Pelanda, H. Cedar, A. Chess, and Y. Bergman. 1998. Kappa chain monoallelic demethylation and the establishment of allelic exclusion. *Genes Dev* **12**:1801-11.
 116. Murphy, B. J. 2004. Regulation of malignant progression by the hypoxia-sensitive transcription factors HIF-1alpha and MTF-1. *Comp Biochem Physiol B Biochem Mol Biol* **139**:495-507.
 117. Murphy, B. J., G. K. Andrews, D. Bittel, D. J. Discher, J. McCue, C. J. Green, M. Yanovsky, A. Giaccia, R. M. Sutherland, K. R. Laderoute, and K. A. Webster. 1999. Activation of metallothionein gene expression by hypoxia involves metal response elements and metal transcription factor-1. *Cancer Res* **59**:1315-22.
 118. Murphy, B. J., T. Kimura, B. G. Sato, Y. Shi, and G. K. Andrews. 2008. Metallothionein induction by hypoxia involves cooperative interactions between metal-responsive transcription factor-1 and hypoxia-inducible transcription factor-1alpha. *Mol Cancer Res* **6**:483-90.
 119. Murphy, B. J., B. G. Sato, T. P. Dalton, and K. R. Laderoute. 2005. The metal-responsive transcription factor-1 contributes to HIF-1 activation during hypoxic stress. *Biochem Biophys Res Commun* **337**:860-7.
 120. Nash, A. A., B. M. Dutia, J. P. Stewart, and A. J. Davison. 2001. Natural history of murine gamma-herpesvirus infection. *Philos Trans R Soc Lond B Biol Sci* **356**:569-79.
 121. Niller, H. H., H. Wolf, and J. Minarovits. 2009. Epigenetic dysregulation of the host cell genome in Epstein-Barr virus-associated neoplasia. *Semin Cancer Biol* **19**:158-64.
 122. Okano, M., D. W. Bell, D. A. Haber, and E. Li. 1999. DNA methyltransferases Dnmt3a and Dnmt3b are essential for de novo methylation and mammalian development. *Cell* **99**:247-57.
 123. Okano, M., S. Xie, and E. Li. 1998. Cloning and characterization of a family of novel mammalian DNA (cytosine-5) methyltransferases. *Nat Genet* **19**:219-20.
 124. Pantry, S. N., and P. G. Medveczky. 2009. Epigenetic regulation of Kaposi's sarcoma-associated herpesvirus replication. *Semin Cancer Biol* **19**:153-7.

125. **Paulson, E. J., J. D. Fingerroth, J. L. Yates, and S. H. Speck.** 2002. Methylation of the EBV genome and establishment of restricted latency in low-passage EBV-infected 293 epithelial cells. *Virology* **299**:109-21.
126. **Paulson, E. J., and S. H. Speck.** 1999. Differential methylation of Epstein-Barr virus latency promoters facilitates viral persistence in healthy seropositive individuals. *J Virol* **73**:9959-68.
127. **Pavlova, I., C. Y. Lin, and S. H. Speck.** 2005. Murine gammaherpesvirus 68 Rta-dependent activation of the gene 57 promoter. *Virology* **333**:169-79.
128. **Pavlova, I. V., H. W. t. Virgin, and S. H. Speck.** 2003. Disruption of gammaherpesvirus 68 gene 50 demonstrates that Rta is essential for virus replication. *J Virol* **77**:5731-9.
129. **Polcicova, K., Z. Hrabovska, J. Mistrikova, J. Tomaskova, J. Pastorek, S. Pastorekova, and J. Kopacek.** 2008. Up-regulation of Murid herpesvirus 4 ORF50 by hypoxia: possible implication for virus reactivation from latency. *Virus Res* **132**:257-62.
130. **Prang, N., H. Wolf, and F. Schwarzmann.** 1999. Latency of Epstein-Barr virus is stabilized by antisense-mediated control of the viral immediate-early gene BZLF-1. *J Med Virol* **59**:512-9.
131. **Puglielli, M. T., N. Desai, and S. H. Speck.** 1997. Regulation of EBNA gene transcription in lymphoblastoid cell lines: characterization of sequences downstream of BCR2 (Cp). *J Virol* **71**:120-8.
132. **Puglielli, M. T., M. Woisetschlaeger, and S. H. Speck.** 1996. oriP is essential for EBNA gene promoter activity in Epstein-Barr virus-immortalized lymphoblastoid cell lines. *J Virol* **70**:5758-68.
133. **Ragoczy, T., L. Heston, and G. Miller.** 1998. The Epstein-Barr virus Rta protein activates lytic cycle genes and can disrupt latency in B lymphocytes. *J Virol* **72**:7978-84.
134. **Ragoczy, T., and G. Miller.** 2001. Autostimulation of the Epstein-Barr virus BRLF1 promoter is mediated through consensus Sp1 and Sp3 binding sites. *J Virol* **75**:5240-51.
135. **Rajcani, J., D. Blaskovic, J. Svobodova, F. Ciampor, D. Huckova, and D. Stanekova.** 1985. Pathogenesis of acute and persistent murine herpesvirus infection in mice. *Acta Virol* **29**:51-60.
136. **Reik, W., A. Collick, M. L. Norris, S. C. Barton, and M. A. Surani.** 1987. Genomic imprinting determines methylation of parental alleles in transgenic mice. *Nature* **328**:248-51.
137. **Rickabaugh, T. M., H. J. Brown, T. T. Wu, M. J. Song, S. Hwang, H. Deng, K. Mitsouras, and R. Sun.** 2005. Kaposi's sarcoma-associated herpesvirus/human herpesvirus 8 RTA reactivates murine gammaherpesvirus 68 from latency. *J Virol* **79**:3217-22.
138. **Rickert, R. C., J. Roes, and K. Rajewsky.** 1997. B lymphocyte-specific, Cre-mediated mutagenesis in mice. *Nucleic Acids Res* **25**:1317-8.
139. **Robertson, K. D., and A. P. Wolffe.** 2000. DNA methylation in health and disease. *Nat Rev Genet* **1**:11-9.
140. **Rogers, R. P., M. Woisetschlaeger, and S. H. Speck.** 1990. Alternative splicing dictates translational start in Epstein-Barr virus transcripts. *Embo J* **9**:2273-7.

141. **Sangster, M. Y., D. J. Topham, S. D'Costa, R. D. Cardin, T. N. Marion, L. K. Myers, and P. C. Doherty.** 2000. Analysis of the virus-specific and nonspecific B cell response to a persistent B-lymphotropic gammaherpesvirus. *J Immunol* **164**:1820-8.
142. **Schaefer, B. C., J. L. Strominger, and S. H. Speck.** 1997. Host-cell-determined methylation of specific Epstein-Barr virus promoters regulates the choice between distinct viral latency programs. *Mol Cell Biol* **17**:364-77.
143. **Schaefer, B. C., M. Woisetschlaeger, J. L. Strominger, and S. H. Speck.** 1991. Exclusive expression of Epstein-Barr virus nuclear antigen 1 in Burkitt lymphoma arises from a third promoter, distinct from the promoters used in latently infected lymphocytes. *Proc Natl Acad Sci U S A* **88**:6550-4.
144. **Shapiro-Shelef, M., K. I. Lin, L. J. McHeyzer-Williams, J. Liao, M. G. McHeyzer-Williams, and K. Calame.** 2003. Blimp-1 is required for the formation of immunoglobulin secreting plasma cells and pre-plasma memory B cells. *Immunity* **19**:607-20.
145. **Shapiro-Shelef, M., K. I. Lin, D. Savitsky, J. Liao, and K. Calame.** 2005. Blimp-1 is required for maintenance of long-lived plasma cells in the bone marrow. *J Exp Med* **202**:1471-6.
146. **Simas, J. P., and S. Efstathiou.** 1998. Murine gammaherpesvirus 68: a model for the study of gammaherpesvirus pathogenesis. *Trends Microbiol* **6**:276-82.
147. **Sinclair, A. J.** 2003. bZIP proteins of human gammaherpesviruses. *J Gen Virol* **84**:1941-9.
148. **Song, M. J., S. Hwang, W. H. Wong, T. T. Wu, S. Lee, H. I. Liao, and R. Sun.** 2005. Identification of viral genes essential for replication of murine gamma-herpesvirus 68 using signature-tagged mutagenesis. *Proc Natl Acad Sci U S A* **102**:3805-10.
149. **Speck, S. H.** 2002. EBV framed in Burkitt lymphoma. *Nat Med* **8**:1086-7.
150. **Speck, S. H., and J. L. Strominger.** 1985. Analysis of the transcript encoding the latent Epstein-Barr virus nuclear antigen I: a potentially polycistronic message generated by long-range splicing of several exons. *Proc Natl Acad Sci U S A* **82**:8305-9.
151. **Staudt, M. R., and D. P. Dittmer.** 2007. The Rta/Orf50 transactivator proteins of the gamma-herpesviridae. *Curr Top Microbiol Immunol* **312**:71-100.
152. **Stedman, W., H. Kang, S. Lin, J. L. Kissil, M. S. Bartolomei, and P. M. Lieberman.** 2008. Cohesins localize with CTCF at the KSHV latency control region and at cellular c-myc and H19/Igf2 insulators. *Embo J* **27**:654-66.
153. **Steed, A., T. Buch, A. Waisman, and H. W. t. Virgin.** 2007. Gamma interferon blocks gammaherpesvirus reactivation from latency in a cell type-specific manner. *J Virol* **81**:6134-40.
154. **Steed, A. L., E. S. Barton, S. A. Tibbetts, D. L. Popkin, M. L. Lutzke, R. Rochford, and H. W. t. Virgin.** 2006. Gamma interferon blocks gammaherpesvirus reactivation from latency. *J Virol* **80**:192-200.
155. **Stewart, J. P., E. J. Usherwood, A. Ross, H. Dyson, and T. Nash.** 1998. Lung epithelial cells are a major site of murine gammaherpesvirus persistence. *J Exp Med* **187**:1941-51.

156. **Strickler, J. G., L. A. Movahed, K. J. Gajl-Peczalska, C. A. Horwitz, R. D. Brunning, and L. M. Weiss.** 1990. Oligoclonal T cell receptor gene rearrangements in blood lymphocytes of patients with acute Epstein-Barr virus-induced infectious mononucleosis. *J Clin Invest* **86**:1358-63.
157. **Suganuma, T., and J. L. Workman.** 2008. Crosstalk among Histone Modifications. *Cell* **135**:604-7.
158. **Sun, R., S. F. Lin, L. Gradoville, Y. Yuan, F. Zhu, and G. Miller.** 1998. A viral gene that activates lytic cycle expression of Kaposi's sarcoma-associated herpesvirus. *Proc Natl Acad Sci U S A* **95**:10866-71.
159. **Sun, R., S. F. Lin, K. Staskus, L. Gradoville, E. Grogan, A. Haase, and G. Miller.** 1999. Kinetics of Kaposi's sarcoma-associated herpesvirus gene expression. *J Virol* **73**:2232-42.
160. **Sunil-Chandra, N. P., J. Arno, J. Fazakerley, and A. A. Nash.** 1994. Lymphoproliferative disease in mice infected with murine gammaherpesvirus 68. *Am J Pathol* **145**:818-26.
161. **Sunil-Chandra, N. P., S. Efstathiou, and A. A. Nash.** 1992. Murine gammaherpesvirus 68 establishes a latent infection in mouse B lymphocytes in vivo. *J Gen Virol* **73 (Pt 12)**:3275-9.
162. **Swenson, J. J., E. Holley-Guthrie, and S. C. Kenney.** 2001. Epstein-Barr virus immediate-early protein BRLF1 interacts with CBP, promoting enhanced BRLF1 transactivation. *J Virol* **75**:6228-34.
163. **Szyf, M., L. Eliasson, V. Mann, G. Klein, and A. Razin.** 1985. Cellular and viral DNA hypomethylation associated with induction of Epstein-Barr virus lytic cycle. *Proc Natl Acad Sci U S A* **82**:8090-4.
164. **Tadokoro, Y., H. Ema, M. Okano, E. Li, and H. Nakauchi.** 2007. De novo DNA methyltransferase is essential for self-renewal, but not for differentiation, in hematopoietic stem cells. *J Exp Med* **204**:715-22.
165. **Tao, Q., H. Huang, T. M. Geiman, C. Y. Lim, L. Fu, G. H. Qiu, and K. D. Robertson.** 2002. Defective de novo methylation of viral and cellular DNA sequences in ICF syndrome cells. *Hum Mol Genet* **11**:2091-102.
166. **Tao, Q., K. D. Robertson, A. Manns, A. Hildesheim, and R. F. Ambinder.** 1998. The Epstein-Barr virus major latent promoter Qp is constitutively active, hypomethylated, and methylation sensitive. *J Virol* **72**:7075-83.
167. **Tarakanova, V. L., F. Suarez, S. A. Tibbetts, M. A. Jacoby, K. E. Weck, J. L. Hess, S. H. Speck, and H. W. t. Virgin.** 2005. Murine gammaherpesvirus 68 infection is associated with lymphoproliferative disease and lymphoma in BALB beta2 microglobulin-deficient mice. *J Virol* **79**:14668-79.
168. **Tierney, R. J., H. E. Kirby, J. K. Nagra, J. Desmond, A. I. Bell, and A. B. Rickinson.** 2000. Methylation of transcription factor binding sites in the Epstein-Barr virus latent cycle promoter Wp coincides with promoter down-regulation during virus-induced B-cell transformation. *J Virol* **74**:10468-79.
169. **Tripp, R. A., A. M. Hamilton-Easton, R. D. Cardin, P. Nguyen, F. G. Behm, D. L. Woodland, P. C. Doherty, and M. A. Blackman.** 1997. Pathogenesis of an infectious mononucleosis-like disease induced by a murine gamma-herpesvirus: role for a viral superantigen? *J Exp Med* **185**:1641-50.

170. **Ueda, Y., M. Okano, C. Williams, T. Chen, K. Georgopoulos, and E. Li.** 2006. Roles for Dnmt3b in mammalian development: a mouse model for the ICF syndrome. *Development* **133**:1183-92.
171. **Upton, J. W., and S. H. Speck.** 2006. Evidence for CDK-dependent and CDK-independent functions of the murine gammaherpesvirus 68 v-cyclin. *J Virol* **80**:11946-59.
172. **Virgin, H. W. t., P. Latreille, P. Wamsley, K. Hallsworth, K. E. Weck, A. J. Dal Canto, and S. H. Speck.** 1997. Complete sequence and genomic analysis of murine gammaherpesvirus 68. *J Virol* **71**:5894-904.
173. **Virgin, H. W. t., R. M. Presti, X. Y. Li, C. Liu, and S. H. Speck.** 1999. Three distinct regions of the murine gammaherpesvirus 68 genome are transcriptionally active in latently infected mice. *J Virol* **73**:2321-32.
174. **Wade, P. A.** 2001. Methyl CpG-binding proteins and transcriptional repression. *Bioessays* **23**:1131-7.
175. **Wade, P. A.** 2001. Methyl CpG binding proteins: coupling chromatin architecture to gene regulation. *Oncogene* **20**:3166-73.
176. **Wang, S. E., F. Y. Wu, H. Chen, M. Shamay, Q. Zheng, and G. S. Hayward.** 2004. Early activation of the Kaposi's sarcoma-associated herpesvirus RTA, RAP, and MTA promoters by the tetradecanoyl phorbol acetate-induced AP1 pathway. *J Virol* **78**:4248-67.
177. **Wang, S. E., F. Y. Wu, Y. Yu, and G. S. Hayward.** 2003. CCAAT/enhancer-binding protein-alpha is induced during the early stages of Kaposi's sarcoma-associated herpesvirus (KSHV) lytic cycle reactivation and together with the KSHV replication and transcription activator (RTA) cooperatively stimulates the viral RTA, MTA, and PAN promoters. *J Virol* **77**:9590-612.
178. **Wang, Y., P. Zhang, W. Li, L. Hou, J. Wang, Y. Liang, and H. Han.** 2006. Mouse follicular and marginal zone B cells show differential expression of Dnmt3a and sensitivity to 5'-azacytidine. *Immunol Lett* **105**:174-9.
179. **Weck, K. E., M. L. Barkon, L. I. Yoo, S. H. Speck, and H. I. Virgin.** 1996. Mature B cells are required for acute splenic infection, but not for establishment of latency, by murine gammaherpesvirus 68. *J Virol* **70**:6775-80.
180. **Weck, K. E., S. S. Kim, H. I. Virgin, and S. H. Speck.** 1999. B cells regulate murine gammaherpesvirus 68 latency. *J Virol* **73**:4651-61.
181. **Weck, K. E., S. S. Kim, H. I. Virgin, and S. H. Speck.** 1999. Macrophages are the major reservoir of latent murine gammaherpesvirus 68 in peritoneal cells. *J Virol* **73**:3273-83.
182. **Whitehouse, A., I. M. Carr, J. C. Griffiths, and D. M. Meredith.** 1997. The herpesvirus saimiri ORF50 gene, encoding a transcriptional activator homologous to the Epstein-Barr virus R protein, is transcribed from two distinct promoters of different temporal phases. *J Virol* **71**:2550-4.
183. **Willer, D. O., and S. H. Speck.** 2005. Establishment and maintenance of long-term murine gammaherpesvirus 68 latency in B cells in the absence of CD40. *J Virol* **79**:2891-9.
184. **Willer, D. O., and S. H. Speck.** 2003. Long-term latent murine Gammaherpesvirus 68 infection is preferentially found within the surface immunoglobulin D-negative subset of splenic B cells in vivo. *J Virol* **77**:8310-21.

185. **Wilson, S. J., E. H. Tsao, B. L. Webb, H. Ye, L. Dalton-Griffin, C. Tsantoulas, C. V. Gale, M. Q. Du, A. Whitehouse, and P. Kellam.** 2007. X box binding protein XBP-1s transactivates the Kaposi's sarcoma-associated herpesvirus (KSHV) ORF50 promoter, linking plasma cell differentiation to KSHV reactivation from latency. *J Virol* **81**:13578-86.
186. **Woisetschlaeger, M., J. L. Strominger, and S. H. Speck.** 1989. Mutually exclusive use of viral promoters in Epstein-Barr virus latently infected lymphocytes. *Proc Natl Acad Sci U S A* **86**:6498-502.
187. **Woisetschlaeger, M., C. N. Yandava, L. A. Furmanski, J. L. Strominger, and S. H. Speck.** 1990. Promoter switching in Epstein-Barr virus during the initial stages of infection of B lymphocytes. *Proc Natl Acad Sci U S A* **87**:1725-9.
188. **Wu, T. T., L. Tong, T. Rickabaugh, S. Speck, and R. Sun.** 2001. Function of Rta is essential for lytic replication of murine gammaherpesvirus 68. *J Virol* **75**:9262-73.
189. **Wu, T. T., E. J. Usherwood, J. P. Stewart, A. A. Nash, and R. Sun.** 2000. Rta of murine gammaherpesvirus 68 reactivates the complete lytic cycle from latency. *J Virol* **74**:3659-67.
190. **Xu, Y., D. P. AuCoin, A. R. Huete, S. A. Cei, L. J. Hanson, and G. S. Pari.** 2005. A Kaposi's sarcoma-associated herpesvirus/human herpesvirus 8 ORF50 deletion mutant is defective for reactivation of latent virus and DNA replication. *J Virol* **79**:3479-87.
191. **Yang, Z., H. Tang, H. Huang, and H. Deng.** 2009. RTA promoter demethylation and histone acetylation regulation of murine gammaherpesvirus 68 reactivation. *PLoS One* **4**:e4556.
192. **Yasui, D. H., S. Peddada, M. C. Bieda, R. O. Vallero, A. Hogart, R. P. Nagarajan, K. N. Thatcher, P. J. Farnham, and J. M. Lasalle.** 2007. Integrated epigenomic analyses of neuronal MeCP2 reveal a role for long-range interaction with active genes. *Proc Natl Acad Sci U S A* **104**:19416-21.
193. **Ye, J., D. Shedd, and G. Miller.** 2005. An Sp1 response element in the Kaposi's sarcoma-associated herpesvirus open reading frame 50 promoter mediates lytic cycle induction by butyrate. *J Virol* **79**:1397-408.
194. **Young, L. S., and A. B. Rickinson.** 2004. Epstein-Barr virus: 40 years on. *Nat Rev Cancer* **4**:757-68.
195. **Yu, F., J. Feng, J. N. Harada, S. K. Chanda, S. C. Kenney, and R. Sun.** 2007. B cell terminal differentiation factor XBP-1 induces reactivation of Kaposi's sarcoma-associated herpesvirus. *FEBS Lett* **581**:3485-8.
196. **Yu, Y., J. B. Black, C. S. Goldsmith, P. J. Browning, K. Bhalla, and M. K. Offermann.** 1999. Induction of human herpesvirus-8 DNA replication and transcription by butyrate and TPA in BCBL-1 cells. *J Gen Virol* **80 (Pt 1)**:83-90.
197. **Zalani, S., E. Holley-Guthrie, and S. Kenney.** 1996. Epstein-Barr viral latency is disrupted by the immediate-early BRLF1 protein through a cell-specific mechanism. *Proc Natl Acad Sci U S A* **93**:9194-9.
198. **Zalani, S., E. A. Holley-Guthrie, D. E. Gutsch, and S. C. Kenney.** 1992. The Epstein-Barr virus immediate-early promoter BRLF1 can be activated by the cellular Sp1 transcription factor. *J Virol* **66**:7282-92.
199. **Zheng, Z. M.** 2003. Split genes and their expression in Kaposi's sarcoma-associated herpesvirus. *Rev Med Virol* **13**:173-84.

200. **zur Hausen, H., F. J. O'Neill, U. K. Freese, and E. Hecker.** 1978. Persisting oncogenic herpesvirus induced by the tumour promotor TPA. *Nature* **272**:373-5.